

# D1.4 PREDICTIVE MODELS OF R- LABSCAPES



Funded by  
the European Union

Funded by the European Union. Views and opinions expressed are however those of the author(s) only and do not necessarily reflect those of the European Union or Research Executive Agency (REA). Neither the European Union nor the granting authority can be held responsible for them.

<b>Deliverable No.</b>	<b>D1.4</b>
<b>Work Package</b>	WP1
<b>Dissemination Level</b>	PU
<b>Author(s)</b>	María Ayelen Calvet (TEC), Beñat Abajo (TEC), Alessandra Gandini (TEC), Aitziber Egusquiza (TEC), Benedetta Baldassarre (UNIBO), Jacob Frederic Schlechtendahl (UNIBO), Claudia de Luca (UNIBO), Natasa Manojilovic (TUHH), Oxana Karatnik (TUHH)
<b>Co-author(s)</b>	
<b>Contributor(s)</b>	Daniel Navarro (TEC), Andrea Di Maggio (LINKS), Nicoletta Portunato (PORTOVENERE, CINQUE TERRE AND THE ISLANDS), Babis Fassoulas (PSILORITIS GEOPARK), Chara Papailiou (PSILORITIS GEOPARK), Catharina Greve (HAM), Josip Milić (ZADAR), Lola Almazan (LNV), Julian Soriano (LNV), Maria Luisa Quarta (SIST), Katharina Milde (FhG), Irene Ghezzi (UNIBO), Sofia Moschetta (UNIBO), Simona Bravaglieri (UNIBO), Angela Santangelo (UNIBO)
<b>Due date</b>	30/04/2025
<b>Actual submission date</b>	13/06/2025
<b>Status</b>	Submitted
<b>Revision</b>	Version 1.0
<b>Reviewed by (if applicable)</b>	Dana Salpina (CMCC), Soheil Mohammadi (CMCC), Catharina Greve (HAM)

Summary	7
List of figures	8
List of tables	10
List of Acronyms	12
<b>1 Introduction</b>	<b>13</b>
1.1 Aims and objectives	13
1.2 Relation with other project activities	14
1.3 Report structure	15
<b>2 Rationale for local impact models' development</b>	<b>16</b>
2.1 Island of Neuwerk in Hamburg	17
2.2 Psiloritis Geopark	19
2.3 Portovenere, Cinque Terre and the Islands	21
2.4 Defensive system of Zadar	22
2.5 L'Horta de València	24
<b>3 Theoretical framework</b>	<b>27</b>
<b>4 Methodological approach</b>	<b>30</b>
4.1 General methodology	30
4.1.1 Selection of key risks and identification of emission scenarios and periods of study	31
4.1.2 Data model design and data collection	32
4.1.3 Building of risk components based on data from R-Labs and on specific models for each case study	33
4.1.4 Development of indicator and index databases	34
4.1.5 Normalization of indicators and indices	34
4.1.6 Expert-based weight assignment	35
4.1.7 Combination of indicators to obtain the hazard, exposure and vulnerability indices	36

4.1.8	Combination of hazard, exposure and vulnerability indices to obtain risk indices	36
4.1.9	Creation of Geo datasets and maps	37
4.1.10	Analysis of results	38
<b>4.2</b>	<b>Island of Neuwerk in Hamburg</b>	<b>38</b>
4.2.1	Hazard	38
4.2.2	Exposure	44
4.2.3	Vulnerability	44
4.2.4	Risk assessment	48
<b>4.3</b>	<b>Psiloritis Geopark</b>	<b>48</b>
4.3.1	Hazard	49
4.3.2	Exposure	53
4.3.3	Vulnerability	54
4.3.4	Risk assessment	62
<b>4.4</b>	<b>Portovenere, Cinque Terre and the Islands</b>	<b>63</b>
4.4.1	Hazard	63
4.4.2	Exposure	69
4.4.3	Vulnerability	69
4.4.4	Risk assessment	73
<b>4.5</b>	<b>Defensive system of Zadar</b>	<b>73</b>
4.5.1	Hazard	74
4.5.2	Exposure	79
4.5.3	Vulnerability	80
<b>4.6</b>	<b>L'Horta de València</b>	<b>81</b>
4.6.1	Hazard	81
4.6.2	Exposure	83
4.6.3	Vulnerability	84
4.6.4	Risk assessment	89
<b>5</b>	<b>Results</b>	<b>90</b>
<b>5.1</b>	<b>Island of Neuwerk, Hamburg</b>	<b>90</b>
	Impacts of coastal floods on the buildings and agricultural lands	90

5.1.1	RCP 8.5 2100	90
<b>5.2</b>	<b>Psiloritis Geopark</b>	<b>92</b>
	Impact of changes in temperature on culture	92
5.2.1	Historical period (1980-2004)	92
5.2.2	RCP 4.5 (2025-2049)	93
5.2.3	RCP 8.5 (2025-2049)	94
	Impact of changes in precipitation patterns on culture	94
5.2.4	Historical period (1980-2004)	94
5.2.5	RCP 4.5 (2075-2099)	95
5.2.6	RCP 8.5 (2075-2099)	96
<b>5.3</b>	<b>Portovenere, Cinque Terre and the Islands</b>	<b>97</b>
	Impacts of landslides on the terraced landscape	97
5.3.1	Historical period (1981-2010)	97
5.3.2	RCP 4.5 scenario (2071-2100)	99
5.3.3	RCP 8.5 scenario (2071-2100)	100
<b>5.4</b>	<b>Defensive system of Zadar</b>	<b>100</b>
<b>5.5</b>	<b>L'Horta de València</b>	<b>102</b>
	Impact of torrential rainfall on the agricultural heritage system	102
5.5.1	Historical period (1971-2000)	102
5.5.2	RCP 4.5 (2071-2100)	104
5.5.3	RCP 8.5 (2071-2100)	105
	Impact of droughts on the agricultural heritage system	106
5.5.4	Historical period (1971-2000)	106
5.5.5	RCP 4.5 (2071-2100)	108
5.5.6	RCP 8.5 (2071-2100)	109
<b>5.6</b>	<b>Comparing the local outcomes with the global outcomes</b>	<b>110</b>
<b>6</b>	<b>Conclusions</b>	<b>114</b>
<b>7</b>	<b>References</b>	<b>118</b>
<b>8</b>	<b>Appendices</b>	<b>125</b>

<b>Annex 1. R-Labs Data models</b>	<b>125</b>
<b>Annex 2. Risk maps</b>	<b>135</b>
PSILORITIS GEOPARK	135
L'HORTA DE VALENCIA	137
PORTOVENERE, CINQUE TERRE AND THE ISLANDS	140

## Summary

This document presents a comprehensive risk assessment for the five RescueME Labscapes, developed through predictive models of the impacts of climate change on these landscapes, specifically focusing on ecosystem services and local heritage values.

A multi-scale approach was employed to identify key risks and hazards affecting each R-Lab, including coastal flooding, changes in precipitation patterns and temperature, torrential rainfalls, droughts, and landslides. Indicators were developed to measure vulnerability, exposure, and hazard, which were then combined to create risk maps for each Labscape. The indicators were normalized and weighted according to their relative importance, with experts from each R-Lab providing input on the weighting process. This allowed for the integration of local knowledge and priorities into risk assessment. The resulting risk maps reveal the spatial distribution of risk and provide a valuable tool for visualizing the potential impacts of climate change.

The analysis shows that climate change poses a significant threat to these cultural landscapes, with many areas expected to experience high or medium-high risk levels by the end of the century. For example, in Neuwerk, storm-related hazards are projected to pose a medium risk to those parcels further away from the dyke system, i.e., located towards the centre of the island, while in L'Horta de Valencia, the impact of torrential rainfall on agricultural heritage is expected to increase over the course of the century.

Some landscapes, such as Portovenere, Cinque Terre and the Islands, are expected to experience a significant increase in risk from landslides, while in Psiloritit, temperature changes are projected to increase risk levels substantially. In Zadar, approximately half of the buildings analyzed are expected to experience medium to higher levels of vulnerability. The study highlights the importance of considering the intrinsic characteristics of each landscape, including ecosystem services and local heritage values, when assessing risk. Vulnerability consistently received the highest weight across all case studies, emphasizing the need to prioritize measures that reduce vulnerability, such as conservation and restoration efforts.

This assessment provides a valuable framework for understanding the complexities of climate risk and for developing effective strategies to support the adaptation of cultural landscapes.

## List of figures

Figure 1. Relation between Task 1.3 and other project activities.	14
Figure 2. Risk and its components. Source: IPCC (2021)	27
Figure 3. Methodological steps carried out for the analysis of risk in each case study.	30
Figure 4. Hazard modelling of the Hamburg-Neuwerk; left: The calibrated North Sea Model indicating the R-Lab area (using the 2D model TELEMAC; right: The refined 2D mesh in the R-Lab)	39
Figure 5. Model storm of 2013 considering the influence of the SLR (green: Reference scenario; yellow: SLR 0.3 m; red: SLR 1.0 m)	40
Figure 6. Heights (m) of the Digital Terrain Model (LGV 2022) of the island of Neuwerk with a raster of 1 m x 1 m. The indicated cross-section A-A is presented in Figure 7.	41
Figure 7. The water levels for the reference storm and the projected storm including the scenario with the wave run up (Ru2%) here presented for the cross-section A-A ; blue: water level for the storm 2013; dash blue line: water level for the storm 2013 + Ru2%; yellow: water level for the scenario SLR 0.3 m; dash yellow line: water level for the scenario SLR 0.3 m and Ru2%; red: water level for the scenario SLR 1.0 m; red dash: water level for the scenario SLR 1.0 m and Ru2%	42
Figure 8. The modelling results/ water depths [m] for Neuwerk taking the storm event of 2013 as a reference and considering SLR of 1.0 m RCP 8.5 and RU2%; Time horizon 2100.	43
Figure 9. WRFEC climate change differences for daily maximum temperature (2025–2049 minus 1980–2004 and 2075–2099 minus 1980–2004) for RCP 4.5 and RCP 8.5. (Areas with no dots specify statistically significant changes using a Student’s t-test at the 95 % confidence level) (taken from Politi et., al.) (red rectangular indicates the study area).	50
Figure 10 a WRFEC mean historical climatology, b annual mean precipitation relative changes given by WRFEC for RCP 4.5 and RCP 8.5 (2075–2099 minus 1980–2004)/1980–2004. (Areas with dots specify changes not statistically significant using a student’s t test at the 95 % confidence level) (taken from Politi et., al. 2023) (red rectangular indicates the study area).	51
Figure 11. The map indicating the measuring stations on the island of Crete (Source: Greek Water Authority)	52
Figure 12. Runoff retention values of Psiloritis Geopark in m <sup>3</sup> . Computed using InVEST® Urban Flood Risk Mitigation model (Natural Capital Project, 2023).	61
Figure 13. Cooling capacity values of Psiloritis Geopark. Computed using InVEST® Urban Cooling model (Natural Capital Project, 2023).	61
Figure 14. The principle of the intersection of the raster data sets for R99 and R99PTOT and the spatial units of the R-Lab. The datasets were provided by Fagian & Trevisol, 2024	65

Figure 15. Rainfall thresholds obtained for the possible initiation of shallow landslides and mud/debris flows on the Portofino promontory corresponding to a 5 % exceedance probability level (red curve) and associated uncertainty (grey pattern) Taken from Rocatti, et al., (2020).	67
Figure 16. Water level series of gauge Tarifa from 1st October 2012 to 1st January 2013.	75
Figure 17. The developed hydrodynamic model with the boundary conditions (inflows) for the Zadar R-Lab. The basemap taken from USGS, (2025).	77
Figure 18. Resolution of the calculation mesh in the area of interest. The basemap taken from USGS, (2025)	77
Figure 19. The results of the hazard modelling, water depths, for the Zadar R-Lab given for the storm of 2012 with a SLR of 0.2 m.	78
Figure 20. The results of the hazard modelling, water depths, for the Zadar R-Lab given for the storm of 2012 with a SLR of 0.7 m.	79
Figure 21. The AdapteCCa platform with the main features and elements relevant for the hazard modelling in the L'Horta de Valencia R-Lab; red rectangular- selection of the variables; yellow rectangular: RCPs; blue rectangular: time horizons; violet rectangular: study area; black rectangular: scale of analysis, here the municipal scale	82
Figure 22. Runoff retention values of Valencia in m <sup>3</sup> . Computed using InVEST® Urban Flood Risk Mitigation model (Natural Capital Project, 2023).	87
Figure 23. Impacts of coastal floods on the buildings and agricultural lands in the island of Neuwerk.	91
Figure 24. Impact of changes in temperature on culture. Historical period (1980-2004).	92
Figure 25. Impact of changes in temperature on culture. RCP 4.5 (2025-2049)	93
Figure 26. Impact of changes in precipitation on culture. Historical period (1980-2004).	95
Figure 27. Impact of changes in precipitation on culture. RCP 4.5 (2075-2099).	96
Figure 28. Impact of changes in precipitation on culture. RCP 8.5 (2075-2099)	97
Figure 29. Impacts of landslides on the terraced landscape.	98
Figure 30. Impacts of landslides on the terraced landscape. RCP 4.5 (2071-2100).	100
Figure 31. Climate change vulnerability. Source: UNIBO, using data collected through a survey conducted with R-Lab experts.	101
Figure 32. Impacts of torrential rainfall on the agricultural heritage system. Historical period (1971-2000).	103
Figure 33. Impacts of torrential rainfall on the agricultural heritage system. RCP 4.5 (2071-2100).	104
Figure 34. Impacts of torrential rainfall on the agricultural heritage system. RCP 8.5 (2071-2100).	105
Figure 35. Impact of droughts on the agricultural heritage system. Historical period (1971-2000).	107
Figure 36. Impact of droughts on the agricultural heritage system. RCP 4.5 (2071-2100).	108
Figure 37. Impact of droughts on the agricultural heritage system. RCP 8.5 (2071-2100).	109

Figure 38. Impact of changes in precipitation patterns on culture. RCP 4.5 (2025-2049)	135
Figure 39. Impact of changes in precipitation patterns on culture. RCP 8.5 (2025-2049)	136
Figure 40. Impact of changes in temperature on culture. RCP 8.5 (2025-2049)	136
Figure 41. Impact of droughts on the agricultural heritage system. RCP 8.5 (2011-2040)	137
Figure 42. Impact of droughts on the agricultural heritage system. RCP 8.5 (2041-2070)	138
Figure 43. Impacts of torrential rainfall on the agricultural heritage system. RCP 4.5 (2011-2040)	138
Figure 44. Impacts of torrential rainfall on the agricultural heritage system. RCP 4.5 (2041-2070)	139
Figure 45. Impacts of landslides on the terraced landscape. RCP4.5 (2021-2050)	140
Figure 46. Impacts of landslides on the terraced landscape. RCP4.5 (2041-2070)	140
Figure 47. Impacts of landslides on the terraced landscape. RCP8.5 (2021-2050)	141
Figure 48. Impacts of landslides on the terraced landscape. RCP8.5 (2041-2070)	141

## List of tables

Table 1. Risks studied, study periods, and emission scenarios for R-Labs.	31
Table 2. Components assessed in each R-Lab	34
Table 3. Indicators employed in the assessment of exposure on Neuwerk Island (Hamburg), along with their corresponding weights.	44
Table 4. List of indicators used for HV assessment of Neuwerk.	45
Table 5. List of indicators used for ES assessment of Neuwerk.	46
Table 6. Indicators and indices used in the vulnerability assessment of Neuwerk Island (Hamburg), along with their corresponding weights.	47
Table 7. Risk components' weights on Neuwerk Island (Hamburg).	48
Table 8 The indicators describing the changes in temperature and precipitation patterns used in the Psiloritis R-Lab. In addition to the indicators provided in the study of Politi et., al (2023), the observed data for the max daily temperatures have been taken into account.	52
Table 9. Indicators employed in the assessment of exposure on Psiloritis, Crete, along with their corresponding weights.	53
Table 10. List of indicators used for HV assessment of Psiloritis Geopark.	54
Table 11. Indicators and indices used in the vulnerability assessment of Psiloritis (Crete), along with their corresponding weights.	62
Table 12. Risk components and weights on Psiloritis, Crete.	62
Table 13. Indicators employed in the assessment of exposure on Portovenere, Cinque Terre and the islands, along with their corresponding weights.	69
Table 14. List of indicators used for HV assessment of Portovenere, Cinque Terre, and the Islands.	70

Table 15. List of indicators used for ES assessment of Portovenere, Cinque Terre and the Islands.	71
Table 16. Indicators and indices used in the vulnerability assessment of Portovenere, Cinque Terre and The Islands, along with their corresponding weights	72
Table 17. Risk components' weights on Portovenere, Cinque Terre and the Islands.	73
Table 18. Input data and their sources that has been used to set up the 2d hydrodynamic model for Zadar R-Lab. They are based on the publicly available sources	74
Table 19. Considered discharges into the Mediterranean Sea.	76
Table 20. A set of indicators for the analysis of changes in precipitation patterns to address both, droughts and torrential floods in the L'Horta de Valencia R-Lab	82
Table 21. Indicators employed in the assessment of exposure on L'Horta de Valencia, along with their corresponding weights.	84
Table 22. List of indicators used for HV assessment of Valencia.	84
Table 23. List of indicators used for ES assessment of Valencia.	86
Table 24. Indicators and indices used in the vulnerability assessment of Valencia, along with their corresponding weights	88
Table 25. Risk components' weights on l'Horta de Valencia	89

# List of Acronyms

Acronym	Full name
CL	Cultural Landscape
CORDEX	Coordinated Regional Climate Downscaling Experiment
CNR	National Research Council of Italy
DAAC	Distributed Active Archive Center
ESA	European Spatial Agency
ES	Ecosystem Services
ETCCDI	Expert Team on Climate Change Detection and Indices
FAO	Food and Agriculture Organization
GIAHS	Globally Important Agricultural Heritage System
GHG	Greenhouse gas
GIS	Geographic Information System
GISIG	Geographic Information Systems International Group
HV	Heritage Values
IFFI	Italian Landslide Inventory
ICCSA	International Conference on Computational Science and Its Applications
IPCC	Intergovernmental Panel on Climate Change
LTI	Landslide Trigger Index
NASA	National Aeronautics and Space Administration
NHESS	Natural Hazards and Earth System Sciences
ORNL	Oak Ridge National Laboratory
ORNLDAAC	Oak Ridge National Laboratory Distributed Active Archive Center
PDO	Protected Designation of Origin
RCP	Representative Concentration Pathway
R-Lab	R-Labscape (resilience landscape laboratories)
SCS	Soil Conservation Service
SETS	Socio-ecological-technical systems
SLR	Sea Level Rise
SSP	Shared Socioeconomic Pathways
TEC	Tecnalia
TUHH	Hamburg University of Technology
UNIBO	University of Bologna
WMO	World Meteorological Organization
WRF	Weather Research and Forecasting Model
WRFEC	Weather Research and Forecasting Model Environmental Chemistry
WP	Work Package

# 1 Introduction

## 1.1 Aims and objectives

This document describes the work undertaken as part of Task 1.3, which aimed to develop a comprehensive **multiscale risk and resilience assessment of coastal Cultural Landscapes (CL)**. This assessment supports the creation of predictive impact models for each R-Lab that focus on assessing risks to cultural landscapes from different hazards, while specifically addressing ecosystem services and local heritage values in accordance with the RescueME framework.

To achieve this, the task has been divided into three interconnected subtasks. The first subtask (ST1.3.1) involves analysing and **quantifying ecosystem services** and **characterizing local heritage values**, ensuring that tangible and, whenever applicable and feasible, intangible cultural values are reflected in the models. The second subtask (ST1.3.2) focuses on **hazard modelling** for each case study. This work builds on model simulations and statistical analysis and covers the relevant hazards identified and prioritized by the R-Labs, including coastal floods, rainfall, temperature and precipitation patterns changes, droughts and landslides. The third subtask (ST1.3.3) focuses on the development of **predictive impact modelling for each R-Lab**. These models simulate the impact of relevant hazards in different scenarios, capturing the effects on socio-ecological-technical systems from a strong heritage-centric perspective, incorporating the different dimensions and capitals that are essential to cultural landscapes. Each model produces a baseline relative risk index that integrates the three key components of risk: hazard, exposure, and vulnerability.

The overall analysis aligns with the conceptual framework proposed in the Fifth and Sixth Assessment Reports of the Intergovernmental Panel on Climate Change (IPCC), ensuring methodological consistency with the internationally recognized standards for risk assessment. The indicators used for the analysis - the relative risk indices and the scaled components of hazard, exposure, and vulnerability - were linked to the Geographic Information System (GIS) layers of each R-Lab through unique spatial unit codes, allowing for spatially explicit modelling and interpretation.

A collection of risk maps was produced for each R-Lab based on these spatial data layers, representing the risks under the different climate change scenarios considered. These maps served as key tools for visualising the spatial distribution of risk and supporting further analysis.

## 1.2 Relation with other project activities

Task 1.3 is connected with several other activities within the RescueME project, both conceptually and methodologically (Figure 1). Its main foundation lies in the primary resilience assessment framework developed in Task 1.1: The Actionable Resilient Historic Landscape Framework. This framework conceptualizes Cultural Landscapes as socio-ecological-technical systems (SETS), structured around five key capitals: natural, built, social, human, and financial. It also introduced a multi-level approach, integrating both top-down and bottom-up perspectives, which was applied throughout Task 1.3.

This task also builds directly on the outcomes of Task 4.2, in which baseline resilience assessments were conducted for each R-Lab. These formed a crucial input to the development of predictive models. Building on the complexity of the impact chains defined in WP4 earlier, Task 1.3 began with a refinement process involving stakeholder prioritization exercises. These exercises helped to narrow the scope of the analysis by identifying the core elements of each R-Lab's System and its primary expected impacts.

In addition, key support for Task 1.3 was provided by WP3, particularly Task 3.1, which defined the technical specifications and supported data preparation. The development of a common data model in Task 3.1 ensured methodological consistency across case studies, aligning the conceptual framework from WP1 with the practical needs and requirements of the R-Labs.

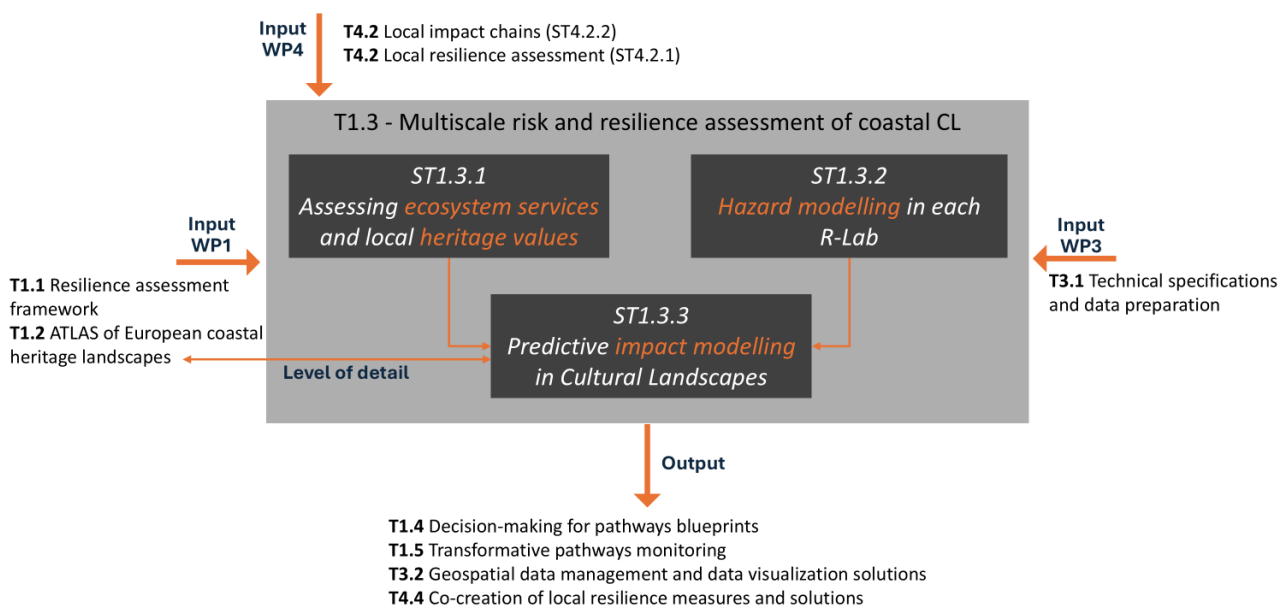


Figure 1. Relation between Task 1.3 and other project activities.

Furthermore, the predictive impact assessment models being developed under Task 1.3 are integral to the broader project vision. These models, which integrate hazard, exposure, and vulnerability components, will be used to inform the design of transformative pathways and their subsequent monitoring (Task 1.4 and Task 1.5), that will be further integrated into the Incremental Spatial Decision Support System. Partial results, as the ecosystem services maps, and relevant data for each R-Lab will be included and visualised in the geospatial data intelligent platform (Task 3.2). Results will also serve as a starting point for the serious game and the development of local resilience measures (Task 4.4). Finally, the relation with the ATLAS of European coastal landscapes (Task 1.2) is bidirectional: from one side, the ATLAS provided the refinement of some indicators definition and calculation, from the other side, Task 1.3 results are used to compare global and local outcomes, which together provide a regional broad overview, and more nuanced patterns shaped by specific characteristics.

## 1.3 Report structure

This document is structured into the following sections:

- a description of the approach used to define the model in each R-Lab
- the theoretical framework that underpins this study
- the general methodology and the methodological description of each R-Lab
- the results obtained from the applied methodology.

The methodology section also provides a detailed explanation of the data generation process for the different risk components: hazard, exposure, and vulnerability, as well as the overall risk assessment methodology. Finally, the conclusions of this work are presented.

## 2 Rationale for local impact models' development

This section outlines the approach used to define and develop local risk models for each R-Lab. Although each site has different cultural, social and environmental characteristics and data availability, the selection of relevant hazards, the identification of exposed elements and the assessment of vulnerability were guided by the indicators framework, with its system, capital and dimension structure, as described in the Actionable Resilient Historic Landscape Framework (Gandini and Egusquiza 2023). As reference, the following table reports the structure of the systems, their associated capitals and dimensions, which are measured by indicators.

System	Capital	Dimension
Social	Social capital	Diversity
		Intangible cultural heritage
		Social value
		Governance
		Demographics
	Financial capital	Economy
		Tourism
	Human capital	Training
		Education
Ecological	Natural capital	Natural heritage

System	Capital	Dimension
Technical	Built capital	Green and blue infrastructure
		Agriculture
		Topography and morphology
		Energy
Technical	Built capital	Infrastructure
		Buildings
		Tangible cultural heritage

The following subsections describe the rationale behind the choices made in the project, following outcomes of the resilience baseline assessment and the impact chain workshops (Wischott et al. 2024), and paying attention to the availability of data, cultural heritage priorities, and stakeholder input. The steps undertaken in the risk analysis methodology and the detailed approach followed for each R-Lab are described in dedicated chapters (4.2 to 4.6) of this document.

## 2.1 Island of Neuwerk in Hamburg

The island of Neuwerk is one of three islands in the Hamburg Wadden Sea National Park. The other two islands Scharhörn and Nighhörn are uninhabited and belong to the wilderness zone. The national park, with a total areas of 137,5 km<sup>2</sup>, has over 90% undisturbed wilderness and is also recognised as a UNESCO Biosphere Reserve. It forms part of the larger UNESCO Wadden Sea World Heritage Site. The national park is recognised for its ecosystems and biodiversity.

The island is defined by its remoteness, limited population, and dependence on seasonal tourism and low-intensity livestock farming, all of which shape its socio-economic and environmental dynamics. Central to its identity is the historic Neuwerk Tower, dating back

to 1310, now a landmark for visitors as well as an emergency shelter during severe storm events.

Despite strong local governance and relatively equitable gender representation in employment, the island faces long-term demographic challenges with an ageing population and a lack of young people moving to the island, according to the resilience baseline assessment. Business ownership, including grazing leases, is predominantly held by older individuals, and there are few mechanisms in place to attract young businesses to move to the island who also engage in grazing leases. Neuwerk benefits financially from its protected status, cultural history and values. However, limited disaster preparedness funding and infrastructure capacity pose ongoing risks, especially during peak tourism periods. Environmentally, the national park maintains strong conservation commitments, but data gaps limit the ability to respond to climate change and human-induced hazards effectively. Built infrastructure supports heritage preservation and environmentally friendly transport, yet emergency services may not be able to cope during a crisis. During the summer season, the increase in visitors, overnight and day tripper, raises concerns about social cohesion and long-term community sustainability. Overall, Neuwerk exemplifies both the opportunities and vulnerabilities typical of remote, protected cultural landscapes facing demographic change, economic transition, and environmental uncertainty.

Neuwerk faces several climate-related challenges, particularly sea level rise and coastal storm events causing storm surges. These events endanger the island's natural systems and infrastructure. These risks were addressed during the project's impact chains workshop by using two scenarios: a sudden disaster involving dyke failure during a storm surge causing the island to flood and a gradual rise in sea level up to one metre. The analysis revealed that the key exposure systems are the island's residents and seasonal workers; critical infrastructure, including supply, disposal, and protection infrastructure; and biodiversity-rich habitats, such as salt marshes and bird nesting areas. Access to the island is limited to a passenger ferry from the mainland, horse carriages, or on foot over the tidal flats, and these routes will also be affected.

According to the above-mentioned results and following bilateral meetings with Neuwerk's key stakeholders, a tailored local impact model was developed to assess the **risks of coastal flooding** – including sea level rise and storm surges – on the island's **buildings and agricultural lands**. The model uses **cadastral lots** as the unit of analysis, allowing for a detailed and spatially differentiated assessment of exposure and vulnerability within the inhabited terrestrial area of the island.

The decision to focus the model on coastal flooding was based on the fact that it represents the island's most critical hazard. The combination of rising sea levels and more intense storm events increases the risk of overtopping or damaging the island's protective ring dyke

system, which could result in the inundation of the residential and agricultural zones. The assessment considered both the reference period (2013 storm event) and future sea level rise scenarios, using cadastral lots as the appropriate spatial units and taking advantage of the available hydrological data to simulate detailed flood scenarios for the island.

The model focuses on **built, financial, and social capital** as the core **exposure** dimensions. Built capital includes number of properties, while financial capital refers to tourism and economic dimensions, considering agricultural holdings, tourism establishments, houses with summer-use, and overnight accommodation. Social capital is addressed by examining the potential impact on the resident population.

When considering **vulnerability**, data availability and the ability to reflect meaningful differences across cadastral lots were key factors. While many variables, such as building typologies and farming systems, are consistent across the island, making them less useful for distinguishing vulnerability at a parcel level, other factors like internet connection, number of emergency operators, number and location of cultural facilities, land use and area with outdoor recreation potential vary spatially and were incorporated into the model. For capitals such as human and financial, information was only available at the island-wide scale and could not be downscaled to individual parcels. These were nonetheless important for contextual analysis. In environmental terms, the surrounding Wadden Sea ecosystem provides a degree of natural protection by buffering wave energy and for this reason the role of **ecosystem services** was considered as one of the main components of vulnerability, together with the **heritage values** that encompass the natural, social and built capitals.

In summary, the local impact model emphasizes a cadastral-scale assessment of risk, particularly focusing on residential properties, tourism-related infrastructure, and agricultural holdings. While all five capitals – natural, social, human, financial, and built – were considered, the analysis concentrates on those dimensions that display meaningful variation between parcels. This allows for a better understanding of vulnerability and adaptation potential, which is essential for informed decision-making and targeted resilience planning on the island.

## 2.2 Psiloritis Geopark

The Psiloritis UNESCO Global Geopark is in central Crete and covers an area of 1,272 km<sup>2</sup>. This diverse region spans from coastal zones along the Aegean Sea to mountainous areas exceeding 2,000 meters in elevation, encompassing 96 villages across eight municipalities. Its landscape combines exceptional geodiversity—including volcanic, sedimentary, and metamorphic rock formations, caves, fossil sites, and karstic systems—with a rich cultural and archaeological heritage. Psiloritis is recognized not only for its geological features but

also for the traditional villages, ancient archaeological sites, and important religious monuments. These are complemented by vibrant intangible cultural traditions, including the Mediterranean culinary tradition, dry-stone walling, and traditional pastoral practices, many of which are protected under national and UNESCO heritage frameworks.

While the inland and coastal zones of the Geopark vary significantly in their exposure to risks, the northern coastal region – specifically the municipalities of Mylopotamos and Rethymno – were selected as the main area of interest among the eight municipalities of the territory. This area is more vulnerable due to its higher concentration of human activity and exposure to climate-related hazards such as droughts, floods, earthquakes, and tsunamis.

The resilience baseline assessment of Psiloritis revealed strengths in areas such as gender equity, youth participation in farming, and strong governance engagement with national strategies. However, there are still challenges regarding accessibility and land tenure in relation to heritage protection, as well as gaps in data, particularly economic and tourism-related information. Despite a slight population decline, local traditions remain vibrant, and the area benefits from both national and EU-level funding for landscape protection. Nonetheless, water scarcity, seasonal tourism pressures, and limited transport infrastructure are critical concerns.

The impact chain workshops focused on heatwaves and rising average temperatures, particularly affecting parts of Mylopotamos and Rethymno municipalities. The Eastern Mediterranean region is projected to face some of the most severe climate impacts in Europe, including a temperature rise of up to 2.4 °C and a 16 % drop in precipitation by 2100. These trends are expected to exacerbate drought, water shortages, and desertification, threatening the two main economic sectors of the northern coastal area: agriculture and tourism. Both sectors are competing increasingly for limited natural resources, particularly water, which is critical for heritage continuity.

Two impact models were developed to address the effects of **rising temperatures and changing rainfall patterns** in communities belonging to the two above mentioned municipalities of Mylopotamos and Rethymno, which are considered to be at the greatest risk from climate-related hazards in the area. These climatic changes pose a significant hazard to the region's **natural systems, socio-economic stability, and cultural continuity**.

The model identifies **social, natural and financial capital** as the primary **exposed** elements, considering demographics and economy as main domains affected, reflecting the local dependency on two key economic sectors: **agriculture and tourism**. These sectors are not only vital sources of employment and income but also closely interlinked with the region's identity and land use patterns.

The **vulnerability** dimension of the model places emphasis on the region's **ecosystem services**, particularly regarding their cooling capacity and runoff retention. These services are crucial in buffering the impacts of temperature extremes and irregular precipitation. Additionally, the model integrates elements of **natural and social capital** related to **heritage value**. This includes both **tangible assets** – such as protected natural areas and cultural sites – and **intangible heritage**, encompassing local traditions, agricultural practices, and social values embedded in the region's identity. These components are critical for understanding the broader implications of climate impacts on cultural continuity. Other aspects of **human and social** vulnerability were also incorporated, including training and education, governance, and the age structure of the population.

## 2.3 Portovenere, Cinque Terre and the Islands

The Italian focus of the RescueME project is the UNESCO World Heritage Site comprising of Portovenere, the five coastal villages of Cinque Terre (Monterosso al Mare, Vernazza, Corniglia, Manarola, and Riomaggiore), and the islands of Palmaria, Tino, and Tinetto. Designated a World Heritage Site in 1997 for its exceptional cultural landscape, this region represents the integration of human settlement with a challenging coastal terrain. The area is characterized by steep cliffs, terraced agriculture, and compact villages that have adapted to the environment. Over centuries, local communities have constructed extensive dry-stone terraces to cultivate vineyards and olive trees, reflecting collective land stewardship and agricultural cooperation. A historic network of walking paths links the villages and was once the sole means of travel between them. This interconnected landscape reflects not only architectural and environmental adaptation but also a living cultural tradition that continues to shape the region's socio-economic fabric. The region's scenic beauty, traditional lifestyles, and cultural assets have made it a major destination for tourism – an important, yet pressure-inducing, economic driver.

The resilience baseline assessment revealed a mixture of strengths and vulnerabilities. Although there has been improvement in terms of social equity, youth involvement in agriculture and gender equality, governance participation remains limited and land tenure and accessibility continue to present challenges. Declining population trends and incomplete demographic data further complicate community planning. While intangible heritage is widely celebrated, policy gaps hinder its broader protection and accessibility. Human capital in the area is constrained by limited educational opportunities and training in farming practices. Local engagement in landscape conservation is robust, but inconsistent funding and mounting tourism pressures are putting a strain on available resources. From an ecological point of view, traditional agriculture benefits from the products recognised by the

EU, but there are still risks in terms of water scarcity, biodiversity and land use. The built environment has basic infrastructure and an active energy transition but lack comprehensive plans for heritage preservation and urban resilience.

In the two impact chain workshops, landslides caused by extreme precipitation were identified as the most relevant hazard and their impacts were discussed for different areas of the pilot region. Landslides are a widespread and pressing hazard throughout the site due to a combination of factors, including steep topography, fragile rock formations, climate variability, and human activity. Intensifying rainfall, vegetation loss from wildfires or deforestation, and poorly managed land use practices all contribute to an increase in slope instability. Abandoning agricultural practices and the collapse of dry-stone walls further increase the risk. Exposed elements identified in the workshops include agriculture, cultural heritage, residents, tourists, and infrastructure.

According to the described analysis, the selected impact model focuses on the effects of **landslides on the terraced cultural landscape**, with municipalities serving as the unit of analysis. This choice was driven by the identification of **landslides triggered by extreme precipitation** as the **most critical hazard** in the area, due to their occurrence and destructive potential. These events **expose** the population, the economic and touristic dimensions, in terms of agricultural holdings, tourist establishment and overnight accommodation as well as education facilities, which are central components of **social, financial** and **human** capitals in the region.

The **vulnerability** of the area is tied to its distinctive **agricultural heritage value system**, embodied in the traditional practices that define the landscape. The terraces are not only cultural symbols but also critical components of the region's **ecosystem services**, particularly in relation to the topographic characteristics and human cultivation of the natural capital. In addition, socio-economic and demographic factors further contribute to vulnerability. These include challenges such as depopulation, limited economic diversification, and the morphological settings of the area.

This impact model thus reflects both the **physical and cultural risks** of the landscape, ensuring that the analysis captures the complex interaction between natural hazards, human presence and heritage preservation.

## 2.4 Defensive system of Zadar

The RescueME project focuses on the historic Defensive System of Zadar, part of the larger UNESCO World Heritage Site titled “Venetian Works of Defence between the 16th and 17th Centuries: Stato da Terra – Western Stato da Mar.” This transnational site includes six

fortified locations that once protected the Republic of Venice, including Zadar, a critical Adriatic port and former capital of Venetian Dalmatia. Strategically situated on a peninsula along the eastern Adriatic coast in the Dalmatian region, Zadar was a key maritime and military hub for the Republic of Venice.

Zadar today exemplifies a strong commitment to preserving its cultural heritage and integrating sustainable energy measures within its historical infrastructure. However, challenges remain. While the city has made progress in inclusive governance and gender equity, more efforts are needed to promote intangible cultural heritage, address demographic trends, and enhance civic participation. The human capital benefits from strong cultural education and adult learning initiatives, yet broader public engagement is needed. Financial strategies show alignment with sustainability goals, although data collection and disaster preparedness need to be strengthened. Environmental efforts are commendable, but vulnerabilities persist – particularly in adapting to climate-related hazards.

Two impact chain workshops highlighted Zadar’s exposure to climate hazards. The first workshop identified heatwaves as a growing hazard due to the city’s coastal Mediterranean climate, with severe impacts on agriculture, ecosystems, infrastructure, and the economy. The second workshop focused on pluvial flooding and storm surges, which significantly affect residents and tourists. Extreme weather events, such as heavy rainfall and high winds, pose substantial risks to heritage sites, buildings and key economic sectors.

The development of a local impact model for Zadar involved several iterations and the application of a tailored methodology to address the specific context of the site. Although heatwaves were initially considered as a relevant hazard – given their growing impact on Zadar – they were ultimately excluded from the model. This decision was based on two main considerations: first, temperature variations across the peninsula are minimal and not spatially differentiated enough to provide meaningful analysis at the local level; second, the primary elements at risk from heatwaves are humans and agriculture. Since the latter is not present within the fortified peninsula, the relevance to the cultural aspects of the case study was limited. Furthermore, the assessment of the effects of heat on built heritage would have required detailed material characterization and an in-depth analysis of hygrothermal stress cycles, which was beyond the scope of this project. Similarly, pluvial flooding was not included in the final model. Although relevant, the uniform distribution of flood hazard values across the study area prevented meaningful spatial differentiation. This, combined with the very low data availability and resolution, was hindering a comparative risk assessment matching intra-peninsula units of analysis. In contrast, **coastal flooding and storm surge** were identified as more suitable hazards for analysis. These allow for greater spatial specificity in determining exposure levels, particularly for **built heritage** and **infrastructure** located along the waterfront.

In terms of **exposure**, the focus was placed on the **built heritage elements** that define Zadar's cultural landscape, including the medieval fortifications as part of the designated UNESCO site. Due to limited availability of detailed data at the individual building level, a **customized approach** was developed to **assess vulnerability**. Many of the proposed initial indicators, such as tourism, were only available at the city scale and could not be disaggregated to the level of the fortified peninsula.

To overcome this challenge, a Geographic Information System (GIS) database was created, incorporating data from UNESCO, the Croatian Geoportal for Cultural Property, and national geographical sources. The building's functions were supplemented using publicly available information, including Google Maps. To refine and contextualize the model, a survey was conducted with local stakeholders to assess and assign cultural heritage values, thereby ensuring that the model reflected the local significance and use of individual heritage.

## 2.5 L'Horta de València

RescueME focuses on the Historical Irrigation System of l'Horta de València, a site of global significance recognised by the FAO as a Globally Important Agricultural Heritage System (GIAHS). L'Horta spans 17 km<sup>2</sup> across 45 municipalities, forming a coastal plain that gently descends toward the Mediterranean Sea. It represents one of Europe's most emblematic Mediterranean farming landscapes, characterized by a rich mosaic of agroecological zones. Despite ongoing urban pressures, the area maintains a high level of productive, environmental, cultural, and aesthetic value. The land is primarily organized into small agricultural plots that rely on historic irrigation channels governed by long-standing water distribution norms. The southern edge connects with the Albufera Natural Park, where rice paddies and small-scale fisheries coexist.

Agriculture focuses on citrus fruits, fresh vegetables and rice, contributing not only to local food systems but also to cultural identity. The irrigation system is deeply embedded in the community's heritage, reflected in institutions like the Tribunal de las Aguas – Europe's oldest functioning court of justice – and in the region's unique architectural, linguistic, and social traditions.

The baseline assessment of the area's resilience reveals a complex interplay of assets across the five capitals. Socially, the system shows strengths in gender employment equity and in the existence of long-standing governance structures. However, there are limitations in the involvement of the younger generation, accessibility for people with disabilities, and coordination among the many municipalities that share responsibility for the landscape. From a human capital perspective, while traditional knowledge remains strong, there are

gaps in adult education and vocational training. The employment sector also suffers from a scarcity of stable employment opportunities, which may hinder long-term stewardship and generational renewal. Financial capital is supported by funding and policy initiatives at the local, regional, and national levels, reflecting a general institutional commitment to environmental protection and community welfare. Yet, the area struggles to create employment in the cultural and creative industries, signalling limited economic diversification. The site's natural capital is marked by the availability of water resources and the production of certified agricultural goods (such as those with Protected Designation of Origin or Geographical Indication status). However, limited crop diversity could heighten vulnerability in the face of climate change. Built capital is progressively being strengthened through efforts to promote cultural heritage, though the lack of a dedicated conservation plan, along with insufficient information on housing dynamics and renewable energy use, indicates areas for further development.

As discussed in the first impact chain workshop, local farmers are well-acquainted with the Mediterranean pattern of alternating droughts and heavy rainfall. Historically, this cyclical variability has shaped farming practices and water management. However, recent climate shifts are disrupting these cycles, as extreme weather events are becoming less predictable and more intense, with longer dry spells and increasingly intense, unseasonal rainfall events. These changes are challenging the adaptive strategies that have historically sustained the region. Workshop participants identified several vulnerable systems – including infrastructure, soils, biodiversity, agriculture, fisheries, and the built environment. Building on the resilience assessment and stakeholder insights gathered, the local impact model was developed with the aim of better understanding the risk of **changing precipitation patterns** on the l'Horta de València **agricultural heritage system**. In this case, the model is built considering the municipal level as unit of analysis, examining how hydrological shifts intersect with the area's cultural, ecological, and socio-economic fabric.

In terms of **hazard**, the analysis concentrates on two key variables—**droughts and torrential rainfall**—both evaluated through statistical modelling. These factors are both essential for the area, where the reduction of water resources, prolonged droughts and out-of-season rainfall events threatens the equilibrium of traditional agricultural cycles. These risks, affecting both water supply and agriculture, are also recognised by the Regional Government (BOE-A-2023-4378).

**Exposure** within the model focuses on elements that represent the foundation of the landscape. These aspects are related to the **natural capital**, such as the extent of the agricultural land itself; the **financial capital**, represented by the number of agricultural holdings across the municipalities and the **social capital** captured by the size and distribution of the population.

The **vulnerability** component takes a broader, **more layered view** of what represents the cultural landscape's resilience. Here, the model places particular emphasis on the elements that define l'Horta's cultural **heritage value**. These include the traditional irrigation practices, local crop varieties, particularly those with Protected Designation of Origin (PDO) status, and the preservation of historic structures such as irrigation channels, watermills and examples of vernacular architecture. The extent to which these features are protected or officially recognised also contributes to the vulnerability assessment, as areas with higher levels of legal protection or designated cultural value may be more actively maintained.

**Ecosystem services**, as a key dimension of natural capital, are central to evaluating vulnerability. The availability and sustainability of water resources, land use, and organic farming are not only essential for continued agricultural productivity but also for maintaining the cultural identity and ecological functionality of the region. In parallel, the human, social, and financial capitals are also considered. Factors such as access to training, local governance mechanisms, and the economic viability of continuing traditional agricultural activities all play a role in determining the community's capacity to adapt.

Overall, the model provides a specific understanding of the local impacts of climate vulnerability on l'Horta de València. It recognises that the effects of changing precipitation patterns are not only ecological in nature, but are deeply entwined with the historical, economic, and cultural systems that sustain this unique agricultural heritage site.

### 3 Theoretical framework

The following analysis is aligned with the conceptual framework proposed in the Fifth and Sixth Assessment Reports of the IPCC (known as AR5 and AR6, respectively), which is based on an understanding of climate change-related risk as a “social construct,” as illustrated in the following figure:

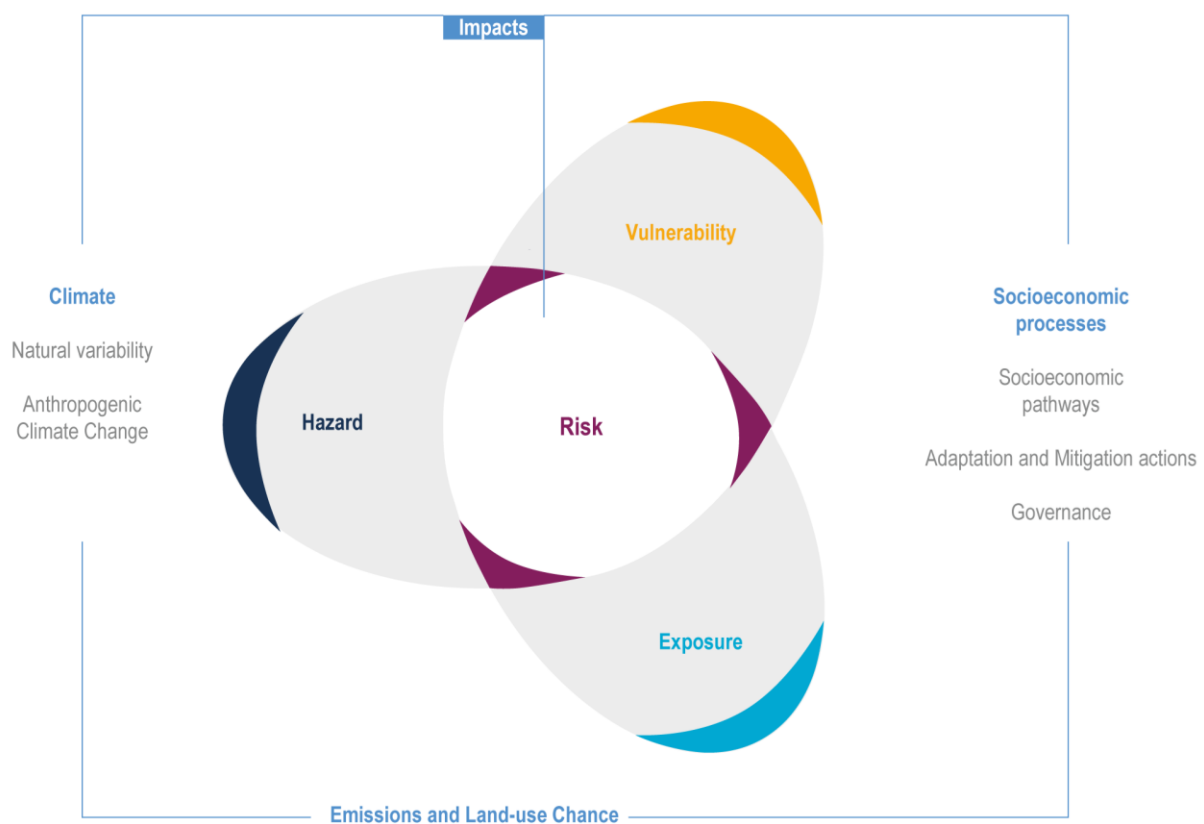


Figure 2. Risk and its components. Source: IPCC (2021)

The glossary included in the AR6 report provides the following definitions for the three main components of risk:

- Hazard:** The potential occurrence of a physical event or trend, whether of natural or human-induced origin, that may cause loss of life, injury, or other health impacts, as well as damage and loss to property, infrastructure, livelihoods, service provision, ecosystems, and environmental resources. In this study, the term refers specifically to hazards associated with climate change.

- **Exposure:** The presence of people; livelihoods; species or ecosystems; environmental functions, services, and resources; infrastructure; or social, cultural, or economic assets in places and settings that could be adversely affected.
- **Vulnerability:** The propensity or predisposition to be adversely affected. Vulnerability encompasses a range of concepts and elements, including sensitivity or susceptibility to harm and lack of capacity to cope and adapt.
  - Sensitivity: the degree to which a system is affected, either adversely or beneficially, by climate variability or change.
  - Adaptive capacity: the ability of systems, institutions, humans, and other organisms to adjust to potential damage, to take advantage of opportunities, or to respond to consequences.

It is important to note that throughout this report, two key concepts have been used to interpret whether the variables characterizing vulnerability, exposure, and hazard contribute to increasing or decreasing risk. These concepts are referred to as positive polarity and negative polarity, respectively. Within this framework, an indicator of sensitivity has a positive polarity and an indicator of adaptive shows negative polarity. In contrast, indicators related to exposure and hazard are always assigned a positive polarity, as a greater number of exposed units or a higher intensity of the hazard directly translates into a higher level of risk.

As this is a multiscale risk and resilience assessment of coastal CL, both the intrinsic value of cultural heritage and the resilience potential provided by the ecosystem services of surrounding or constitutive natural environments, depending on the context, are of significant relevance. These two elements, describing the condition of cultural heritage and ecosystems that may enhance their resilience to specific hazards, have been integrated into the vulnerability component of the assessment.

In fact, the vulnerability component connected to heritage values (HV) has been investigated based on previous experience and reference to articles such as those by Lombardini and Scorza (2016), Osman (2022), Peña-Alonso et al. (2017), Tekken et al. (2017) and Ravankhah et al. (2021). The key issue is how heritage values or services can be considered within the risk assessment.

Heritage can be functionally considered as a means of reducing vulnerability. Sites such as the Neuwerk Tower and the defensive walls of Zadar can be considered for their authenticity, historical, and technological value, as well as their potential to provide shelter. Furthermore, they may attract tourists which bring revenue and financial means, therefore enhancing the area's resilience indirectly.

These values, however, don't necessarily stem only from built cultural heritage. To reflect this, a holistic approach to heritage values was applied. Specifically, this means that wherever possible, the assessment also incorporated heritage values relating to the natural environment and intangible aspects (Azzopardi et al., 2023).

This intrinsically links the concept of heritage value to that of ecosystem services (ES), another crucial element of resilience. Following the definition of the Millenium Ecosystem Assessment (2005), ecosystem services are linkages between ecosystems and human well-being. Based on Peng et al. (2024), an adapted framework for risk assessment was developed here which considers the capacity of ecosystem services to reduce disaster risk as part of the vulnerability component. This highlights the characteristics of ecosystem services as means to reduce susceptibility and simultaneously emphasises their potential for increased adaptive capacity. It furthermore serves to draw attention to vulnerability being a complex social-ecological concept.

Ecosystem services are typically clustered into four categories based on their function: **Provisioning** services are the products obtained from ecosystems and include for example food, water and timber. **Regulating** services are benefits obtained through the regulation of ecological processes like air quality, water and climate regulation. **Cultural** services provide nonmaterial benefits, among others recreation, spiritual enrichment and cognitive development. **Supporting** services are the base of all other ecosystem services and consist of processes such as soil formation, primary production and nutrient cycling (Millenium Ecosystem Assessment, 2005).

Since indicators reflecting ecosystem services might overlap with those of natural heritage values, indicators which are related to both heritage values as well as ecosystem services – such as recreational potential – were included only within the component of heritage values. The ecosystem service analysis on the other hand was limited to regulating ecosystem services. This highlights the ability of ecosystem services to influence and modulate disaster risk directly. For each hazard and R-Lab, an appropriate methodology was chosen to determine how ecosystem service interact with the hazards of coastal flooding, changing precipitation patterns, rising temperatures and landslides respectively.

In addition, the vulnerability assessment has considered other factors beyond ecosystem services and local heritage values. These factors included governance and institutional capacity, farm structure and labour, human capital and training, socio-demographic aspects, and sustainable and innovative practices, among others.

# 4 Methodological approach

## 4.1 General methodology

The general risk analysis methodology is summarized in the following steps (Figure 3). However, a detailed explanation of the specific methodology for each R-Lab is provided in the following sections.

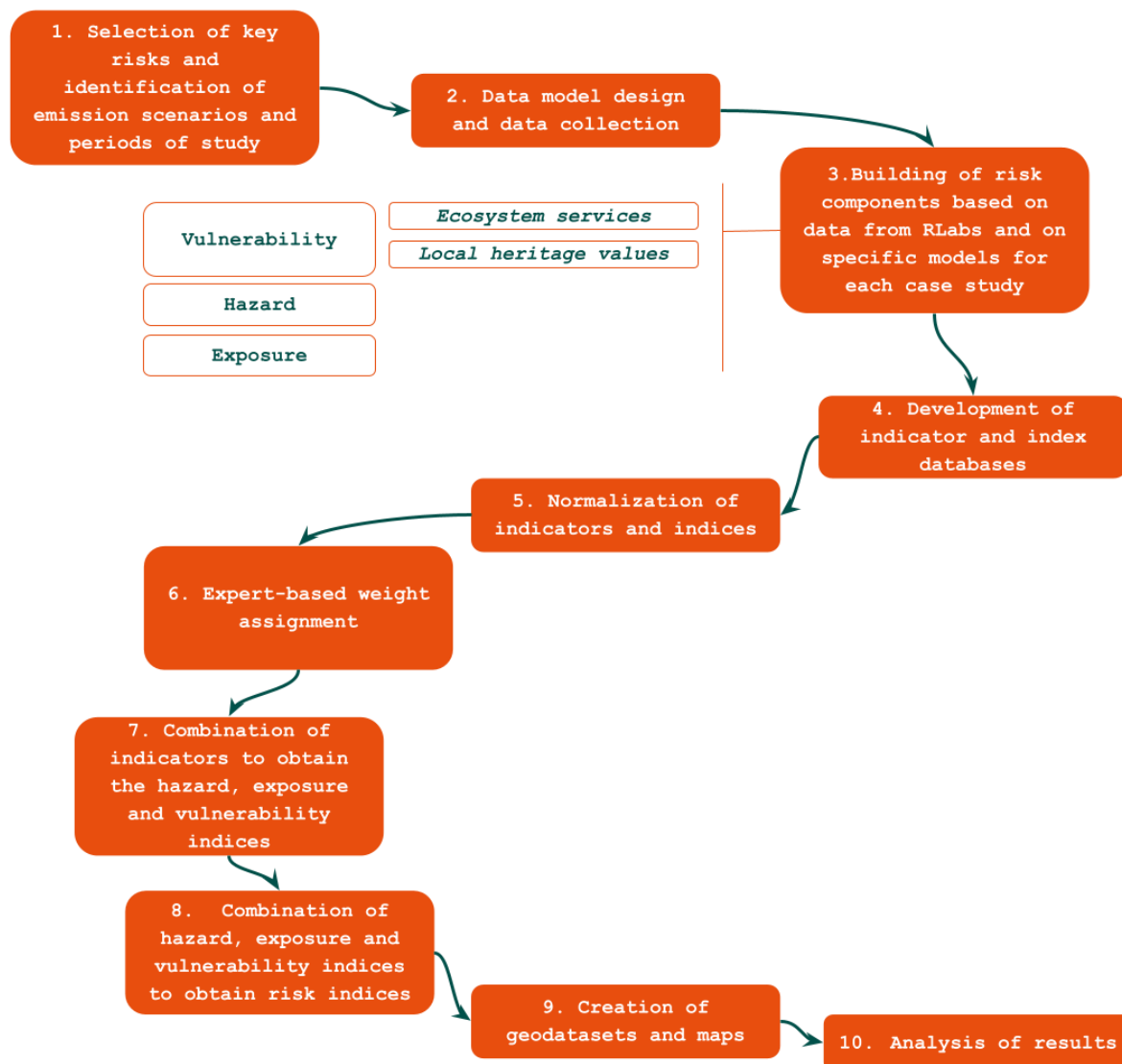


Figure 3. Methodological steps carried out for the analysis of risk in each case study.

## 4.1.1 Selection of key risks and identification of emission scenarios and periods of study

The selection of risks in each R-Lab followed a structured process combining existing knowledge with local expertise. As a starting point, impact chains developed in Task 4.2 (Wischott et al. 2024) were reviewed. Given their complexity, a prioritization exercise with stakeholders was carried out to refine the scope, identify key elements, and focus on primary impacts, ensuring alignment with project goals and comparability across cases.

An initial questionnaire assessed the feasibility of model development, followed by bilateral meetings with each R-Lab to solve uncertainties and finalise the models. These discussions focused on identifying major hazards, analysing exposed elements and vulnerabilities, and determining the appropriate spatial resolution and assessment detail—balancing data availability with analytical depth.

Building on these steps, the final selection of risks for each R-Lab was informed by:

- i) previously identified issues and potential impacts likely to intensify in the future.
- ii) local knowledge provided by technical staff from each R-Lab.

In addition, the selection of time periods and emission scenarios for each case was primarily guided by the availability of relevant data.

The selected risks, study periods, and emission scenarios for each R-Lab are summarized in Table 1.

*Table 1. Risks studied, study periods, and emission scenarios for R-Labs.*

R-Lab	Risk or vulnerability studied	Periods of study	Emission scenario
Neuwerk, Hamburg, Germany	Impacts of coastal floods on the buildings and agricultural lands on the island of Neuwerk	2013, 2050, 2100	RCP 8.5 <sup>1</sup>

<sup>1</sup> The reason for choosing the RCP8.5 scenario lies in the fact that it is currently the standard scenario used by coastal authorities and the coastal flood community, particularly in Germany, for the design and planning of coastal flood protection infrastructure. This also applies to the city of Hamburg and its coastal flood management. In contrast, RCP4.5 is rarely used for making representative or operationally relevant projections. To ensure consistency, this approach has also been applied to the Zadar R-Lab.

R-Lab	Risk or vulnerability studied	Periods of study	Emission scenario
Psiloritis Geopark, Crete, Greece	Impact of changes in precipitation patterns on culture	1980-2004, 2025-2049 and 2075-2099	RCP 4.5 and RCP 8.5
	Impact of changes in temperature on culture	1980-2004, 2025-2049 and 2075-2099	RCP 4.5 and RCP 8.5
Portovenere, Cinque Terre and the Islands, Italy	Impacts of landslides on the terraced landscape	1980-2004, 2021-2050, 2041-2070 and 2071-2100	RCP 4.5 and RCP 8.5
Defensive System of Zadar, Croatia	Impacts of coastal floods on cultural heritage buildings	2012, 2050, 2100	RCP 8.5
Historical Irrigation System at l'Horta de València, Spain	Impact of torrential rainfall on the agricultural heritage system	1971-2000, 2011-2040, 2041-2070 and 2071-2100	RCP 4.5 and RCP 8.5
	Impact of droughts on the agricultural heritage system		

### 4.1.2 Data model design and data collection

The selection of indicators used in the analysis of the various risks was based on their relevance, reliability, and suitability to the spatial scale of each R-Lab. These indicators are directly related to the risks being assessed, encompassing socio-ecological-technical systems, and related natural, build, social, human and financial capitals. At the same time, they are linked to one of the previously mentioned components of risk: hazard, exposure, or vulnerability.

The process began with the development of a proposed indicator system, informed by the agreed models and building on the Actionable Resilient Historic Landscape Framework (Gandini and Egusquiza, 2023) and the refined indicators from the ATLAS (Klose et al., 2024). A preliminary list was created for each R-Lab, considering the specific hazard and key elements prioritized. The R-Labs reviewed and refined this list based on data availability and contextual relevance, ensuring the final selection reflected the most significant aspects of their landscapes.

For certain indicators where data are available at the required scale (for example, at the cadastral parcel level in the case of Neuwerk), only the identification, collection, and compilation of data were necessary. However, in cases where data were not readily available

at the specific scale of analysis for the R-Lab, additional processing was performed using GIS tools to adapt the data accordingly.

For this type of indicators, a weighted average was calculated based on the proportion of the spatial unit covered by each cell value, in order to assign the most accurate information possible given the scale at which the climatic variables are available.

The data model for each R-Lab is detailed in their respective methodological sections. Additionally, the complete data model for each R-Lab can be found in Annex 1.

### 4.1.3 Building of risk components based on data from R-Labs and on specific models for each case study

While the methodology for calculating each component and subcomponent of risk is developed in the dedicated sections for each R-Lab – including the integration approach for indicators and the criteria applied for their selection – it is pertinent at this stage to highlight the general evaluations carried out across the various R-Labs (see Table 2).

In the case of Neuwerk, vulnerability was assessed based on an analysis of heritage values, ecosystem services, and other relevant indicators. The hazard was simulated for three temporal scenarios: a historical baseline, a projection for 2050, and a projection for 2100. However, the presence of a protective dyke on the island reduced the hazard to zero in the first two scenarios, meaning that the risk assessment was only technically meaningful under the most pessimistic scenario (2100).

A similar situation was observed in Zadar, where, across all scenarios (historical, 2050, and 2100), wave action was estimated to affect no more than 3 % of the built environment. As a result, a risk assessment was not technically justified, and the analysis focused exclusively on climate change vulnerability.

For Psiloritis, L'Horta de València, and Portovenere, Cinque Terre and the Islands, a comprehensive evaluation was conducted, incorporating ecosystem services, cultural heritage values, and additional indicators aimed at approximating vulnerability. Furthermore, exposure, hazard, and risk were analysed according to the temporal and emissions scenarios defined in Table 2.

Table 2. Components assessed in each R-Lab

R-Lab	Vulnerability			Exposure	Hazard	Risk
	Ecosystem services assessment	Local heritage value assessment	Other indicators			
Island of Neuwerk in Hamburg	x	x	x	x	x	x
Psiloritis Geopark	x	x	x	x	x	x
Portovenere, Cinque Terre and the Islands	x	x	x	x	x	x
Defensive system of Zadar		x		x	x	
L'Horta, València	x	x	x	x	x	x

#### 4.1.4 Development of indicator and index databases

The focus of this stage was the development of a tabular indicator database. For each spatial unit, the table contains all the relevant indicator values relating to the specific risks being studied. The table contains as many rows as spatial units exist within each R-Lab, and as many columns as indicators have been compiled or obtained for the set of key risks. In this stage, the polarity of each indicator is defined. A positive polarity indicates that an increase in the indicator leads to an increase in risk, while a negative polarity indicates that a decrease in the indicator leads to an increase in risk.

Since the results must be suitable for spatial representation, each row includes a column with a unique identifier code that distinguishes each territorial unit.

#### 4.1.5 Normalization of indicators and indices

As the indicators used in the vulnerability analysis were expressed in different units of measurement, it was necessary to standardise their scales using a normalisation process. This step enables values from a variety of different metrics and scales to be integrated and apply weightings to them (OECD, 2008; Kuhn, Wickham & Hvitfeldt, 2025; Pedregosa et al., 2011).

To facilitate data aggregation, the normalization was performed so that the minimum value in the distribution corresponds to 1 and the maximum value to 2. The formula used for this process is as follows:

$$v = \frac{x - \min(x)}{\max(x) - \min(x)} + 1$$

Where  $v$  denotes the normalized value, and  $x$  represents the set of observed values for the indicator under analysis

## 4.1.6 Expert-based weight assignment

To incorporate local knowledge into the risk analysis, weights assigned by technical staff (OECD, 2008; Greco et al., 2019) from each of the R-Labs (hereafter referred to as expert-based weighting) were considered. These weights were applied to both exposure and vulnerability indicators (hazard typically consists of only one indicator, except in a single case where equal weights were assigned to both indicators) as well as to the overall risk components.

In this context, each R-Lab weighted the vulnerability indicators by assigning a conversion factor to each, ensuring that the sum of all assigned weights equals 1. The same procedure was applied to exposure indicators and to the three components of risk. It should be noted that each R-Lab conducted the expert-based weighting exercise using an independent approach. In each R-Lab, the number of experts involved varied, and each conducted an individual scoring process. However, all R-Labs shared certain common criteria.

For the risk components, experts agreed that vulnerability should be assigned a higher weight, as it encompasses both ecosystem services and cultural heritage, and represents the component most susceptible to improvement through human intervention. Regarding exposure, it was argued that a greater presence of people, infrastructure or assets (as applicable in each R-Lab) increases the level of risk, even when these exposed units are relatively well-prepared. Therefore, exposure was also generally assigned a high weight. In contrast, hazard was typically given a lower weight, based on the argument that the hazards identified had not demonstrated substantial impacts in the observed context. As for the indicators, the weights assigned by experts were justified based on their direct influence on risk. Particular emphasis was placed on indicators related to the vulnerability of cultural heritage and ecosystem services, which were considered more relevant than others. In all cases, the ecosystem services index received a high weight within the vulnerability component, as it was regarded as a key factor in providing natural protection against hazards.

## 4.1.7 Combination of indicators to obtain the hazard, exposure and vulnerability indices

The calculations of the relative exposure (E) and vulnerability (V) indices were carried out using processes analogous to those proposed in other methodologies in which the different risk components are integrated (Tapia et al, 2017; ESPON, 2022; Navarro et al., 2023). Their calculations were performed using the following formulas:

$$E = \sum_{j=1}^n w_j \cdot I_j$$

Where  $w_j$  is the weight assigned by the experts to the indicator;  $I_j$  is the value of indicator  $j$ ; and  $n$  is the total number of indicators considered.

$$V = \sum_{i=1}^n w_i \cdot I_i$$

Where  $w_i$  is the weight assigned by the experts to the indicator;  $I_i$  is the value of indicator  $i$ ; and  $n$  is the total number of indicators considered.

In the case of the hazard component, being a single variable or at most two variables, a similar formula was not applied, but the weight was attributed equally, i.e. 1 in the case of only one variable or 0.5 in the case of two variables.

To facilitate the interpretation and discussion of the results in this study, the values of each relative index were grouped into five classes using quantiles as classification method: “Higher,” “Medium-High,” “Medium,” “Medium-Low,” and “Lower.”

## 4.1.8 Combination of hazard, exposure and vulnerability indices to obtain risk indices

Subsequently, the composite relative risk indices for each spatial unit were calculated based on the relative indices of hazard, exposure, and vulnerability associated with each risk (ESPON, 2022; Klose et al., 2024). The following formula was used:

$$R = H^{1/wh} \cdot E^{1/we} \cdot V^{1/wv}$$

Where  $R$  represents the relative risk for a given spatial unit;  $H$ ,  $E$ , and  $V$  are the relative indices of hazard, exposure, and vulnerability, respectively, for the same spatial unit; and  $w_h$ ,  $w_e$  and  $w_v$  are the weights assigned by the experts to the hazard, exposure and vulnerability components, respectively.

In line with the previous section and to facilitate interpretation and discussion of the results in this study, the values of the relative risk indices were also grouped into five classes using quantiles as classification method: Higher, “Medium-High,” “Medium,” “Medium-Low,” and Lower.

## 4.1.9 Creation of Geo datasets and maps

The indicators used for the analysis of each key risk, along with their original values prior to normalization, were geographically linked to the GIS layer of each R-Lab using the unique spatial unit code. This way a new vector file in standard GeoPackage format was generated for each of the key risks. Each GeoPackage includes several layers corresponding to the scenarios analyzed within each case study. The contents of these vector files can be accessed using standard GIS applications.

Similarly, for each risk within each R-Lab, an additional vector file – also in GeoPackage format – was created, containing the relative risk values and their corresponding risk components, all normalized to a value range between 1 and 2. Besides, for each risk component, as well as for the overall risk, fields were added indicating the corresponding classes

A collection of risk maps was also produced based on these files, corresponding to the climate change scenarios considered for each of the risks analysed.

It should be noted at this point that the steps “*Combination of indicators to obtain the hazard, exposure, and vulnerability indices*,” “*Combination of hazard, exposure, and vulnerability indices to obtain risk indices*,” and “*Creation of geo datasets and maps*” (sections 4.1.7, 4.1.8 and 4.1.9, respectively) were carried out using the SIRVA<sup>2</sup> software, developed by Tecnia, which enables the assessment of climate change risk based on territory-related indicators.

---

<sup>2</sup> Register TX 9-116-358 (Scalable Integrated Risk and Vulnerability Assessment Tool for Climate Change Adaptation)

## 4.1.10 Analysis of results

Finally, an analysis and interpretation of the results were conducted, aiming to explore the relationships between the risk indices of the spatial units and the values of the indicators. This was done to understand which factors have the greatest influence or best explain the observed differences between the territorial units.

Additionally, where more than one scenario was considered in a R-Lab, a comparative analysis of the risk indices was carried out to assess how the results varied under different conditions. This approach highlighted patterns within each case study and identified specific differences across analysed areas. This not only facilitates the interpretation of the maps, but also enhances the understanding of spatial dynamics, contributing to more informed decision-making and supporting territorial management efforts.

## 4.2 Island of Neuwerk in Hamburg

The analysis of the **impact of coastal flooding on the buildings and agricultural land on the island of Neuwerk** was carried out at the cadastral parcel scale and is limited to the area protected by the ring dyke system (i.e., salt marshes and areas outside the ring dyke were excluded).

The hazard was simulated based on a storm event in 2013, and projections were made for two future scenarios under RCP 8.5: one for the year 2050 (assuming an average sea level rise of 0.3 meters) and another for 2100 (with an assumed rise of 1 meter). However, in both the baseline and the 2050 scenario, the island's protective dyke system prevents projected coastal flooding/storm surges from flooding the area behind the dyke. Therefore, the risk analysis has been conducted for the 2100 scenario only.

### 4.2.1 Hazard

For the hazard assessment, a hydrodynamic numerical modelling approach has been adopted to characterise and quantify the hazard due to coastal floods and storm surges, the island is exposed to. A series of focused meetings and discussions with the R-Lab partners preceded the final decision on the type and the scale of the approach, building upon the previous studies and experience available in the area such as the Project TideelbeKlima (Fröhle et., al, 2022).

The adopted approach for the hazard assessment included the following steps:

- (1) Data Survey and analysis
- (2) Model set up

- (3) Model calibration and run
- (4) Hazard assessment considering the climate scenarios

A comprehensive data survey was conducted to verify the accuracy and relevance of existing datasets and to update them where necessary (1). The update primarily included the incorporation of a new Digital Terrain Model (DTM) provided by LGV (2022), a re-evaluation of potential design storms for modelling, and the integration of relevant climate scenarios, including projections of sea level rise (SLR).

Subsequently, a 2D hydrodynamic model was set up using the TELEMAC modelling platform (2). To support the spatial resolution and scope required for the RescueME risk assessment, the existing North Sea hydrodynamic model, originally developed by TUHH, was adapted and refined. The model mesh was enhanced with triangular elements of 30 x 30 meters to capture detailed topographic and hydraulic features, including flood protection infrastructure. This refinement ensures that the influence of such structures on flood dynamics and hazard propagation on the island is adequately represented in the simulations.

The developed and deployed model is illustrated with an example in Figure 4.

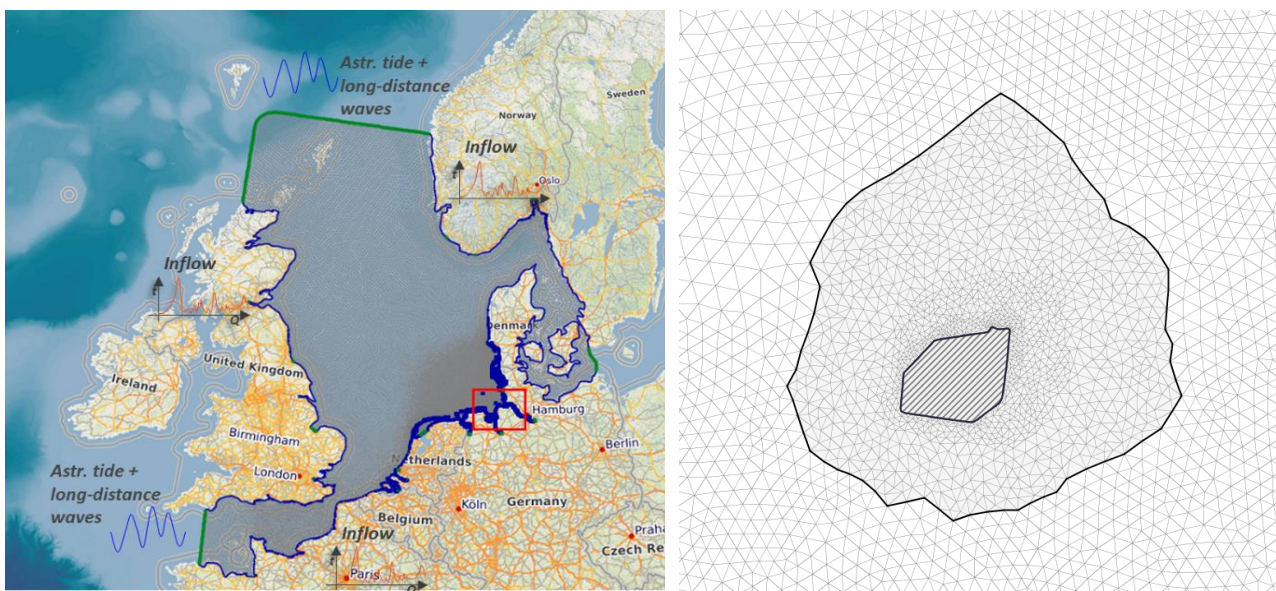


Figure 4. Hazard modelling of the Hamburg-Neuwerk; left: The calibrated North Sea Model indicating the R-Lab area (using the 2D model TELEMAC; right: The refined 2D mesh in the R-Lab)

For the calibration of the hydrodynamic model, the storm of 2013 was adopted as a baseline (3). For the adopted Representative Concentration Pathway RCP 8.5, the future scenarios of the water level were generated as an uplift of the water level time series of the baseline

scenario deploying results of the IPCC AR6 (IPCC, 2023) implemented in the NASA Sea Level Projection Tool (NASA, n.d.) as follows:

- 2050 (assuming an average SLR of 0.3 m)
- 2100 (assuming an average SLR of 1.0 m)

The derived scenarios considering the impact of the SLR on the model storm are presented in Figure 5. It should be noted that water levels below 0 m are not included in the analysis. This is due to limitations of the Neuwerk water level gauge, which does not register values below this threshold owing to its installation height and technical configuration.

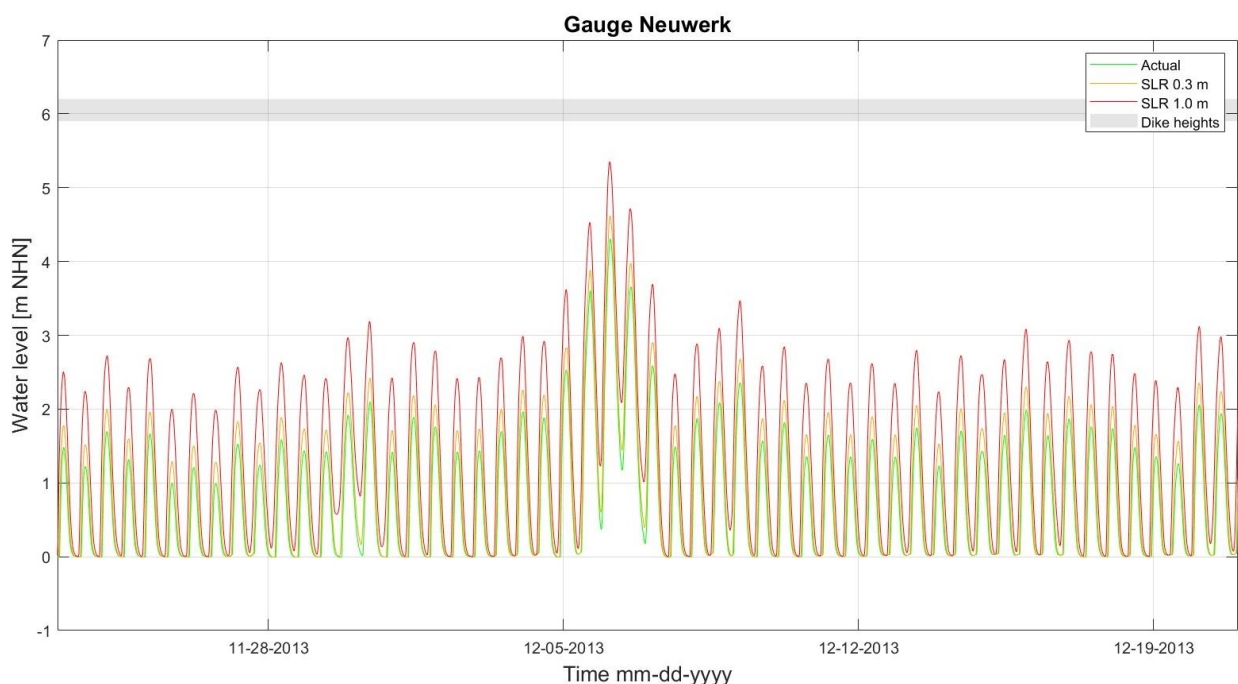


Figure 5. Model storm of 2013 considering the influence of the SLR (green: Reference scenario; yellow: SLR 0.3 m; red: SLR 1.0 m)

In addition to the water level, the wave propagation has been considered using a TOMAWAC model, originally developed by TUHH, delivering the information about the wave direction, wave height and peak period (for the corresponding storm event). These results were further processed to assess the wave run-up ( $R_{u2\%}$ ) and overtopping, using the EurOTop 2018 manual:

- 1) Considering the maximum water level of each storm event calculated
- 2) Adding value of  $R_{u2\%}$  (wave run-up exceeded by 2 % of waves) calculated after EurOTop 2018 as given in Equation 1.

$$\frac{R_{u2\%}}{Hm0} = 1.75 * \gamma_b * \gamma_f * \gamma_\beta * \xi_{m-1.0} \text{ Equation 1}$$

Where:

$H_{m0}$  = significant wave height (m)

$\gamma_b$  = berm influence factor (-)

$\gamma_f$  = roughness influence factor of the dike cover (-)

$\gamma_\beta$  = influence factor for oblique wave attack (-)

$\xi_{m-1.0}$  = wave breaking parameter (-)

- 3) Estimating the wave overtopping discharges into the inward area following the Equation 2:

$$\frac{q}{\sqrt{g \cdot H_{m0}^3}} = \frac{0.026}{\sqrt{\tan \alpha}} * \gamma_b * \xi_{m-1.0} * \exp\left[-\left(2,5 \frac{R_c}{\xi_{m-1.0} * H_{m0} * \gamma_b * \gamma_f * \gamma_\beta * \gamma_v}\right)^{1.3}\right] \text{ Equation 2}$$

Where:

$g$  = gravity (m/s<sup>2</sup>)

$\alpha$  = average slope angle of the dyke (-)

$\gamma_v$  = influence factor for a wall at the end of a slope (-)

$R_c$  = Freeboard of the dike (m)

The results of this analysis are presented in Figure 6 and Figure 7.

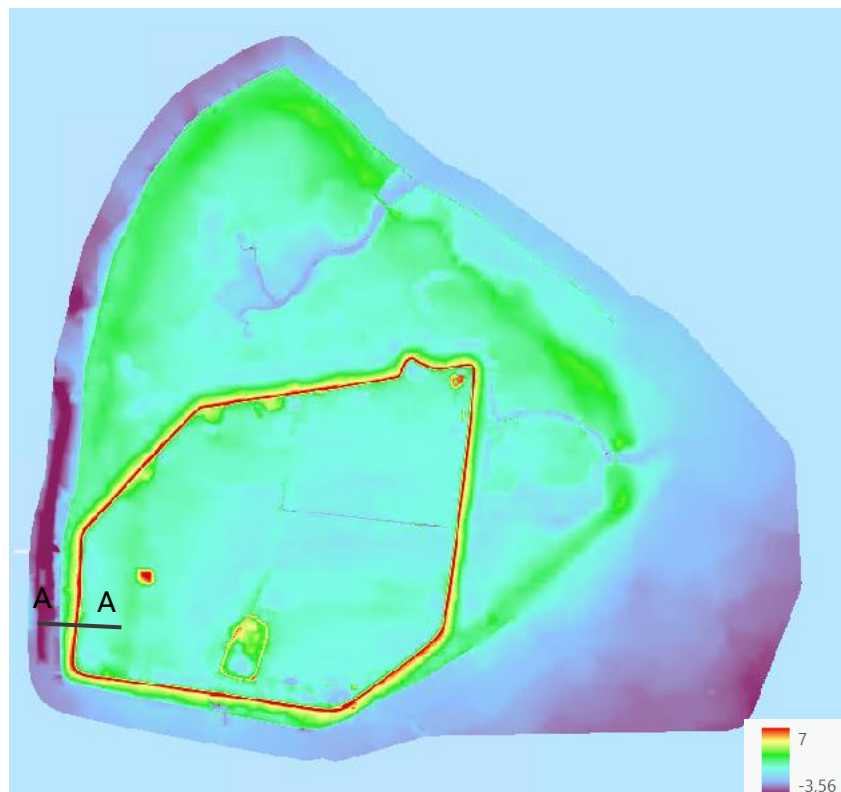


Figure 6. Heights (m) of the Digital Terrain Model (LGV 2022) of the island of Neuwerk with a raster of 1 m x 1 m. The indicated cross-section A-A is presented in Figure 7.

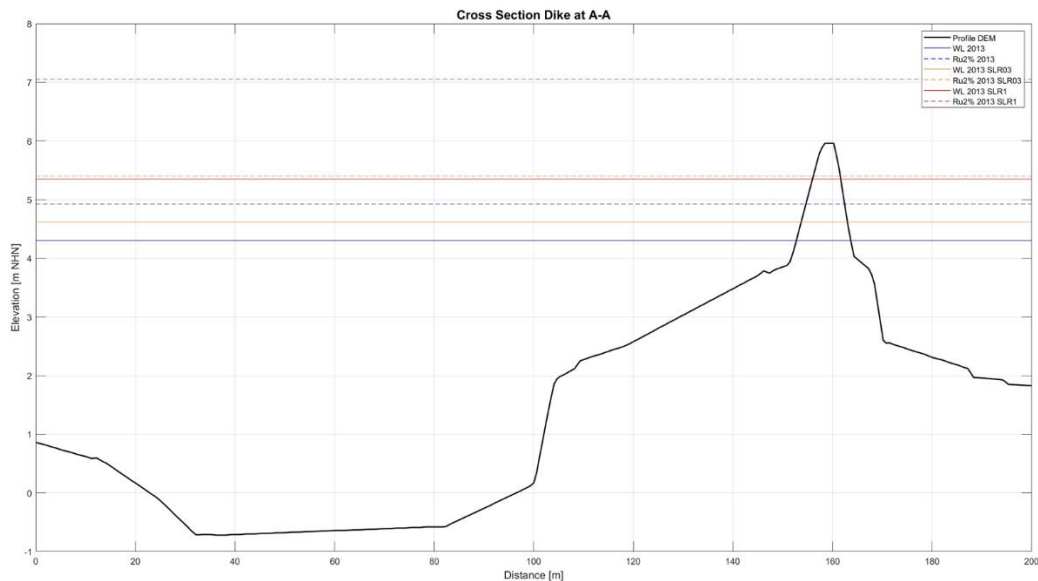


Figure 7. The water levels for the reference storm and the projected storm including the scenario with the wave run up (Ru2%) here presented for the cross-section A-A ; blue: water level for the storm 2013; dash blue line: water level for the storm 2013 + Ru2%; yellow: water level for the scenario SLR 0.3 m; dash yellow line: water level for the scenario SLR 0.3 m and Ru2%; red: water level for the scenario SLR 1.0 m; red dash: water level for the scenario SLR 1.0 m and Ru2%

### Results and limitations of the model

The final output of the hydraulic model consists of water level raster data representing both the baseline (design/model storm) conditions and future scenarios incorporating sea level rise (SLR) estimates for the defined cadastre units as relevant the risk assessment.

Modelling results suggest that the existing flood protection infrastructure is adequate to provide protection for the island under both, the baseline scenario and the 2050 scenario. In these cases, the projected storm surge does not reach inland parcels.

However, under the RCP 8.5 scenario and the 2100-time horizon, which includes an assumed SLR of 1 m, the model indicates that dike overtopping takes place. Figure 8 illustrates this scenario, in which overtopping is intensified by the inclusion of a 2% exceedance wave run-up (Ru2%) based on EurOtop (2018) guidelines. This results in significant flooding of the inland area. Under these high hydrodynamic conditions, the water level inside the dike is given to be equal to that on the seaward side.

It is important to note that the estimation of wave run-up and overtopping using the EurOtop (2018) method is only indicative in this context. However, it provides a level of accuracy that is deemed sufficient for the scope and objectives of this study.

The final output of the hazard assessment, the water depth raster, was calculated as the difference between the simulated water surface levels and the corresponding Digital Terrain Model (DTM), using a raster resolution of 1 meter. To account for worst-case flood conditions,

maximum water depths were extracted for each cadastral unit. These are presented in Figure 8.

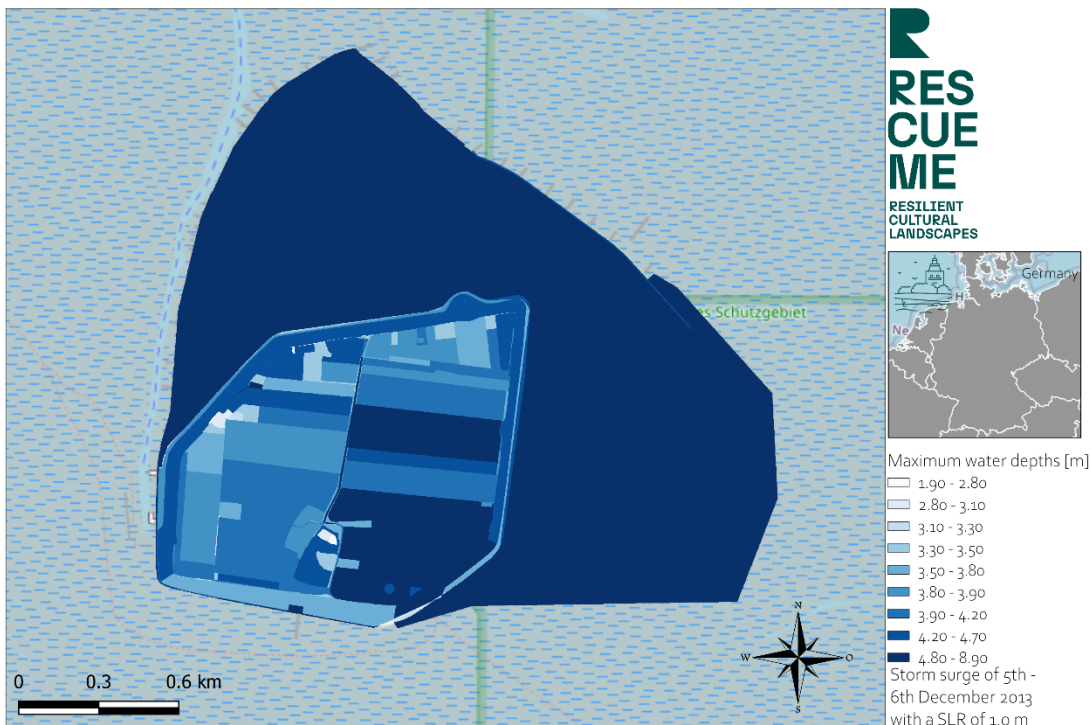


Figure 8. The modelling results/ water depths [m] for Neuwerk taking the storm event of 2013 as a reference and considering SLR of 1.0 m RCP 8.5 and RU2%; Time horizon 2100.

The approach implies the deployment of a high-resolution hydrodynamic model, which has already been tested and used in various projects for different areas in the North Sea region (e.g. for the Elbe Estuary as given in Fröhle, et al, 2022). The required data were mostly readily available, allowing a detailed analysis of the hazard situation in the area.

While the development and calibration of high-resolution hydrodynamic models involve considerable effort, this factor has to be carefully considered when upscaling the methodology to other regions. The process requires significant data availability, technical expertise, and computational resources. Nevertheless, despite the complexity and resources demands, the use of such models is strongly recommended. Their ability to simulate the physics of the processes and the interactions between water levels, terrain, and flood protection infrastructure provides a level of detail and accuracy that is essential for robust flood hazard and risk assessment.

## 4.2.2 Exposure

As previously mentioned, the model prioritizes built, financial, and social capital as the primary dimensions of exposure. Built and financial capitals encompass structures such as properties, agricultural holdings, and tourism facilities, including bed spaces. Social capital is considered by assessing the potential impact on the resident population. The following indicators showed in Table 3 were used to quantify exposure, along with the weights assigned by the R-Lab.

*Table 3. Indicators employed in the assessment of exposure on Neuwerk Island (Hamburg), along with their corresponding weights.*

Capital	Name of indicator	Unit	Weight
Social	Population	Number	0.3
Financial	Bed places	Number	0.2
Financial	Number of agricultural holdings	Number	0.1
Financial	Tourist accommodation establishments	Number	0.15
Built	Owned houses with summer use only	Number	0.1
Built	Number of properties	Number	0.15

## 4.2.3 Vulnerability

The heritage value assessment followed four general steps as outlined in the following section:

### Indicator selection

A list of indicators has been composed to collect relevant data on the vulnerability of local heritage values regarding coastal floods based on the ATLAS (Klose et al. 2024), expert opinions and local knowledge from the R-Lab stakeholders.

### Assessment of polarity and normalization

Afterwards, the indicators were assigned to a specific risk component, namely sensitivity or adaptive capacity, in order to clarify then its relationship within the whole risk analysis. A positive polarity reflects a positive relation, meaning the indicator will increase the vulnerability, while a negative polarity reflects a negative relation, meaning the indicator will decrease the vulnerability<sup>3</sup>. The indicator values were normalised accordingly using the min-max method and rescaled to a range between 1 and 2.

---

<sup>3</sup> It should be noted at this point that a positive polarity does not always correspond to sensitivity, and a negative polarity does not always correspond to adaptive capacity.

### Weighting indicators

In order to be aggregated into composite indices, the indicators should reflect different levels of contribution to the overall risk. In this phase individual weights were assigned to each indicator, considering local conditions and the hazard in question. Several methods could be adopted for assigning weights, based on statistical analysis, expert judgement or local stakeholders' consultations, budget allocation or decision-making processes, as well as existing literature-based approaches (Kabir et al., 2019; Kappes et al., 2012). However, according to Papathoma-Köhle et al. (2019), no established methodology currently exists on how to select the most appropriate weighting scheme, and it represents a highly sensitive step in computing composite risk indices.

Here, this step was conducted through an expert consultation process. In line with the aim of creating a robust multi-perspective risk assessment methodology, this allowed for the inclusion of additional knowledge aside from the local stakeholders already involved in the risk assessment. In total, seven experts from the fields of spatial planning, cultural heritage management and environmental science were asked to fill out a questionnaire: based on the indicator, its unit, the hazard and the location, each indicator received a value between 1 and 5 highlighting its relevance for the risk assessment. The final weights were computed using the averages of the individual expert assignments and converting them to a scale of 0 to 1 with all indicator weights, adding up to a sum of 1.

### Heritage value assessment

Based on the previous steps, the heritage value index was computed as follows:

$$V_{HV} = \sum_{i=1}^n w_i \cdot I_i \text{ where } \sum_{i=1}^n w_i = 1$$

Where:

$w$  is the weight associated to each indicator.

$I$  represents the normalized value of each indicator, selected as relevant for HV.

$n$  is the total number of indicators to consider.

The indicators and their respective weights can be found in Table 4.

Table 4. List of indicators used for HV assessment of Neuwerk.

Risk Element	Capital	Name of indicator	Unit	Polarity	Weight
Adaptive capacity	Built	Number of cultural facilities open to the public and aiming at promoting arts and culture per population	Number/ha	Negative	0.29

Risk Element	Capital	Name of indicator	Unit	Polarity	Weight
	Natural	Area with outdoor recreation potential	% of area	Negative	0.27
	Social	Cultural vibrancy - number of cultural sites exposed to coastal floods	Number/ha	Negative	0.44

### Ecosystem services assessment

A similar approach to the heritage value assessment was applied to the assessment of ecosystem services (ES). The indicator selection, polarity determination and weighting were conducted analogously. Overall, the ES index was computed as follows:

$$V_{ES} = \sum_{i=1}^n w_i \cdot I_i \text{ where } \sum_{i=1}^n w_i = 1$$

Where:

$w$  is the weight associated to each indicator.

$I$  represent the normalized value of each indicator, selected as relevant for ES.

$n$  is the total number of indicators to consider.

As previously described, this assessment focussed on the direct effects of regulating ES as defined by the Millenium Ecosystem Assessment Report (2005). In the case of coastal flooding hazards, this may include the coast stabilisation and runoff retention among others. Due to its small size and low data availability, these ES could not be directly assessed but instead were estimated with land use categories. The expected association between land use and ecosystem service characteristics and scale was approximated by assigning different weights to each land use class present on the island. This represents a simplified approach of respective models such as those of the suite of software tools called InVEST® which aim to value ecosystem services through land use class-based properties and calculations (Natural Capital Project, 2023).

The three land use classes that functioned as indicators for the formation of the ES index can be found in Table 5.

Table 5. List of indicators used for ES assessment of Neuwerk.

Risk Element	Capital	Name of indicator	Unit	Polarity	Weight
Adaptive capacity	Natural	Share of agricultural land	% of area	Negative	0.29
	Natural	Share of forest land	% of area	Negative	0.38

Risk Element	Capital	Name of indicator	Unit	Polarity	Weight
	Natural	Share of natural land+water	% of area	Negative	0.33

### Vulnerability assessment: Indicator and vulnerability indices aggregation

As previously mentioned, both HV and ES indices were aggregated with other indicators (Table 6) into the vulnerability index for Neuwerk Island. The indicators and the weights assigned to each are presented below.

Table 6. Indicators and indices used in the vulnerability assessment of Neuwerk Island (Hamburg), along with their corresponding weights.

Capital	Name of indicator	Unit	Risk component	Polarity	Weight
Natural	ES index	Dimensionless	All the indicators that make up the index belong to the adaptive capacity dimension.	Positive <sup>4</sup>	0,45
Natural, built, social	HV index	Dimensionless	All the indicators that make up the index belong to the adaptive capacity dimension.	Positive <sup>5</sup>	0,15

<sup>4</sup> Clarification: the calculation of the ES index has been carried out in such a way that higher ES index values reflect higher risk. Therefore, the ES index can be interpreted as an indicator of the lack of ecosystem regulatory services. This applies to the ES indices across all R-Labs.

<sup>5</sup> Similarly, the HV index has been estimated under the assumption that higher values represent greater vulnerability of cultural heritage. Consequently, in all HV indices across the R-Labs, higher HV values indicate increased risk.

Capital	Name of indicator	Unit	Risk component	Polarity	Weight
Built	Households with access to the internet at home	Percentage of total	Adaptive capacity	Negative	0,1
Built	Emergency operators	Percentage of total	Adaptive capacity	Negative	0,3

### 4.2.4 Risk assessment

Finally, the risk index was constructed by integrating the exposure, hazard and vulnerability indices (see formula in Section 4.8. Combination of hazard, exposure and vulnerability indices to obtain risk indices). The weights were established following specific consultation with the R-Lab, and the resulting weightings are shown in Table 7.

Table 7. Risk components' weights on Neuwerk Island (Hamburg).

Risk component	Weight
Vulnerability	0.4
Exposure	0.4
Hazard	0.2

## 4.3 Psiloritis Geopark

In the Psiloritis Geopark, two main risks have been identified and analysed: **Impact of changes in precipitation patterns on culture**, and **impact of changes in temperature on culture**.

Both risks were assessed at the community level within the municipalities of Mylopotamos and Rethymno in the Geopark. Communities were chosen as the unit of analysis to allow for greater spatial heterogeneity. However, it should be noted that some indicators were only available at the municipal scale.

Each risk was evaluated under different scenarios. For the impact of changes in precipitation patterns, both RCP 4.5 and RCP 8.5 were considered, as well as three temporal horizons: 1980–2004 (historical scenario), 2025–2049 (near future), and 2075–2099 (far future).

In contrast, for the temperature-related risk, although both RCP scenarios were also analysed, the lack of spatial variability in projected values for the far future across the geopark made it technically unfeasible to conduct a meaningful comparison between spatial units. Consequently, risk calculation in this case were not technically justified.

### 4.3.1 Hazard

In the Psiloritis UNESCO Global Geopark, the shifting temperature and precipitation patterns have been analysed and assessed. The developed approach has been applied to:

- (1) Source the existing data, models and results available to date by screening the public data repositories, reports, publications and websites.
- (2) Select the most appropriate set of data and models and enhance them, if required.
- (3) Apply the selected data and models to the proposed scenarios.

After screening and evaluating the available data and resources (1), the method and scenarios proposed by Politi et al, (2023) were adopted for further processing, providing a resolution of 5 km grid spacing and a 6-hour interval (2). This approach involves deriving high-resolution projections of extreme temperatures and precipitation in Greece using the Weather Research and Forecasting (WRF) model. High-resolution data could be obtained for the historical period (1980–2004) and the near (2025–2049) and far (2075–2099) futures, assuming RCP 4.5 and 8.5. The historical simulation was evaluated against available station observations.

For the purposes of this study, only the processed maps were available and used; access to the corresponding raw data was not provided. The maps that have been used for the statistical analysis are given in Figure 9 and Figure 10.

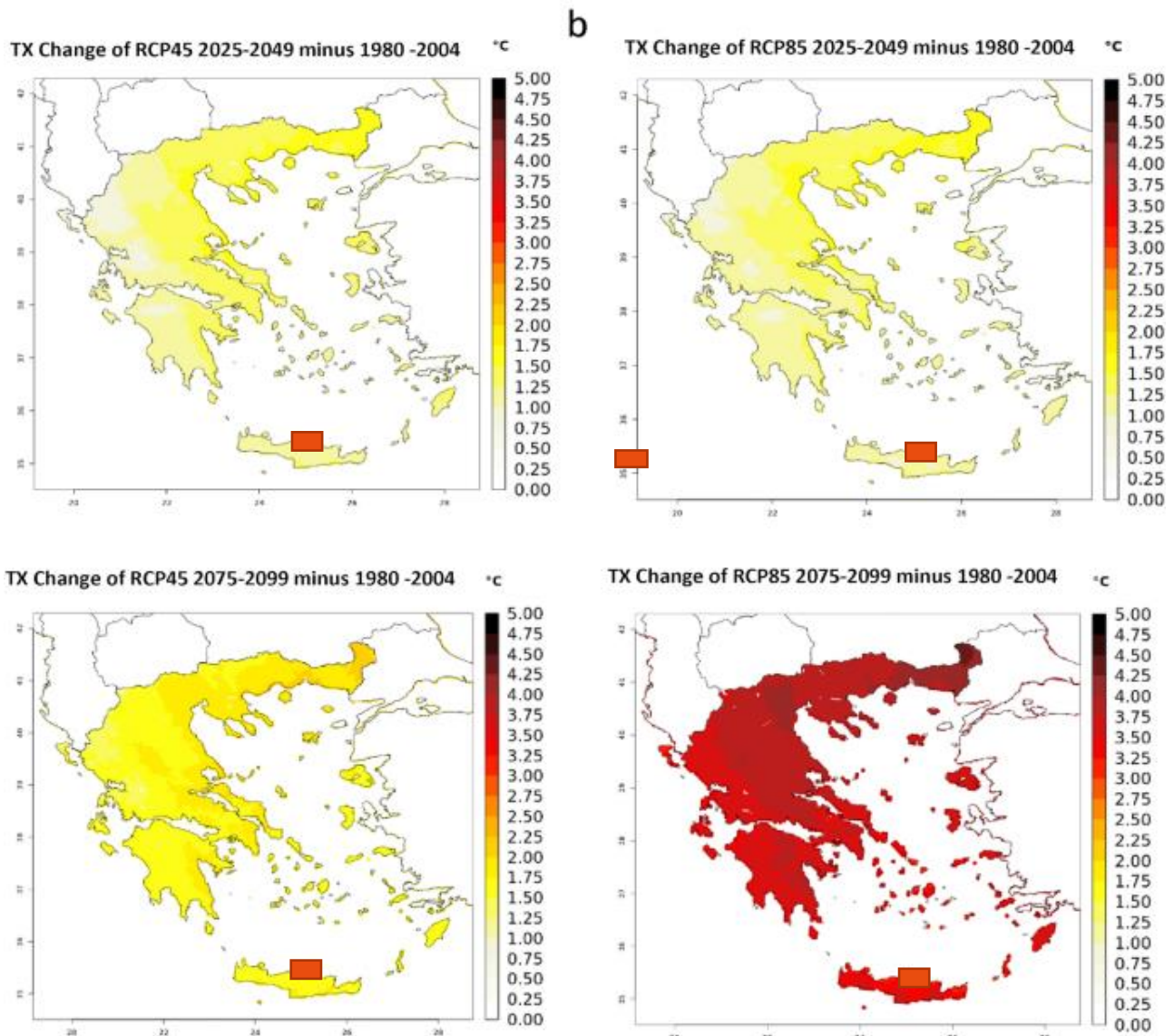


Figure 9. WRFEC climate change differences for daily maximum temperature (2025–2049 minus 1980–2004 and 2075–2099 minus 1980–2004) for RCP 4.5 and RCP 8.5. (Areas with no dots specify statistically significant changes using a Student’s t-test at the 95 % confidence level) (taken from Politi et., al.) (red rectangular indicates the study area).

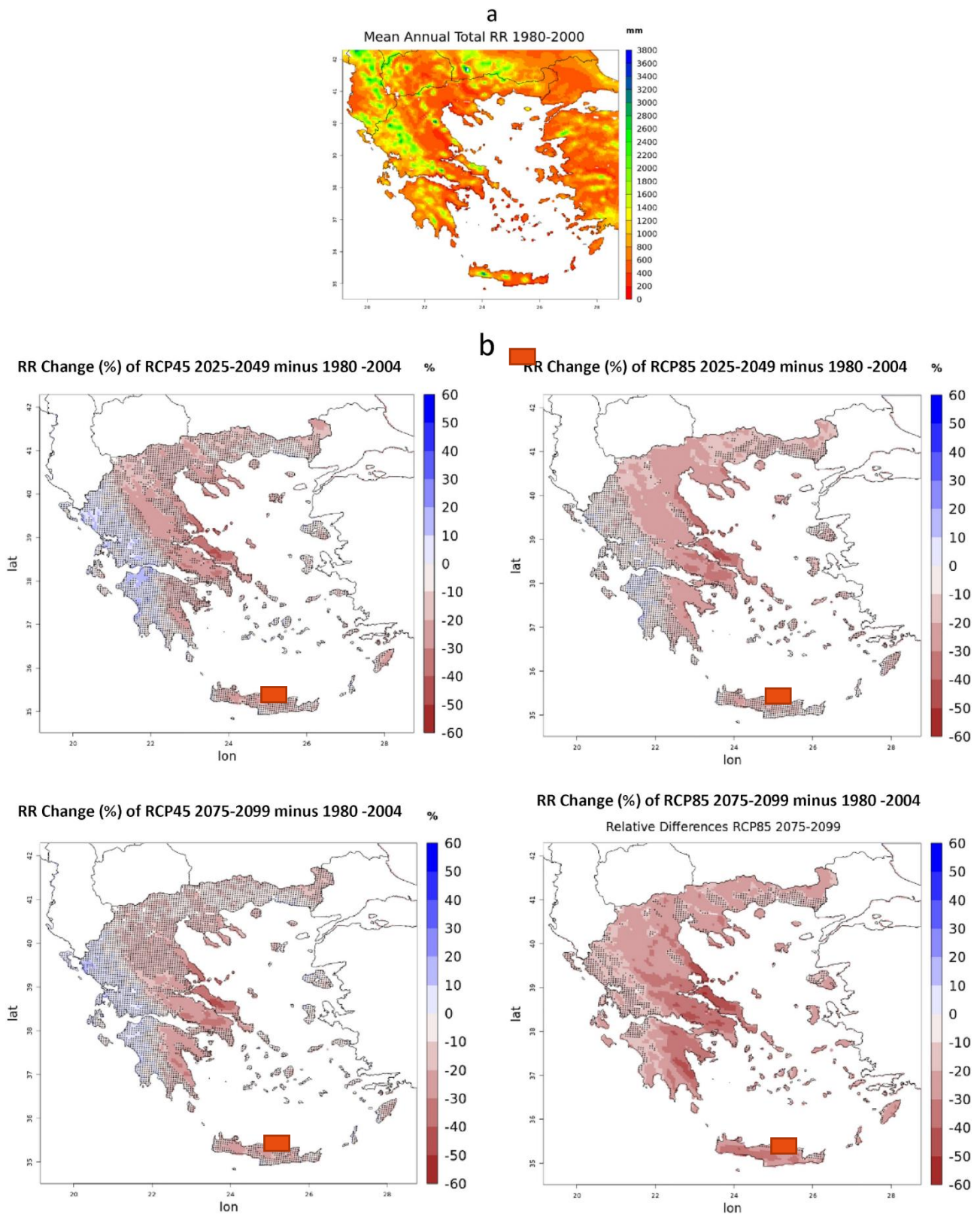


Figure 10 **a** WRFEC mean historical climatology, **b** annual mean precipitation relative changes given by WRFEC for RCP 4.5 and RCP 8.5 (2075–2099 minus 1980–2004)/1980–2004. (Areas with dots specify changes not statistically significant using a student's *t* test at the 95 % confidence level) (taken from Politi *et. al.* 2023) (red rectangular indicates the study area).

In step 3, the set of indicators that has been finally adopted for the hazard assessment is presented in Table 8.

*Table 8. The indicators describing the changes in temperature and precipitation patterns used in the Psiloritis R-Lab. In addition to the indicators provided in the study of Politi et., al (2023), the observed data for the max daily temperatures have been considered.*

Name of indicator	Unit
Maximum temperature (based on the daily values taken from the observation stations)	[°C]
Mean annual precipitation	[mm]

For those indicators/variables the projected changes in relation to the reference period 1980-2002 for RCP 4.5 and RCP 8.5 and time horizons 2025-2049 and 2075-2099 were evaluated.

In addition to the maps and modelling results of Politi et al (2023), the data from the observations stations available at the platform of the Greek Water Authority on the max daily temperature for the reference period have been collected (Figure 11). They were cross-checked with the historical datasets available at the MeteoBlue.

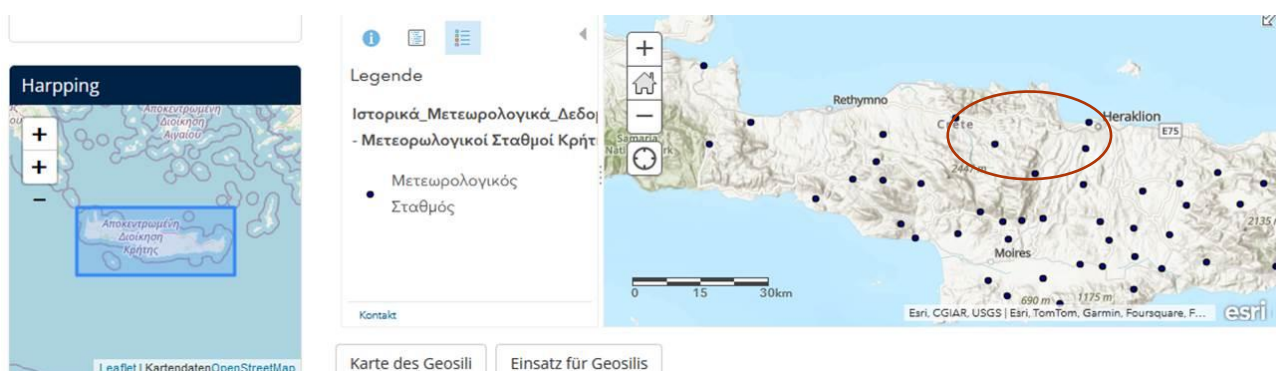


*Figure 11. The map indicating the measuring stations on the island of Crete (Source: Greek Water Authority)*

Finally, the changes in temperature and precipitation patterns have been derived for the spatial units -municipalities, by weighting the values for the indicators from the temperature and precipitation raster for each municipality.

### *Results and limitations of the model*

The results obtained indicate an increase in maximum daily temperatures for all time horizons and both considered RCPs. On the contrary, precipitation is projected to decrease (e.g. -16 % to -30 % for RCP 8.5 and time horizon 2075-2099).

Despite the acknowledged limitations of moderate underestimation of maximum temperatures and slight overestimation of minimum temperatures (Politi et.al., 2023), this approach has been assessed as the most appropriate for the scope of the risk assessment in RESCUEME, providing a good representation of spatial patterns (Politi et.al., 2023) and a sufficient level of detail for the risk assessment (5 km spatial grid), when the raw datasets are taken for the analysis.

Still, the key limitation of this assessment lies in the availability and quality of both, modelled and observed datasets. The analysis was based on the use of processed maps rather than raw data, which constrained the level of detail and, consequently, the accuracy of the results. Furthermore, the observed data from monitoring stations were found to be fragmented, with many datasets being incomplete or containing significant data gaps.

Nevertheless, the results obtained are considered sufficiently accurate for the scope of the project and the level of detail required for the risk assessment in this R-Lab.

Although resources from the IPCC were examined, including reports and the associated data repository, were reviewed, their application in this study was limited. The spatial resolution of available data, primarily at the Mediterranean basin scale, was too coarse to support the fine-scale analysis required in this study.

## 4.3.2 Exposure

This impact model prioritizes population and financial capital as the primary elements of exposure, specifically two key economic sectors: agriculture and tourism. Accordingly, the selected indicators include both total population and employment figures (this last indicator is related to the fact that most of the population is employed in tourism in Psiloritis), as well as the extent of agricultural land, as shown in Table 9.

*Table 9. Indicators employed in the assessment of exposure on Psiloritis, Crete, along with their corresponding weights.*

Capital	Name of indicator	Unit	Weight
Social	Population number	Number	0.3
Financial	Employed persons	Number	0.12

Capital	Name of indicator	Unit	Weight
Natural	Agricultural area	m2	0.58

### 4.3.3 Vulnerability

#### Heritage value assessment

The approach for the heritage value assessment followed the same general structure as the one outlined in the section of Neuwerk. The main difference is that for the R-Lab of Psiloritis Geopark, two separate hazards were considered. To account for this, the analysis was conducted separately for each hazard highlighting specific interrelationships between heritage values and temperature changes or changing precipitation patterns respectively (see Table 10).

Table 10. List of indicators used for HV assessment of Psiloritis Geopark.

Risk Element	Capital	Name of indicator	Unit	Polarity	Weight for changing precipitation patterns	Weight for rising temperatures
Adaptive capacity	Natural	Protected areas under national laws	% of area	Negative	0.17	0.17
	Social	Number of sites accessible by people	Number/km <sup>2</sup>	Negative	0.10	0.11

Risk Element	Capital	Name of indicator	Unit	Polarity	Weight for changing precipitation patterns	Weight for rising temperatures
		with disabilities				
	Social	Annual number of festivals or cultural events connected to traditions/culinary practices/local products	Number/1,000 inhabitants	Negative	0.12	0.13
	Social	Number of local associations connected to traditions/culinary practices/local products	Number/1,000 inhabitants	Negative	0.13	0.12
	Social	Number of shops, restaurants and tourism	Number/1,000	Negative	0.13	0.12

Risk Element	Capital	Name of indicator	Unit	Polarity	Weight for changing precipitation patterns	Weight for rising temperatures
		facilities selling local products (0 Km)	inhabitants			
	Social	Attendance and participation in cultural activities and events	Number/1,000 inhabitants	Negative	0.17	0.18
	Social	Cultural vibrancy - number of cultural sites	Number/km <sup>2</sup>	Negative	0.17	0.16

### Ecosystem services assessment

Like the HV analysis, the ES assessment was conducted separately to account for differences in the functioning of ES in relation to reducing the system’s vulnerability.

### Changing precipitation patterns

For the hazard of changing precipitation patterns, the potential runoff retention was calculated with the help of the Urban Flood Risk Mitigation model by the InVEST® software tool (Natural Capital Project, 2023). The model was originally developed exclusively for pluvial flooding. Yet based on studies such as the one by Ogden et al. (2013), that found synergistic effects between different land use types and their flood and drought mitigation potential, this may serve as a proxy for ES connected to precipitation overall.

To estimate this, the runoff  $Q$  (mm) was calculated using the Curve Number method:

$$Q_{p,i} = \begin{cases} \frac{(P - \lambda \cdot S_{max_i})^2}{P + (1 - \lambda) \cdot S_{max_i}} & \text{if } P > \lambda \cdot S_{max_i} \\ 0 & \text{otherwise} \end{cases}$$

with each pixel  $i$  under the conditions of a heavy rain event with a predefined storm depth  $P$  (mm), the potential retention per pixel  $S_{max}$  (mm) and the rainfall depth needed to initiate runoff  $\lambda \cdot S_{max}$  (with  $\lambda = 0.2$ ).

$S_{max}$  is calculated using the subsequent function based on the curve number  $CN$ , which is a predictor of runoff and infiltration depending on soil hydrologic group and land use class:

$$S_{max_i} = \frac{25400}{CN_i} - 254$$

With the estimated runoff  $Q$  and the design storm depth  $P$ , InVEST® then calculates the runoff retained per pixel compared to the storm volume, the relative runoff retention per pixel  $R_i$  and the absolute runoff retention per pixel in  $m^3$  with  $pixel.area$  in  $m^2$  (Natural Capital Project, 2023):

$$R_i = 1 - \frac{Q_{p,i}}{P}$$

$$Rm3_i = R_i \cdot P \cdot pixel.area \cdot 10^{-3}$$

Lastly, the results were aggregated to represent the average value per municipal unit  $m$  and inverted as follows:

$$V_{ES_m} = 1 - Rm3_m$$

These values were then normalized to a range between 1 and 2 using the min-max approach to form the ES index for this hazard.

Data requirements for the Urban Flood Risk Mitigation model included the following:

Storm depth was set at 67.7 mm. This is equivalent to the maximum daily rainfall of 2024 recorded in May at the Amnatos meteorological station (Petrou, n.d.). Data on soil hydrologic groups were retrieved from the Global Hydrologic Soil Group data set by Ross et al. (2018) at 250 m resolution. Land use/Land cover data were taken from the 2021 WorldCover maps at 10 m resolution by the European Space Agency (Zanaga et al., 2022). Curve number data for each land use class and soil hydrologic group were adapted from Hong & Adler (2008) and Marino et al. (2023).

### *Rising temperatures*

For the hazard of rising temperatures, the InVEST® Urban Cooling model was used to estimate an indicator value for ecosystem services (Natural Capital Project, 2023). The main output of this model is a heat mitigation index which provides a value for the reduction of the urban heat island effect. However, the R-Lab in question is characterized by a rural environment. Therefore, a partial output of the model, the cooling capacity index, was used instead. The model considers multiple factors like crop coefficient, shade, evapotranspiration and albedo which are associated with different land use classes.

First, the evapotranspiration index  $ETI$  for each pixel is computed based on the reference evapotranspiration  $ET_o$ , the maximum value of the reference evapotranspiration within the study area  $ET_{max}$  and the crop coefficient  $K_c$  as follows:

$$ETI = \frac{K_c \cdot ET_o}{ET_{max}}$$

This is then combined with the weighted values for shade (proportion of tree canopy  $\geq 2$  m in height) and albedo (proportion of directly reflected solar radiation) to calculate the cooling capacity per pixel  $CC_i$ :

$$CC_i = 0.6 \cdot shade + 0.2 \cdot albedo + 0.2 \cdot ETI$$

The used weights were chosen based on InVEST® recommendations and underlying empirical studies (Natural Capital Project, 2023; Phelan et al., 2015; Zardo et al., 2017).

To incorporate the cooling capacity into the risk equation, the ES for rising temperatures was determined through aggregating the values per pixel to an average for each municipal unit  $m$  and inverting it:

$$V_{ES_m} = 1 - CC_m$$

The ES index was then formed with the normalised results using the min-max approach with a final range between 1 and 2.

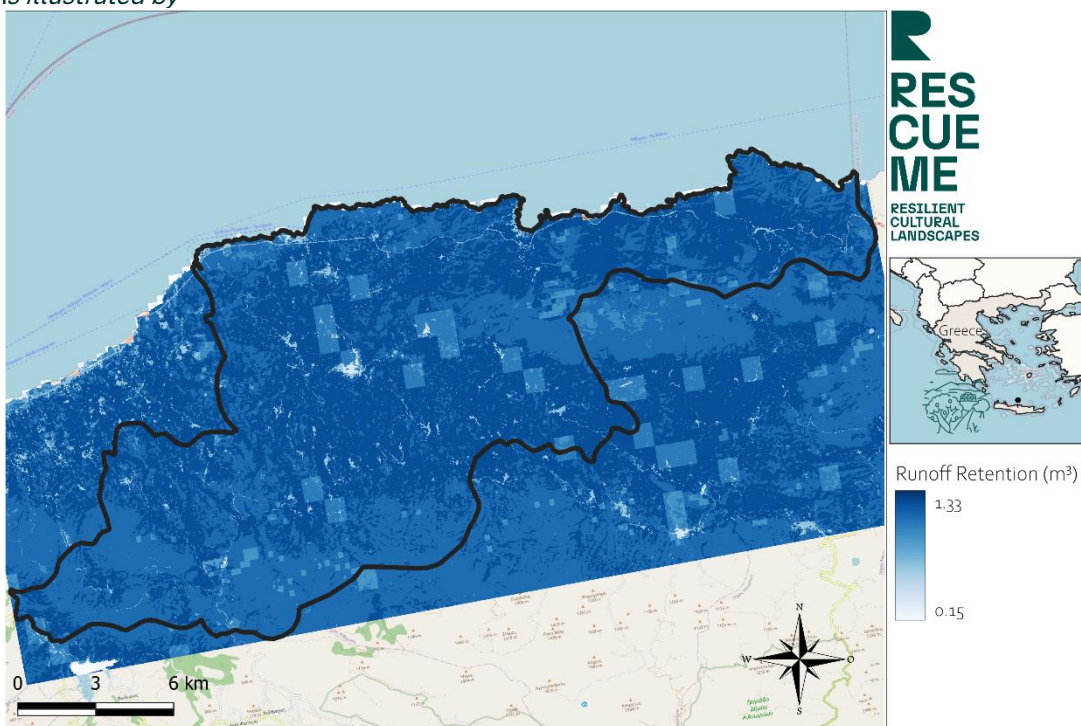
Data requirements for the Urban Cooling Model included the following:

Air Blending Distance was set to 600 m (Lonsdorf et al., 2021). The magnitude of the urban heat island effect was set to 8 °C based on (Kolokotsa et al., 2008) but in this case does not affect the final calculation. 31 °C was chosen as the Reference Air Temperature, which was the maximum monthly mean high temperature of 2024, as measured in June at the Amnatos

meteorological station (Petrou, n.d.). In line with this, Version 3 of the Global Reference Evapotranspiration model for June developed by Zomer et al. (2022) was used as the reference evapotranspiration, following the methodology of Hamel et al. (2024). Land use/Land cover data were obtained from the European Space Agency (Zanaga et al., 2022). Corresponding values for  $K_c$ , shade and albedo were based on and adapted from Hu et al. (2023).

### Results from ES assessment<sup>6</sup>

As illustrated by



<sup>6</sup> The results of intermediate tasks were incorporated into the methodology section in order to concentrate all final risk analysis results in the results chapter.

Figure 12 and

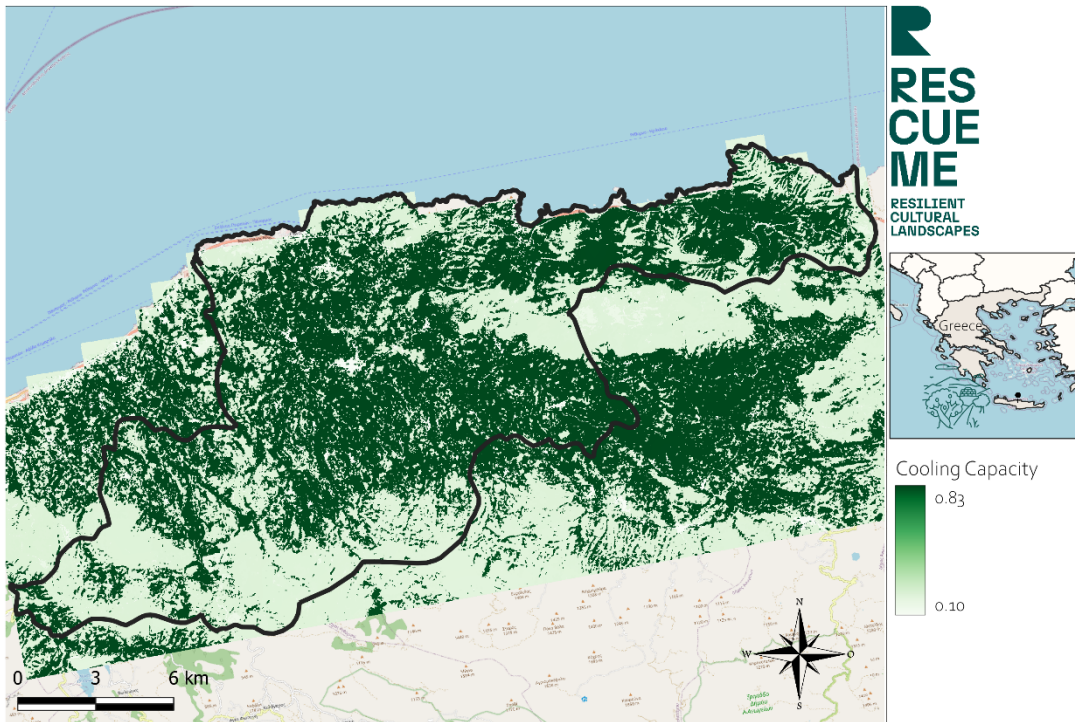


Figure 13, overlapping patterns emerge across the two different ES models applied. The supply of ES mitigating the effects of changing precipitation patterns (runoff retention) and rising temperatures (cooling capacity) seem to have a synergistic relationship. The highest values for both ES, visualised in dark blue and dark green for runoff retention and cooling capacity respectively, are found along the coast and a stretch of land with a parallel east-west orientation further inland.

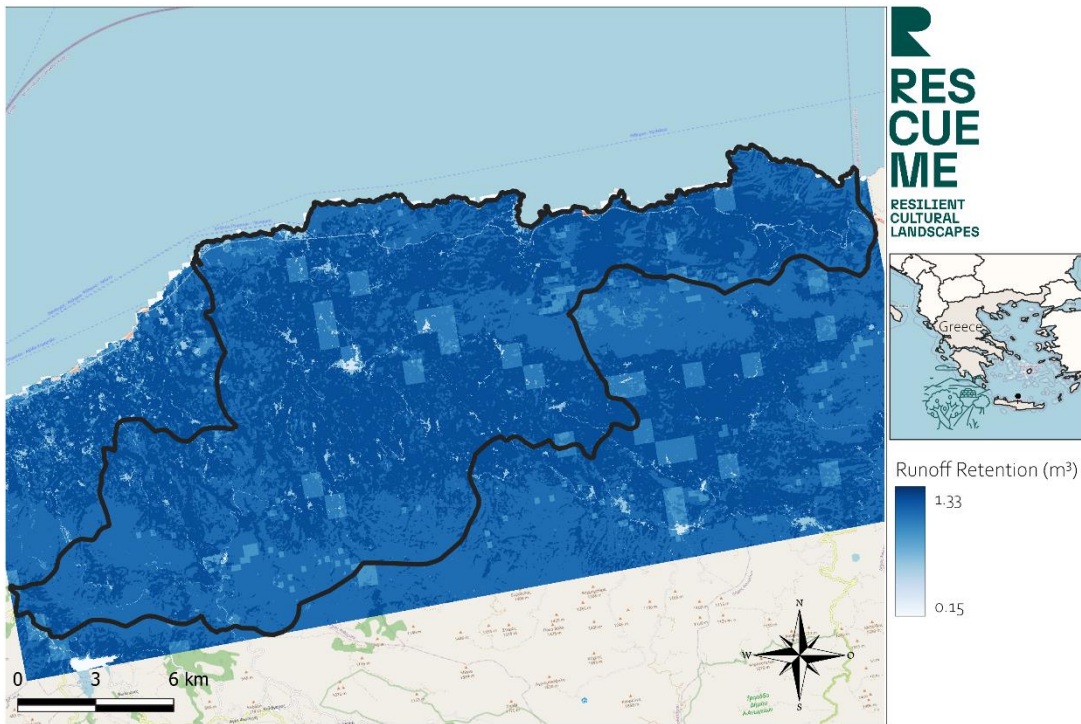


Figure 12. Runoff retention values of Psiloritis Geopark in m<sup>3</sup>. Computed using InVEST® Urban Flood Risk Mitigation model (Natural Capital Project, 2023).

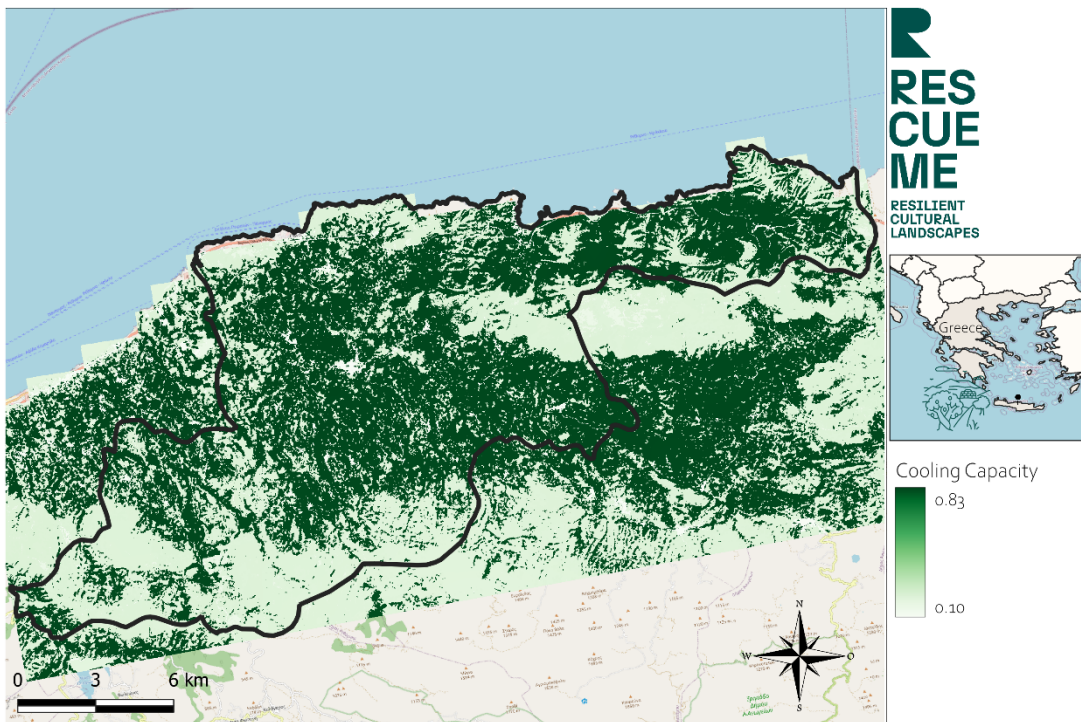


Figure 13. Cooling capacity values of Psiloritis Geopark. Computed using InVEST® Urban Cooling model (Natural Capital Project, 2023).

**Vulnerability assessment: Indicator and vulnerability indices aggregation**

As previously mentioned, both HV and ES indices were aggregated with other indicators (Table 11) into the vulnerability index for Psiloritis Geopark. The indicators and the weights assigned to each are presented below.

*Table 11. Indicators and indices used in the vulnerability assessment of Psiloritis (Crete), along with their corresponding weights.*

Capital	Name of indicator	Unit	Risk component	Polarity	Weight
Natural	ES index	Dimensionless	The only indicator that makes up the index belong to the adaptive capacity dimension.	Positive	0.5
Natural, social	HV index	Dimensionless	All the indicators that make up the index belong to the adaptive capacity dimension.	Positive	0.35
Social	Proportion of population aged 65 years and more	% of total population	Sensitivity	Positive	0.08
Social	Share of tenant agricultural area	% of agricultural area	Adaptive capacity	Negative	0.05
Human	Share of farmers with full or basic agricultural training	% of holdings	Adaptive capacity	Negative	0.02

### 4.3.4 Risk assessment

Ultimately, the risk index was derived by integrating the exposure, hazard, and vulnerability indices, applying the weights detailed in the table below. Those weights were selected by R-Lab experts.

*Table 12. Risk components and weights on Psiloritis, Crete.*

Risk component	Weight
Vulnerability	0.47
Exposure	0.28
Hazard	0.25

## 4.4 Portovenere, Cinque Terre and the Islands

In this R-Lab the analysis focused on the **impacts of landslides on the terraced landscape**, assessed at the local level across seven municipalities: Levanto, Monterosso al Mare, Pignone, Vernazza, Riomaggiore, La Spezia, and Portovenere. Four temporal scenarios were considered: 1980–2004, 2021–2050, 2041–2070, and 2071–2100. For the latter three, both RCP 4.5 and RCP 8.5 emission scenarios were evaluated.

### 4.4.1 Hazard

Shallow landslides induced by rainfall pose a serious hazard to hilly and mountainous areas around the world, such as the Eastern Ligurian Riviera. The mountainous landscape of the R-Lab Cinque Terre, Porto Venere and the Islands, is particularly vulnerable to these landslides, which usually occur on steep, soil-covered slopes because of heavy or intense rainfall. However, they can often evolve into potentially disastrous, flow-like movements (Napoli et al., 2021). They have been identified as the most critical hazard in the area, due to their occurrence and their destructive potential. The impacts of climate change are likely to additionally increase the hazard to rainfall-induced landslides, having an impact on the rainfall patterns.

In order to assess the hazard due to rainfall-induced landslides, the approach with the following steps has been adopted:

- (1) A desk study on the available data, methods, models and tools
- (2) Selection of the method and model to perform the hazard assessment due to rainfall-induced shallow landslides
- (3) Application of the selected method to the R-Lab area

A thorough desk study of the available methods, tools and data has been conducted, including expert interviews and contact with data providers, particularly the National

Research Council of Italy (CNR), Geographic Information Systems Interest Group (GISIG) and Meteolitalia (1).

The methods and publications on the landslides based on the available sources in Google Scholar, Scopus and other scientific publication repositories such as Research Gate were systematically analysed. The objective was to identify approaches relating geographic and/or relevant meteorological and climatological characteristics of an area to the probability of landslide occurrence. To this end, a systematic literature review (e.g. Torres-Carrión et al., 2018) was conducted using the following keywords and their combinations: 'landslides' 'rainfall/precipitation' 'climate change' 'GIS-based' 'geomorphology' 'Cinque Terre' 'Liguria' 'Italy'. Based on the conducted literature review, the following main types of approaches were identified in the scientific literature and are available in practice:

- GIS-based analyses of shallow landslides relating the geographical and geological parameters to the landslide occurrence (e.g., Conforti et al., 2016, Rocatti et al., 2021).
- Analyses of the (heavy) rainfall characteristics including the duration and the intensity of the heavy rainfall that is likely to trigger the landslides (e.g., Bogaard & Greco, 2018, Rocatti et al., 2020).

Methods and approaches that combine GIS with rainfall characteristics, particularly those incorporating climate change perspective, are generally scarce and currently unavailable for the R-Lab area. Given these limitations, this study has adopted a proxy-based approach, using indirect variables to represent the hazard (2). Specifically, proxies related to heavy rainfall were used to describe the hazards due to rainfall-induced landslides. This method enables a preliminary evaluation of hazard dynamics in the absence of more comprehensive, high-resolution data and established models for the region.

Analysis of the available data on heavy rainfall and the corresponding climate projections identified the datasets and model runs by Fagian & Trevisol, (2024) as the most appropriate for analysing rainfall-induced landslides, as these describe current and future heavy rainfall patterns. The analysis utilizes the 99th percentile-based indices, namely the R99 index from the World Meteorological Organization's Expert Team on Climate Change Detection and Indices (WMO ETCCDI) for the historical reference period, and the R99PTOT index for future projections. Future projections are considered for three-time horizons: short-term (2021–2050), medium-term (2041–2070), and long-term (2071–2100). These projections are derived from simulations using 12 high-resolution Euro-CORDEX regional climate models, incorporating both RCP 4.5 and RCP 8.5 scenarios. The R99PTOT index reflects projected precipitation associated with extremely wet days—those exceeding the historical 99th percentile threshold.

Additionally, Italian weather scenario data depicting the 95th percentile of precipitation, which is available from ItaliaMeteo, has been taken into consideration. However, due to the lack of data representing the reference period, this data was deemed unsuitable for consistent analysis and thus excluded from the assessment.

The collected data and the provided datasets and model run by Fagian & Trevisol, (2024) were further processed for the hazard assessment.

Raster datasets with a resolution of 6 km x 6 km that were created for different RCPs and time horizons, containing information about R99 and R99PTOT, were intersected with the spatial units of the risk assessment, which are the municipalities in the R-Lab (Figure 14).

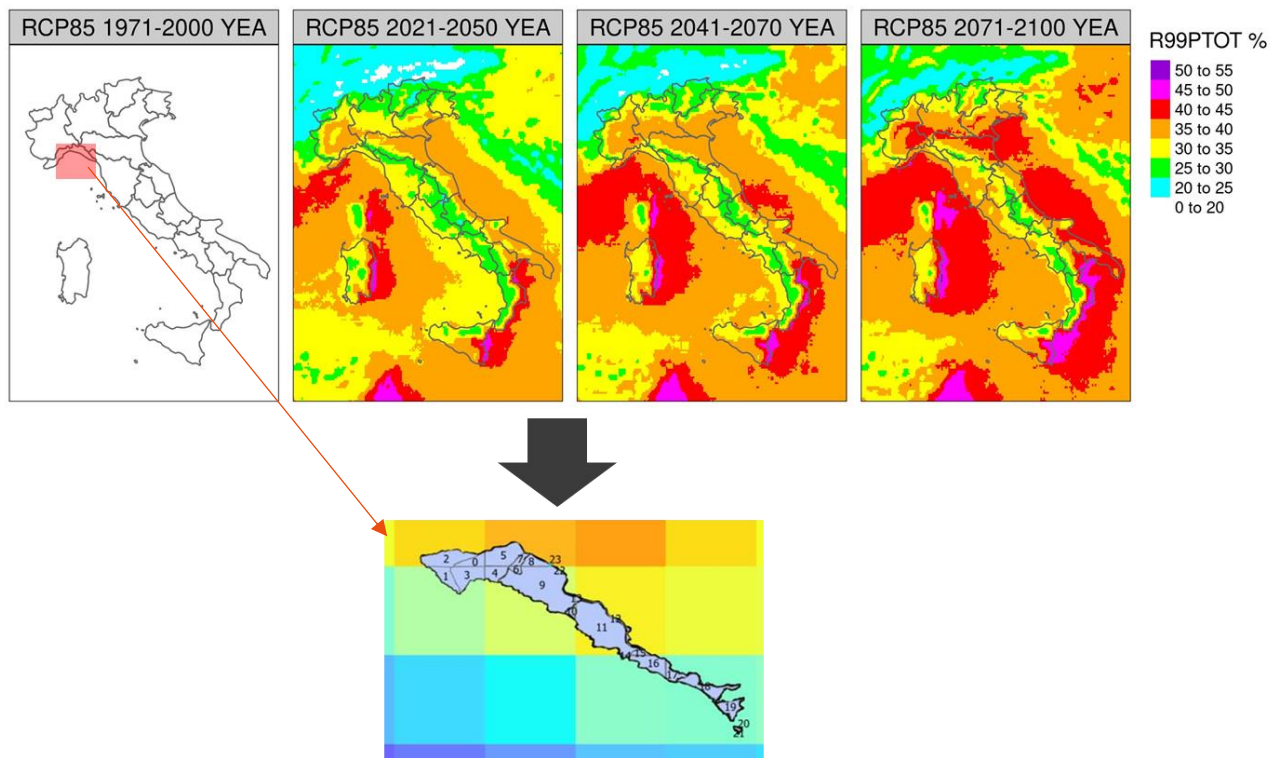


Figure 14. The principle of the intersection of the raster data sets for R99 and R99PTOT and the spatial units of the R-Lab. The datasets were provided by Fagian & Trevisol, 2024

For each spatial unit, the values of the intersecting raster cells were weighted. The outcome of this analysis is weighted R99 in [mm/day] and an R99RTOT in [%] values, which indicate changes in precipitation patterns for different RCPs and time horizons.

Following the spatial analysis of projected changes in the selected proxy indicator (R99PTOT), the relationship between rainfall intensity, duration, and the occurrence of landslides was investigated. To establish this correlation, the methodology proposed by

Rocatti et al., (2020) was adopted. This approach defines empirical rainfall thresholds for the potential initiation of shallow landslides, based on the combined effects of rainfall intensity and duration.

The threshold model was derived from a historical dataset comprising 85 rainfall events that triggered 114 shallow landslides in the Liguria region (Portofino area) over the period 1910–2019. This empirical correlation is presented in  $I = (4.04 \pm 0.14) D^{(-0.46 \pm 0.01)}$  (Equation 3 and illustrated in Figure 15, serving as a basis for evaluating landslide susceptibility under varying rainfall conditions.

$$I = (4.04 \pm 0.14) D^{(-0.46 \pm 0.01)} \text{ (Equation 3)}$$

Where:

$I$  = [mm/h] is the intensity of the rainfall

$D$  = [h] is the rainfall duration

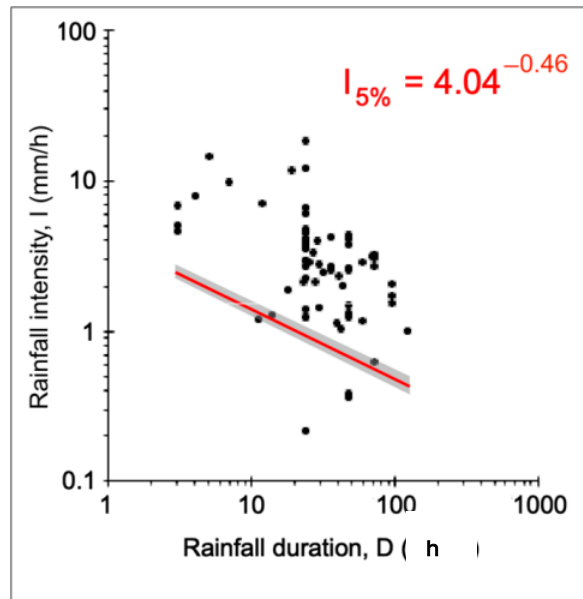


Figure 15. Rainfall thresholds obtained for the possible initiation of shallow landslides and mud/debris flows on the Portofino promontory corresponding to a 5 % exceedance probability level (red curve) and associated uncertainty (grey pattern) Taken from Rocatti, et al., (2020).

The Landslide Trigger Index (LTI) has been defined as a ratio between the analysed/modelled rainfall [mm/day] and the critical rainfall i.e. the one that triggers a landslide according to Equation 3. The LTI is presented in Landslide Trigger Index  $LTI = \frac{\text{Modelled Rainfall}}{\text{Critical rainfall}}$  (Equation 4).

$$\text{Landslide Trigger Index } LTI = \frac{\text{Modelled Rainfall}}{\text{Critical rainfall}} \quad (\text{Equation 4})$$

For the scope of this work, a 24h rainfall duration has been assumed, given the available data and examining the reported observed rainfalls that triggered landslides.

For the LTI for a 24h rainfall duration (given as LTI<sub>24</sub> and used in this study), the critical rainfall is obtained by applying the Equation 3, and assuming the duration of 24h. The modelled rainfall values for different time horizons and RCPs are derived from the dataset provided by Fagian and Trevisol, (2024).

As an additional analysis, the existing repositories of the rainfall-induced landslides have been examined in order to identify the hotspots in the area and cross-check the conducted analysis.

Two main repositories have been identified, being ITALICA and ITALIAN LANDSLIDE INVENTORY (IFFI). ITALICA is claimed to be the largest catalogue of rainfall-induced landslides with accurate spatial and temporal spots currently available in Italy (Brunetti et al., 2024). IFFI delivers an indicator that provides information about the landslide number and their spatial distribution in Italy. However, due to differences in the reporting of rainfall-induced landslides in the area, a direct relationship with the method used could not be established and finally was not considered for the scope of this work. Nevertheless, these records are documented and once the differences have been reassessed, they can be considered for refining the hazard assessment method presented in this work. However, this refinement is beyond the scope of this project.

#### *Results and limitations of the model*

This methodology allowed for the derivation of spatially aggregated, representative LTI24 values for each municipality (in total 7) based on the values given for the raster cells of the provided dataset. Thus, the final output of this analysis consists of weighted LTI24 values for the reference period, as well as for multiple future scenarios based on different RCPs (4.5 and 8.5) and time horizons.

Those results indicate an increase in heavy precipitation and consequently in LTI or LTI 24.

The methodology adopted in this study relies on the use of proxy indicators to assess the potential for rainfall-induced landslides. As such, it is inherently subject to debate regarding the selection and suitability of variables used as proxies. Given that the primary hazard addressed in this study is related to rainfall-triggered processes, heavy rainfall has been selected as the key proxy.

By applying the threshold-based approach developed by Rocatti et al., (2020), geographical and geomorphological factors have been indirectly incorporated, since the threshold values were derived from empirical data specific to the Liguria region, where the R-Lab is also located.

Still, this method does not explicitly integrate geographic or geomorphological variables, which are known to significantly influence landslide susceptibility. Future research should aim to develop integrated models that directly correlate rainfall-induced landslide occurrences with both meteorological and geographic conditions. Such an approach would enhance the spatial accuracy and reliability of hazard assessments. However, it must be acknowledged that the implementation of such models requires extensive, high-quality datasets, including well-documented landslide events and high-resolution climate projections across varying rainfall patterns and intensities.

It should also be noted that climate modelling was beyond the scope of the project. Instead, the available data sources and model runs have been examined.

## 4.4.2 Exposure

This impact model prioritizes population and the agricultural and touristic built infrastructure as the primary elements of exposure. Accordingly, the selected indicators include both total population and other tourism indicators, as well as the extent of agricultural holdings, as shown in Table 13.

*Table 13. Indicators employed in the assessment of exposure on Portovenere, Cinque Terre and the islands, along with their corresponding weights.*

Capital	Name of indicator	Unit	Weight
Social	Population number	Number	0.3
Financial	Bed places	Number	0.1
Financial	Number of Agricultural holdings	Number	0.3
Financial	Tourist accommodation establishments	Number	0.2
Human	Number of educational facilities	Number	0.1

## 4.4.3 Vulnerability

### Heritage vulnerability assessment

The methodology for the overall heritage value assessment again follows the same structure as outlined for Neuwark. However, for this R-Lab, the key focus was terrace cultivation of vineyards and olive trees. Since the latest data regarding their status and potential abandonment was from 2012, an expeditious methodology was developed which aims to update data related to abandonment and changes in cultivation in the terraced areas of the Cinque Terre.

First, the terraces that had previously been mapped were divided among the municipalities in the area based on their location. The classification of terrace land was already completed in 2012 by comparing the state of the terraces with that of 1973. A similar comparison was then made between the 2012 and the current one, to check whether the use of the terraces remained the same or had changed.

The process involved comparing the 2012 data with satellite images obtained from websites such as Google Maps and Google Earth. Occasional verification via Google Street View was used for more uncertain cases visible from roads. During this process, the surface area of some plots had to be adjusted. For instance, some plots appeared partially uncultivated, so

they were divided to better reflect their current state. Additionally, new areas were added, as not all currently existing terraces were mapped and included in the dataset from 2012.

This data was then used to calculate the percentage of abandonment of terraces out of the total terraced area. In this context, “abandoned terraces” included both uncultivated terraces and those overtaken by shrubs or trees.

Lastly, together with other indicators reflecting agricultural heritage and protected areas (see Table 14), the HV index was computed.

*Table 14. List of indicators used for HV assessment of Portovenere, Cinque Terre, and the Islands.*

Risk element	Capital	Name of indicator	Unit	Polarity	Weight
Adaptive capacity	Natural	Share of Natura2000 area	% of area	Negative	0.12
	Natural	Surface cultivated with vineyards	% of area	Negative	0.13
	Natural	Surface cultivated with olive trees	% of area	Negative	0.14
	Natural	Share of protected areas surface	% of area	Negative	0.12
	Natural	Protected natural and agricultural areas with international designation exposed to landslides	% of area	Negative	0.16

Risk element	Capital	Name of indicator	Unit	Polarity	Weight
	Natural	Percentage of terraced vineyards on the total land used for viticulture	% of viticulture area	Negative	0.15
Sensitivity	Natural	Percentage of abandonment of terraces on the total terraced area	% of total terraced areas	Positive	0.17

### Ecosystem services assessment

The methodology for the ecosystem service assessment followed the same structure as the one outlined for the R-Lab of Neuwerk as outlined in page 44. The indicators used for the analysis can be found in Table 15 and were weighted with a particular focus on how different types of land use specifically affect soil stability and subsequently affect the vulnerability to the hazard of landslides.

Table 15. List of indicators used for ES assessment of Portovenere, Cinque Terre and the Islands.

Risk element	Capital	Name of indicator	Unit	Polarity	Weight
Adaptive capacity	Natural	share of forest land	% of area	Negative	0.39
	Natural	Share of agricultural area	% of area	Negative	0.33
Sensitivity	Natural	Degree of urbanisation - Share of urban areas	% of area	Positive	0.28

### Vulnerability assessment: Indicator and vulnerability indices aggregation

As previously mentioned, both HV and ES indices were aggregated with other indicators (Table 16. Indicators and indices used in the vulnerability assessment of Portovenere, Cinque Terre and The Islands, along with their corresponding weights (Table 16) into the vulnerability index for Portovenere, Cinque Terre and the Islands. The indicators and the weights assigned to each are presented below.

*Table 16. Indicators and indices used in the vulnerability assessment of Portovenere, Cinque Terre and The Islands, along with their corresponding weights*

Capital	Name of indicator	Unit	Risk component	Polarity	Weight
Natural	ES index	Dimensionless	The indicators that make up the index belong to the dimensions of adaptive capacity and sensitivity.	Positive	0.2
Natural	HV index	Dimensionless	The indicators that make up the index belong to the dimensions of adaptive capacity and sensitivity.	Positive	0.4
Social	Population density	persons/ km <sup>2</sup>	Sensitivity	Positive	0.05
Social	Population change	number/ 1,000 inhabitants	Adaptive capacity	Negative	0.06
Financial	Unemployment rate	% of Working Age Population (15 and older)	Sensitivity	Positive	0.04
Financial	Arrivals at tourist accommodation establishments per population	number/1,000 inhabitants	Sensitivity	Positive	0.04
Natural	Share of region with high or very high landslide susceptibility	% of region area	Sensitivity	Positive	0.06
Natural	Share of elevation breakdown - low coast	% of region area	Sensitivity	Positive	0.03
Natural	Share of elevation breakdown - high coast	% of region area	Sensitivity	Positive	0.03

Capital	Name of indicator	Unit	Risk component	Polarity	Weight
Natural	Share of elevation breakdow - inland	% of region area	Sensitivity	Positive	0.03
Natural	Share of elevation breakdow - upland	% of region area	Sensitivity	Positive	0.03
Natural	Share of elevation breakdow - mountains	% of region area	Sensitivity	Positive	0.03

#### 4.4.4 Risk assessment

Finally, to construct the risk index, the exposure, hazard, and vulnerability indices were integrated (see formula in Section 4. 8. Combination of hazard, exposure and vulnerability indices to obtain risk indices), using the weights chosen by R-Lab experts. Risk components along with the weights are presented in the table below.

Table 17. Risk components' weights on Portovenere, Cinque Terre and the Islands.

Risk component	Weight
Vulnerability	0.5
Exposure	0.2
Hazard	0.3

## 4.5 Defensive system of Zadar

In Zadar the study addressed the **impacts of coastal flooding on cultural heritage buildings**. Although a coastal flood hazard assessment was performed for the peninsula, the analysis showed that only a few buildings were subject to any level of hazard. Therefore, with both hazard and exposure values essentially at zero, conducting a full risk assessment was not technically feasible. As a result, the analysis was limited to vulnerability assessment alone.

## 4.5.1 Hazard

For Zadar R-Lab the identified hazards coastal flooding and storm surge have been assessed using a detailed hydrodynamic modelling approach, following the steps as given for the Neuwerk, Hamburg R-Lab.

Following the collection and evaluation of available data (1), a decision was made to use the historical storm event that occurred in October–November 2012, driven by Scirocco winds, as the basis for the hazard and risk assessment.

This storm was chosen as the representative design event due to its observed intensity and relevance to the local coastal dynamics. For future scenarios, projected SLR values of 0.2 meters (by 2050) and 0.7 meters (by 2100) were applied. These projections align with the SSP5-8.5 high-emission pathway specific to the Mediterranean region.

The combination of this historical storm with SLR projections enables a robust analysis of current and future flood risks under climate change conditions.

In addition, the storm of January/February 2015 (undocumented Mediane) with the same SLR scenarios was selected in order to provide a better insight into the behaviour of the flood propagation and the susceptibility of the area.

The input parameters used to set up the hydrodynamic model are based on the public sources and are summarised in Table 18.

*Table 18. Input data and their sources that has been used to set up the 2d hydrodynamic model for Zadar R-Lab.*

Input parameter	Data source	Resolution
Bathymetry	General Bathymetric Chart of the Oceans (GEBCO) Compilation Group (2019)	15 arc seconds
DEM	European Environmental Agency (2016)	25 m x 25 m
Wind data	Bollmeyer et al. (2015)	6 x 6 km, hourly
Tidal gauge Tarifa	Puertos del Estado (n.d.)	hourly
River discharges	Poulos (2020) Ludwig et al. (2009)	-

Input parameter	Data source	Resolution
Water level gauges for calibration and validation	Martinsica, Prosika (Croatia): DHMZ (n.d.). Marseille (France): National Oceanography Centre: (n.d.). Valencia (Spain): Puertos del Estado (n.d.) Otranto, Venice: Flanders Marine Institute (VLIZ) (2025).	daily / hourly / 10 - minutely /
SLR scenarios	IPCC (2023)	-

A detailed 2D hydrodynamic numerical model using the TELEMAC platform for the flood hazard assessment has been fully set up within the project (2). The tidal forces are considered using the tidal gauge measurements at Tarifa (Spain) station in the Strait of Gibraltar, which connects the Mediterranean Sea with the Atlantic Ocean (see Figure 16).

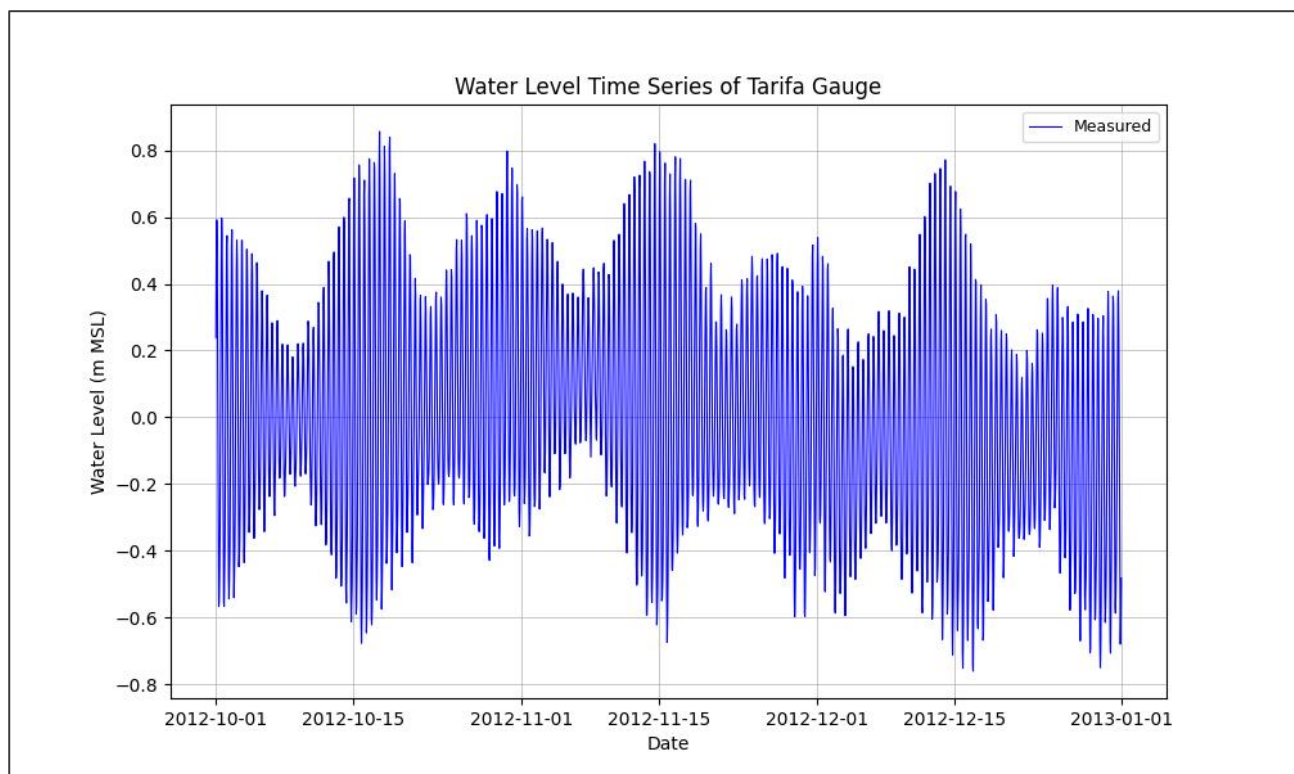


Figure 16. Water level series of gauge Tarifa from 1st October 2012 to 1st January 2013.

Furthermore, the discharges as given in Table 19 from inland areas as well as from the Sea of Marmara (Strait of Dardanelles) have been built into the model.

Table 19. Considered discharges into the Mediterranean Sea.

Discharge area	Water flux [m <sup>3</sup> /s]
Dardanelles	10127
Ebro	547
Jucar	39
Krka	53
Neretva	386
Nile	965
Po	1479
Rhone	1736
Zrmanja	230

The developed hydrodynamic model and the boundary conditions with the astronomical tide and river discharges (inflows) are presented in Figure 17. The spatial resolution of the unstructured, triangular mesh that reaches up to 200 m edge length in the area of interest, is given in Figure 18.

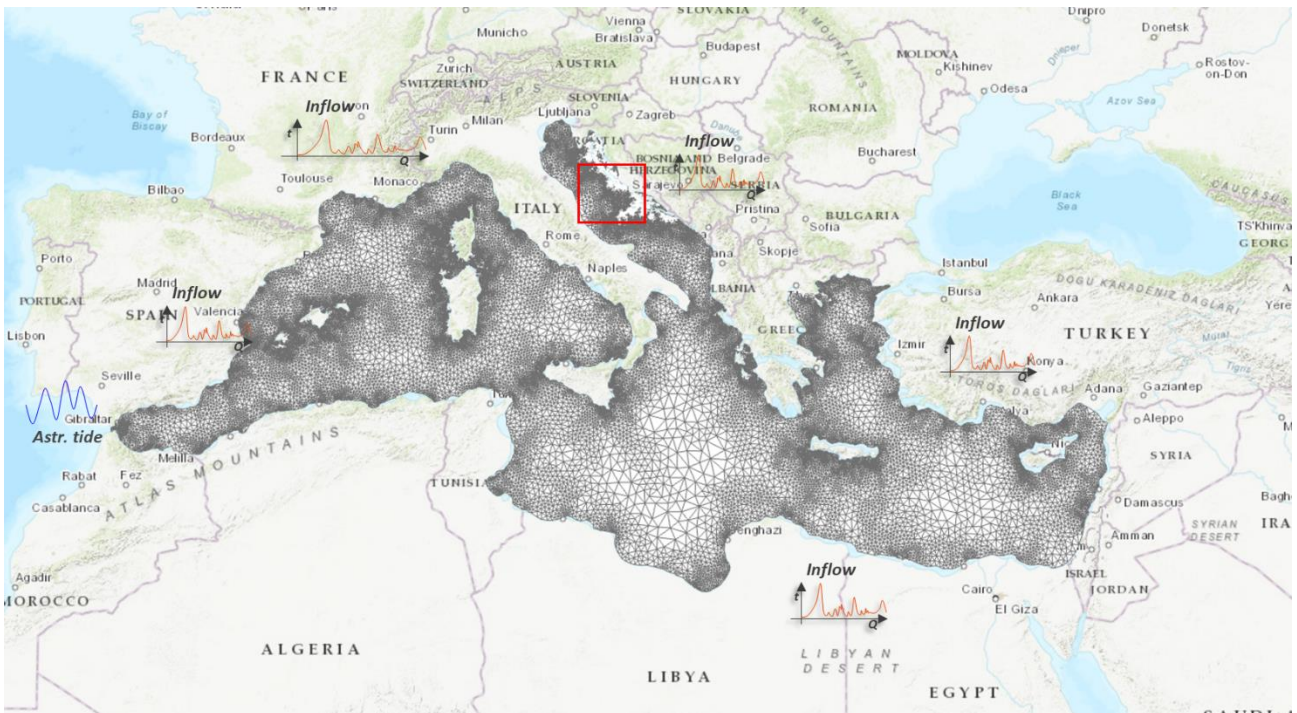


Figure 17. The developed hydrodynamic model with the boundary conditions (inflows) for the Zadar R-Lab. The basemap taken from USGS, (2025).

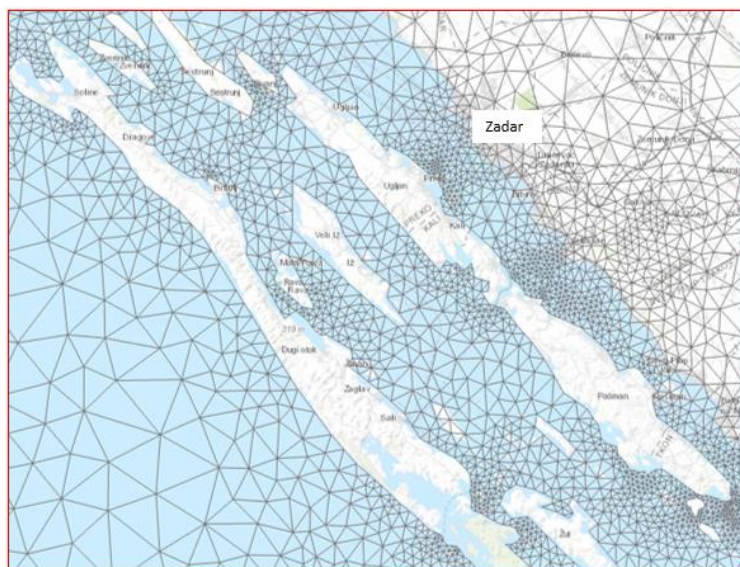


Figure 18. Resolution of the calculation mesh in the area of interest. The basemap taken from USGS, (2025)

### Results and the limitations of the model

The final result of the hazard modelling in the Zadar R-Lab is the water level raster that has been intersected with the DTM, delivering the water depth at the affected locations, which are mainly located along the historic Defensive System of Zadar (3). The results are given for the model/design storm and for the scenarios considering the climate change. The results

for the storm surge of 2012 considering the SLR of 0.2 m and 0.7 m are given in Figure 19 and Figure 20 respectively.

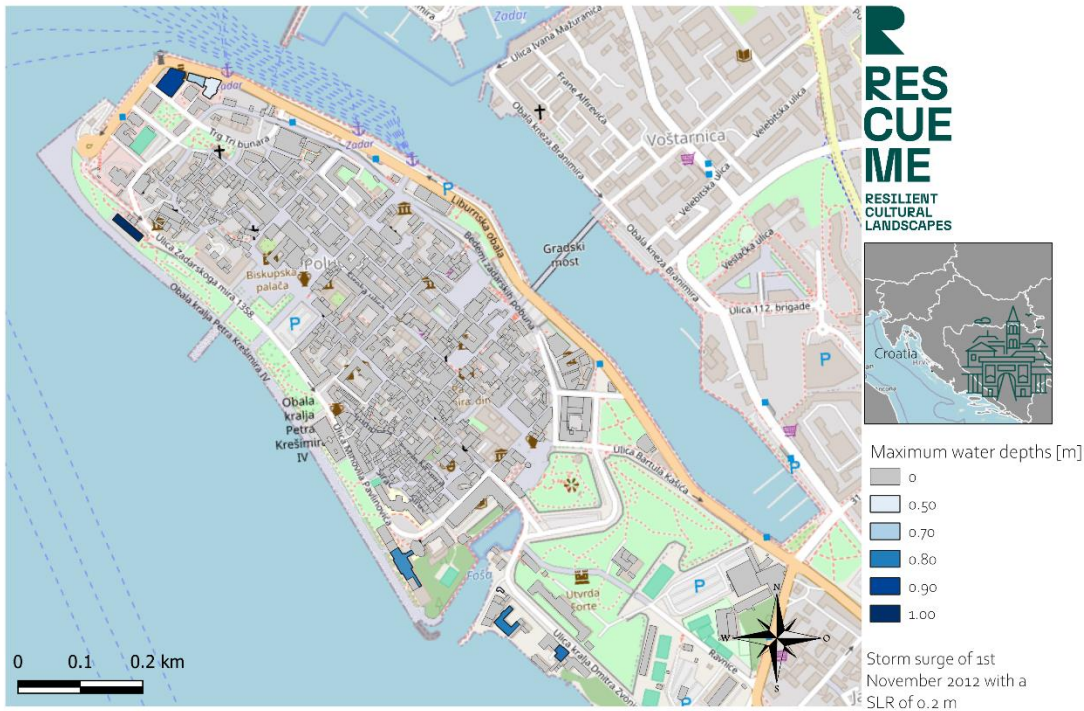


Figure 19. The results of the hazard modelling, water depths, for the Zadar R-Lab given for the storm of 2012 with a SLR of 0.2 m.

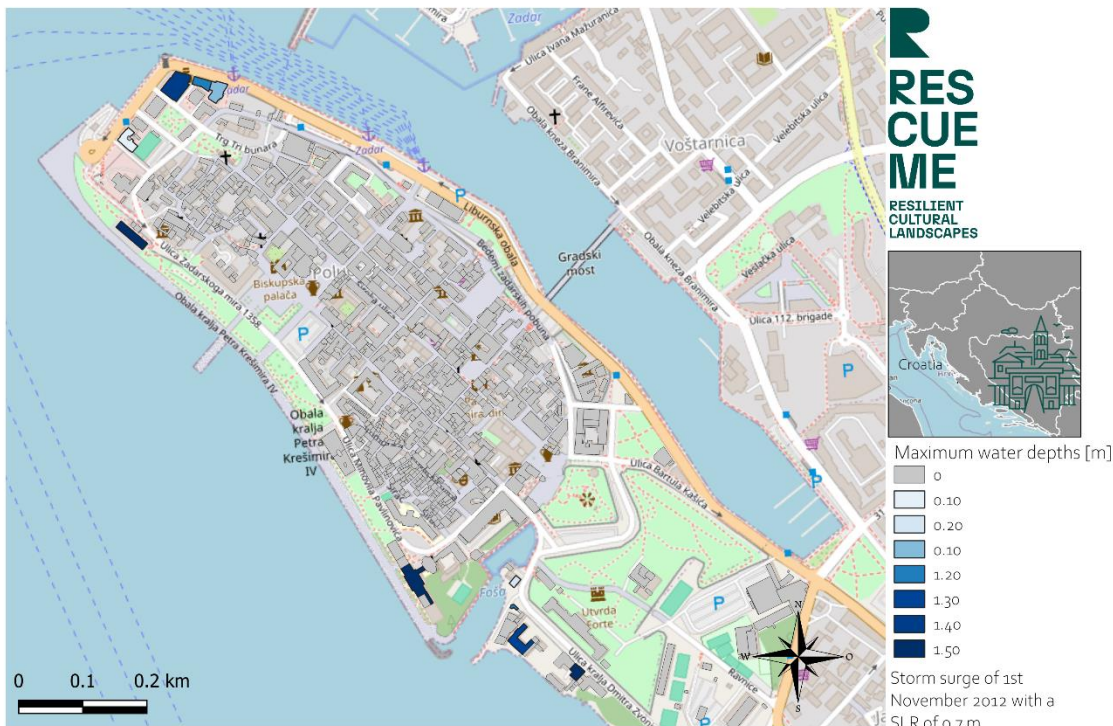


Figure 20. The results of the hazard modelling, water depths, for the Zadar R-Lab given for the storm of 2012 with a SLR of 0.7 m.

While the required data for the Neuwerk R-Lab was largely available and accessible, significant data limitations were encountered in the Zadar Labscape. In particular, the absence of measured data from local gauging stations posed a major challenge, especially for validating the hydrodynamic modelling results. To partially overcome this limitation, data from the broader Adriatic and Mediterranean region was collected and used to feed into the analysis. Moreover, interpolation and extrapolation techniques were applied to estimate values for the Zadar area, allowing the modelling to proceed despite the local data gaps.

Despite the challenges in acquiring the necessary data for hydrodynamic modelling and high efforts to develop such models, the use of such models remains highly recommended. These models are essential for accurately understanding the physical processes driving coastal flooding and for reliably characterizing the associated hazards as they can capture key dynamics such as wave overtopping, flow velocities, or the influence of protective infrastructure, which is usually not the case with the simplified, or static models.

## 4.5.2 Exposure

As shown in the Figure 20, there is a very limited number of buildings exposed to the hazard. This is primarily because the defensive system of Zadar, while originally constructed for military purposes, now function as critical infrastructure in reducing impacts of coastal

floods. Their substantial mass and elevation act as a physical barrier, reducing the direct exposure of the historic peninsula to storm surges and sea level rise. As such, these heritage structures contribute not only to the cultural and historical identity of the city but also to its resilience against climate-induced coastal hazards. Therefore, there is a need to maintain and preserve the walls not solely from a heritage conservation perspective, but also as a component of adaptive coastal risk management. Consequently, future risk assessments should incorporate a targeted analysis of the structural condition and material vulnerability of the walls, particularly regarding hydrodynamic pressures, saltwater intrusion, and long-term erosion processes. This integrated approach will support both heritage safeguarding and of urban flood resilience improvement.

### 4.5.3 Vulnerability

#### Heritage vulnerability assessment

Due to the small extent of the R-Lab and the desired output resolution at building level, a different methodology had to be applied here. First, using available data from the Geoportal of Cultural Property, the geoportal site of Croatia, UNESCO and Google maps, the cultural sites of Zadar have been mapped. For the heritage value assessment, 13 cultural sites which can be assigned to a specific building (complex) were selected. A survey was developed in order to determine their heritage values and relationships with vulnerability across eight HV dimensions. This approach was adapted from the methodology to gather expert opinions on heritage by Ravankhah et al. (2021). The HV dimensions selected were:

- Recreation or aggregation
- Spiritual or religious
- Education
- Workmanship, technological and traditional knowledge
- Authenticity and history
- Individual or collective memory and sense of place
- Entertainment or tourism
- Aesthetic

The survey followed the general structure of asking two questions per site.

Assign a score between 1 (“very low”) and 5 (“very high”) reflecting the cultural significance of the mapped sites/buildings in Zadar for each of the listed eight heritage value dimensions. Considering the scores assigned to each value in the previous question, indicate whether it may increase or decrease the vulnerability of the cultural site in the event of a coastal flooding or if it is not assessable. For instance, considering an historical building with high authenticity value, do you think it may increase vulnerability due to its age and/or conservation state, or it may decrease vulnerability, due to a reinforced sense of place.

The survey was sent out to four experienced local experts, representing the fields of cultural site management, public administration and museum curation.

For the final assessment, the average heritage value scores for each heritage dimension and site were computed and the polarity was determined based on the majority of experts' responses. The heritage value was left unchanged if more experts assumed a positive polarity, meaning a contribution to vulnerability. For the opposite case, meaning a negative polarity and a decrease in vulnerability, the additive inverse of the determined heritage value was considered for the analysis (meaning if the heritage value was 5, in the calculation, it would be considered as -5). If at least 50 percent of experts deemed the polarity to not be assessable, the value dimension was not considered for the analysis. Similarly, if the experts were evenly split between assuming a positive and negative polarity, the respective heritage dimension was discarded for this heritage site.

Subsequently, the unweighted average of all heritage dimensions was computed, individually for each site. Afterwards, the values were normalised using the min-max approach with a final range between 1 and 2. Thus, the final result of this analysis was a heritage value index that contains one value for each site which reflects not only different dimensions of heritage values but also takes into account whether these dimensions contribute to or reduce vulnerability.

## 4.6 L'Horta de València

In the València case study, the focus was on two climate-related risks: the **impact of torrential rainfall** and **the impact of droughts on the agricultural heritage system**. Both risks were assessed at the municipal scale, covering a total of 45 municipalities. The assessment included four temporal periods: 1971–2000, 2011–2040, 2041–2070, and 2071–2100. For the last three, both RCP 4.5 and RCP 8.5 scenarios were used.

### 4.6.1 Hazard

For the L'Horta de Valencia R-Lab, the most dominating hazards are related to droughts and torrential rainfall. In both cases, the changes in precipitation patterns play the key role to understand the future development of those hazards. The following approach has been adopted to explore the shifts in the precipitation patterns for the future climate projections:

- (1) Desk study on the available data, methods and tools.
- (2) Selection of the model and hazard modelling/assessment for the reference and the adopted future scenarios and RCPs.

A desk study of data sources and existing methodologies indicated that the AdapteCCa platform, a joint initiative of the Spanish Climate Change Office and the Biodiversity Foundation (both under the Ministry of Ecological Transition and the Demographic Challenge), is the most comprehensive data repository suitable for the scope of the project. The AdapteCCa platform provides information on various climate variables related to temperature and precipitation for the reference period and time horizons, for different climate scenarios based on various RCPs. These are presented as ensemble model runs or as individual models. For the scope of this work, the ensemble results were used. The overview of the platform’s main features is given in Figure 21.

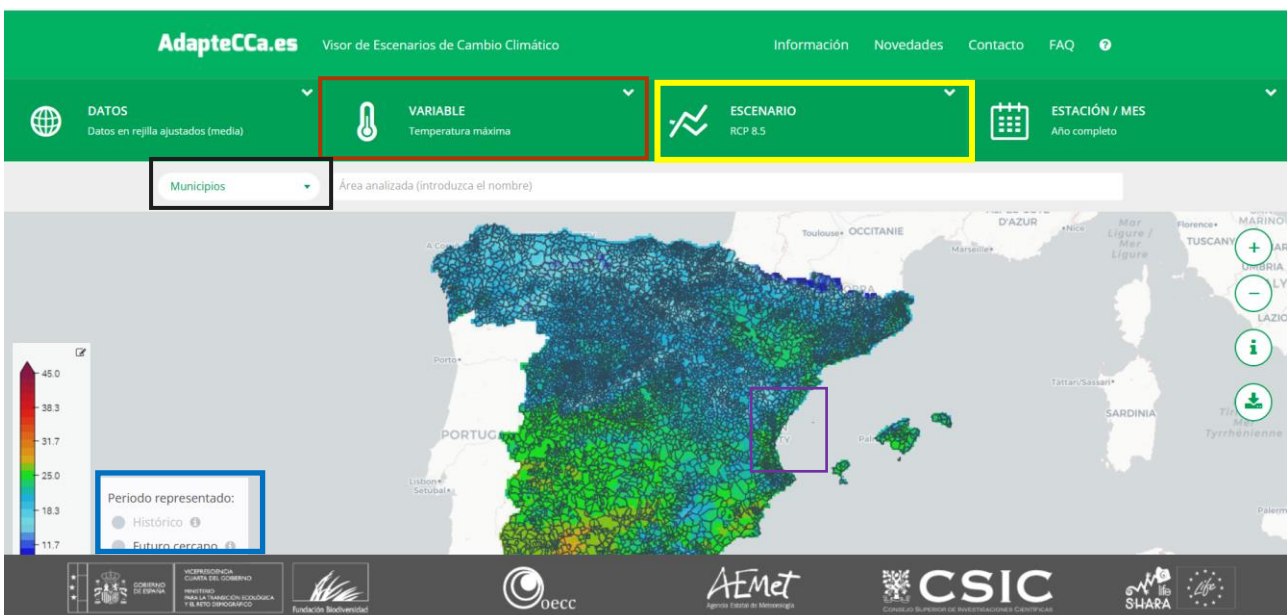


Figure 21. The AdapteCCa platform with the main features and elements relevant for the hazard modelling in the L’Horta de Valencia R-Lab; red rectangular- selection of the variables; yellow rectangular: RCPs; blue rectangular: time horizons; violet rectangular: study area; black rectangular: scale of analysis, here the municipal scale

In order to analyse the changes in precipitation patterns to address both, droughts and torrential floods, a set of indicators/ variables has been selected for the statistical modelling, as given in Table 20.

Table 20. A set of indicators for the analysis of changes in precipitation patterns to address both, droughts and torrential floods in the L’Horta de Valencia R-Lab.

Name of indicator	Unit
95th percentile of daily rainfall	[mm/d]

Name of indicator	Unit
Number of days with rainfall less than 1 mm	days
Accumulated rainfall in 24 h	[mm/a]

They are given for RCP 4.5 and RCP 8.5 and time horizons 2011-2040, 2041-2070 and 2071-2100.

The statistical modelling included the following steps:

- 1 Preprocessing: Downloading the data from the AdapteCCa platform for all variables, scenarios and time horizons and their formatting; In all cases the average values of the provided ensemble modelling results were taken for further processing.
- 2 Processing: statistical modelling, which included the calculation of the mean values and the trend for the 3 variables for the adopted time horizons and RCPs. For the scope of this analysis, the trend was calculated for the validation purposes.
- 3 Postprocessing: preparation and analysis of the data for all municipalities (in total 45).

#### *Results and limitations of the model*

The final output of this analysis is a table containing the values of the selected indicators given in Table 20, for the reference period and for the multiple climate scenarios (RCP 4.5 and RCP 8.5) and different time horizons 2011-2040, 2041-2070 and 2071-2100. These values provide a comparative basis for assessing the changes in precipitation patterns in the L'Horta, Valencia R-Lab.

The changes in precipitation patterns based on the calculated average values vary across different time horizons and RCPs. This variation is attributable to the use of ensemble modelling data, where individual models may produce outlier values that can influence the overall statistical outputs. A more robust understanding of future changes can be obtained by cross-checking these calculated average (mean) values against the long-term trends. Finally, for the scope of the study the average values were taken for further processing towards the risk assessment.

## 4.6.2 Exposure

This impact model prioritizes natural capital – reflected in the extent of agricultural land; financial capital – represented by the number of agricultural holdings per municipality; and social capital – captured through the size and distribution of the population, as the primary components of exposure. Accordingly, the selected indicators include both total population as well as the extent and number of agricultural holdings, as shown in Table 21.

Table 21. Indicators employed in the assessment of exposure on L'Horta de Valencia, along with their corresponding weights.

Capital	Name of indicator	Unit	Weight
Social	Population number	Number	0.3
Financial	Number of agricultural holdings	Number	0.1
Natural	Agricultural area	m <sup>2</sup>	0.6

### 4.6.3 Vulnerability

#### Heritage vulnerability assessment

The approach for the heritage value assessment is identical to the one outlined in the section of Neuwerk. Following the focus on agricultural traditions and the unique irrigation system present in this R-Lab, indicators reflecting this were prioritised as seen in Table 22.

Table 22. List of indicators used for HV assessment of Valencia.

Risk element	Capital	Name of indicator	Unit	Polarity	Weight
Adaptive capacity	Natural	Share of Natura 2000 area	% of area	Negative	0.09
	Natural	Share of protected areas surface	% of area	Negative	0.10
	Financial	Incentives for the maintenance of traditional agricultural activities	€/farmer /year	Negative	0.11
	Natural	Number of PDO/PGI agriculture firms	Number/ km <sup>2</sup>	Negative	0.10

Risk element	Capital	Name of indicator	Unit	Polarity	Weight
	Natural	Area with outdoor recreation potential	% of area	Negative	0.06
	Natural	Protected areas under national laws	% of area	Negative	0.09
	Natural	Diversity of landscape	Number	Negative	0.09
	Built	Traditional channels of irrigation	m/km <sup>2</sup>	Negative	0.14
	Natural	Area used for traditional cultivations	% of area	Negative	0.12
	Built	Number of architectural and infrastructural elements representing the traditional way of living and cultivating	Number/km <sup>2</sup>	Negative	0.10

### Ecosystem services assessment

The ecosystem service assessment method chosen for this R-Lab represents a blended approach between the ones outlined for Neuwerk and Psiloritis Geopark. First, the InVEST® Urban Flood Risk Mitigation model was applied to give an estimate of the runoff retention related to ES.

The input data was chosen as follows:

The rainfall depth on September 28, 2012, was 188.9 mm, the maximum value recorded at the Valencia Airport meteorological station, and was used as the storm depth (AEMET, n.d.). The Global Hydrologic Soil Group data set by Ross et al. (2018) at 250 m resolution was used for the classification into different soil hydrologic groups. Land use/Land cover data were obtained from the European Space Agency (Zanaga et al., 2022). Curve number data were adapted from Hong & Adler (2008) and Marino et al. (2023) for each land use class and soil hydrologic group.

In a subsequent step, the model’s output was used as an indicator for an ES index and integrated with other available data which directly or indirectly reflect ES in relation to changing precipitation patterns. The selection of indicators, including the runoff retention calculated with InVEST®, can be found in Table 23.

Table 23. List of indicators used for ES assessment of Valencia.

Risk element	Capital	Name of indicator	Unit	Polarity	Weight
Adaptive capacity	Natural	Average hydric resources for crops	m <sup>3</sup> /ha/year	Negative	0.20
	Natural	Organic farming activities	% of area	Negative	0.14
	Natural	Share of arable land	% of area	Negative	0.13
	Natural	Permanent cultivations surface	% of area	Negative	0.16
	Natural	Ramsar site wetland area	% of area	Negative	0.17
	Natural	Runoff Retention	m <sup>3</sup> /25m <sup>2</sup>	Negative	0.20

Risk element	Capital	Name of indicator	Unit	Polarity	Weight
		(calculated with InVEST®)			

### Results from ES assessment

Unlike the R-Lab of Psiloritis Geopark, where the same InVEST® model (Urban Flood Risk Mitigation) was applied, the distribution of runoff retention, a crucial ES, is characterised by the presence of urban areas. The city centre and suburbs in particular show lower ES supply values compared to their surroundings, as illustrated by

Figure 22. In general, a consistent pattern can be observed in which the ES supply is higher with increasing distance from both urban environments as well as the coast.

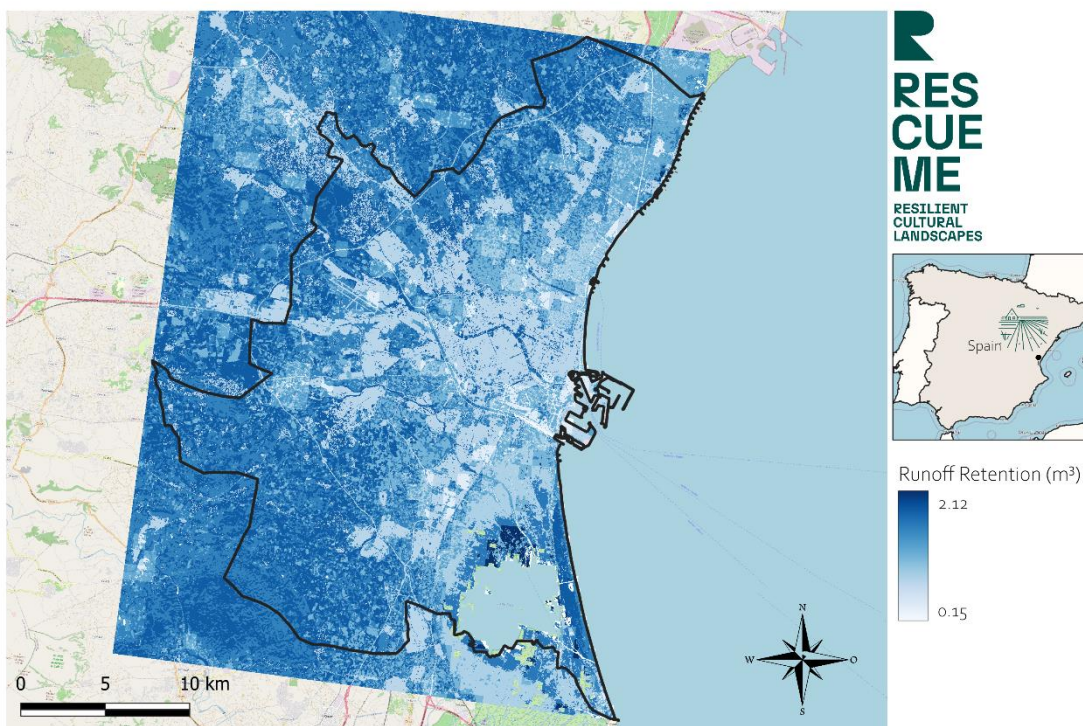


Figure 22. Runoff retention values of Valencia in m<sup>3</sup>. Computed using InVEST® Urban Flood Risk Mitigation model (Natural Capital Project, 2023).

### Vulnerability assessment: Indicator and vulnerability indices aggregation

As previously mentioned, both HV and ES indices were aggregated with other indicators (Table 24) into the vulnerability index for Valencia. The indicators and the weights assigned to each are presented below.

Table 24. Indicators and indices used in the vulnerability assessment of Valencia, along with their corresponding weights

Capital	Name of indicator	Unit	Risk component	Polarity	Weight
Natural	ES index	Dimensionless	All the indicators that make up the index belong to the adaptive capacity dimension.	Positive	0.3
Natural, financial, built	HV index	Dimensionless	All the indicators that make up the index belong to the adaptive capacity dimension.	Positive	0.3
Financial	Unemployment rate	% of Working Age Population (15 and older)	Sensitivity	Positive	0.05
Social	Availability of action plans or adaptation strategies at municipal level	0=has neither nor, 1=has one of them, 2=has both	Adaptive capacity	Negative	0.01
Human	Share of holdings with a full-time manager	Percentage	Adaptive capacity	Negative	0.02
Financial	Social Security affiliation in Agriculture	Percentage	Adaptive capacity	Negative	0.04
Social	Public land tenure	Percentage	Adaptive capacity	Negative	0.01
Social	Share of female farm managers	Percentage	Adaptive capacity	Negative	0.03
Human	Farm manager with agricultural studies	Percentage	Adaptive capacity	Negative	0.03
Financial	Municipal budget	Euro/inhabitant/year	Adaptive capacity	Negative	0.04
Natural	Number of Bio agriculture firms	Percentage	Adaptive capacity	Negative	0.03
Social	Share of young farmers (25 to 34 years)	Percentage	Adaptive capacity	Negative	0.03

Capital	Name of indicator	Unit	Risk component	Polarity	Weight
Social	Number of water management bodies/structures	Percentage	Adaptive capacity	Negative	0.03
Financial	Mid agriculture value	€/ha	Sensitivity	Positive	0.05
Human	Share of farmers with full or basic agricultural training	Percentage	Adaptive capacity	Negative	0.03

#### 4.6.4 Risk assessment

Finally, to construct the risk index, the exposure, hazard, and vulnerability indices were integrated using the weights assigned by R-Lab experts is presented in the table below.

*Table 25. Risk components' weights on l'Horta de Valencia*

Risk component	Weight
Vulnerability	0.5
Exposure	0.3
Hazard	0.2

# 5 Results

## 5.1 Island of Neuwerk, Hamburg

### Impacts of coastal floods on the buildings and agricultural lands

#### 5.1.1 RCP 8.5 2100

On average, the overall risk level across the island is Medium<sup>7</sup>. However, there is significant spatial heterogeneity evident (Figure 23). Since exposure and vulnerability are the most heavily weighted components in the risk index (each with a weighting of 0.4), cadastral parcels with a higher value in these two dimensions tend to have a High risk level. Consequently, High risk values are not necessarily associated with High hazard levels. In other words, areas with greater wave heights do not always correspond to areas with the highest risk.

---

<sup>7</sup> It is important to note that when referring to categories, the term will be capitalized (e.g., Higher, Medium, etc.), whereas when making comparisons between categories, standard capitalization will be used (e.g., x spatial unit has a higher risk than y spatial unit).



Figure 23. Impacts of coastal floods on the buildings and agricultural lands in the island of Neuwerk.

In general terms, parcels located along the island’s perimeter, which are typically associated with coastal infrastructure, exhibit Medium risk levels. This is primarily due to very High vulnerability scores, despite Medium hazard levels in these areas.

Some parcels in the northern and southern part of the island (e.g., 93140 and 94427) present Higher risk levels than those in the central part, where risk tends to be Lower. The elevated risk in these parcels is explained by both High exposure (presence of residents, a high number of bed places, and property assets) and High vulnerability (notably elevated indices of ecosystem services and cultural heritage).

Additionally, twelve parcels fall within the Medium-High risk category. These areas coincide with zones containing property assets and critical infrastructure, such as the wastewater treatment plant. The Medium-High risk levels are largely attributable to elevated vulnerability: these parcels have a high number of bed places for visitors, residents, and above-average scores in ecosystem services (ES) and heritage value (HV) indices.

Finally, most parcels on the island are characterized by Low risk levels. This is mainly due to Low exposure: in areas without residential buildings, tourism infrastructure, or agricultural activity, the risk remains Low because exposure is minimal in comparison to other parcels.

Overall, the distribution of risk across the island is highly heterogeneous, with relatively few parcels in the High or Medium-High risk categories and a large proportion classified as Low risk.

## 5.2 Psiloritis Geopark

### Impact of changes in temperature on culture

#### 5.2.1 Historical period (1980-2004)

In the area covered by the municipalities of Mylopotamos and Rethymno within the Psiloritis Geopark, there is a clear geographic distribution of risk. Communities belonging to Rethymno exhibit Lower risk levels toward the southwest compared to the central and northeastern communities of Mylopotamos. Nevertheless, the overall risk values are generally Medium to Medium-Low. Almost half of the communities are at Medium risk, only one community (MELIDONIOY, 7472) is at Medium-High risk, and the remainder are at Low or Medium-Low risk (Figure 24).

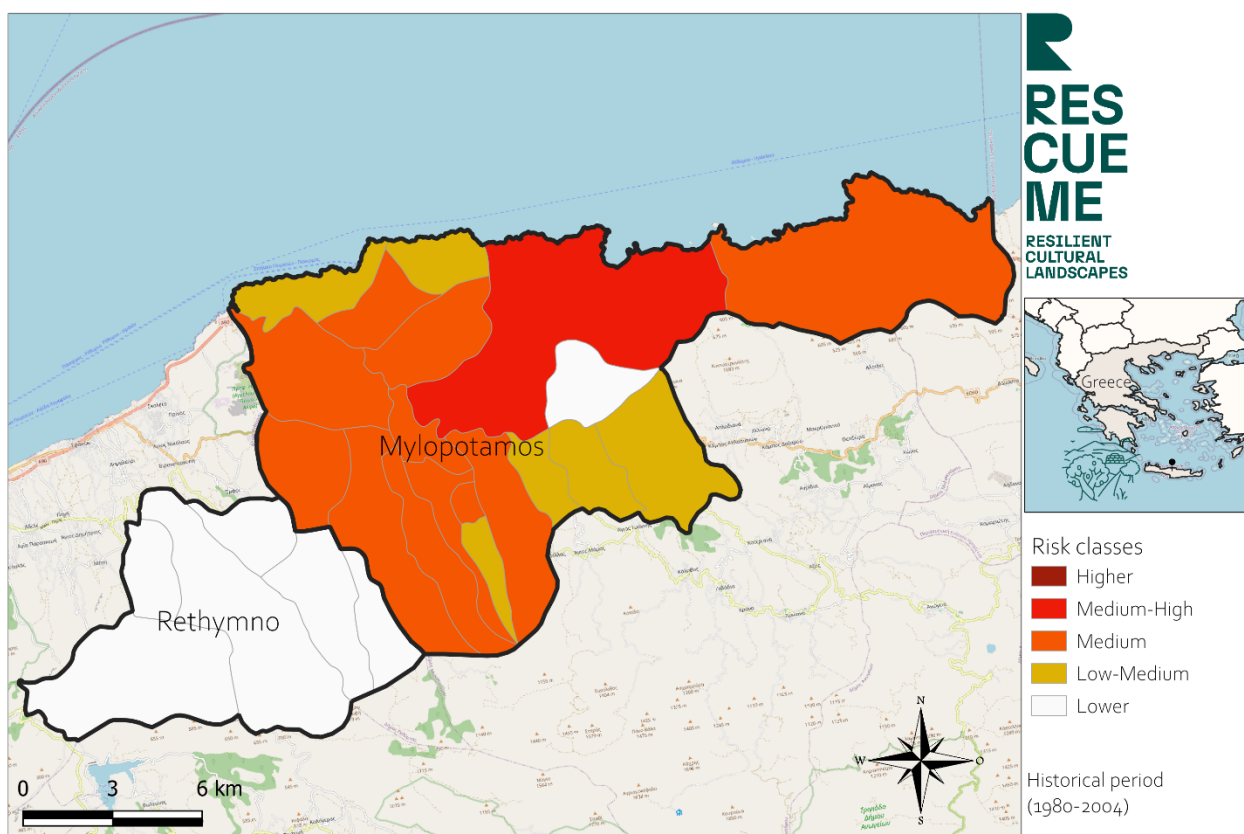


Figure 24. Impact of changes in temperature on culture. Historical period (1980-2004).

The highest risk values are primarily driven by High vulnerability levels, accounting for nearly half of the overall risk weighting. Additionally, the ecosystem services model – specifically the *cooling capacity*– shows Lower values towards the northeast, which further explains the higher risk levels in these areas compared to the southwestern communities.

In all communities where risk is classified as Medium or Medium-High, vulnerability is consistently High, hazard levels are Low, and exposure values range from High to Medium-Low.

### 5.2.2 RCP 4.5 (2025-2049)

In the projected scenario, risk increases significantly: only 7 out of 25 communities exhibit medium-low or low risk values, while 10 communities are classified as high risk (Figure 25). These communities are: K. SISVN, K. ROYMELHS, K. MELIDONIOY, K. AGGELIANVN, K. AXLADE, K. PERAMATOS, K. ALFAS, K. MARGARITVN, K. XOYMERIOY and K. PASALITVN. This indicates that several of these communities have shifted upward by two risk categories within a relatively short time period.

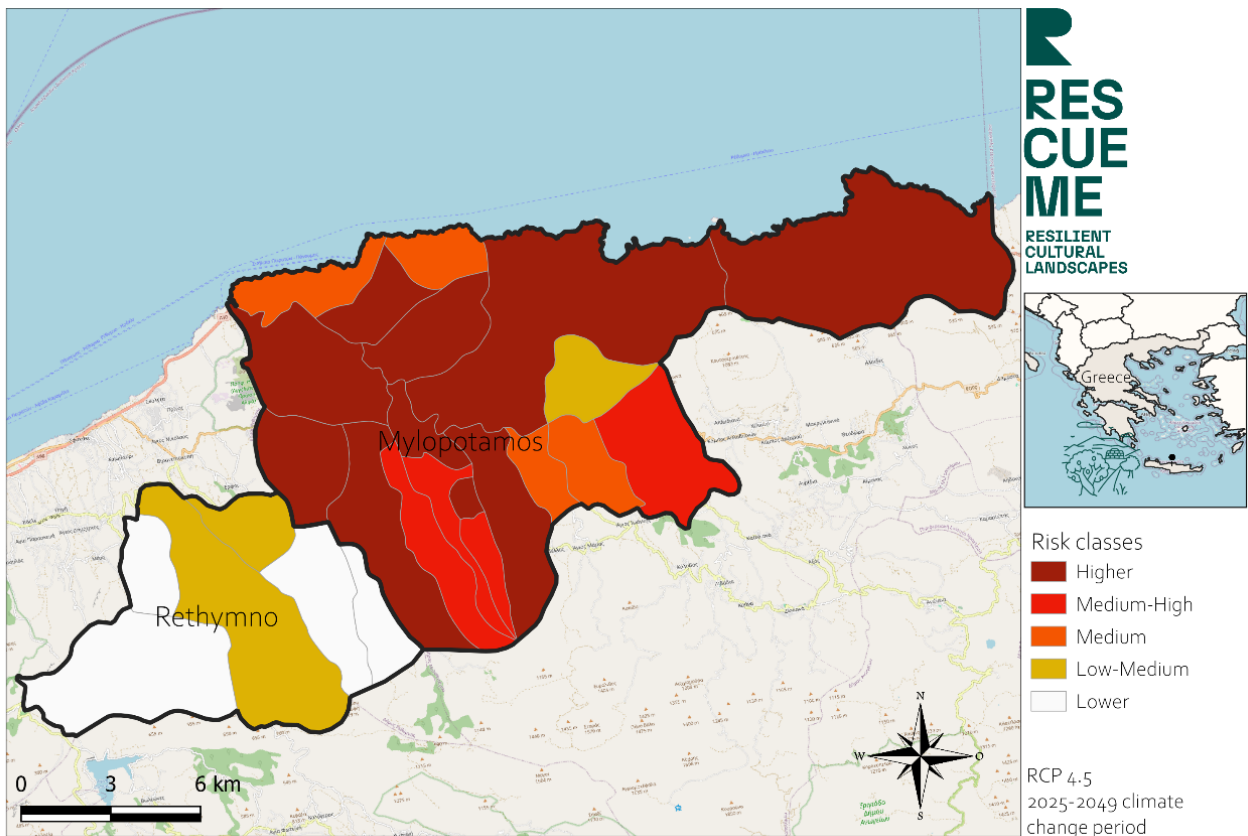


Figure 25. Impact of changes in temperature on culture. RCP 4.5 (2025-2049)

This phenomenon is driven primarily by increases in hazard values. Although hazard levels rise across the entire study area, the increases are more pronounced in Mylopotamos with approximately 1°C compared to Rethymno, where the increase is around 0.5°C. This difference accounts for the less significant risk escalation in the communities of the latter municipality.

In fact, there are some communities where the risk level has increased, but not to the extent that it warrants a shift to a higher risk category.

### 5.2.3 RCP 8.5 (2025-2049)

The literature indicates that hazard levels remain the same under both emission scenarios. For this reason, the risk mapping corresponding to the RCP 8.5 scenario is identical to that of the previous scenario, as the vulnerability and exposure indicators are not projected. This map is provided in Annex 2.

## Impact of changes in precipitation patterns on culture

### 5.2.4 Historical period (1980-2004)

Although in this reference period none of the 25 communities belonging to the Psiloritis study area reach the High risk category, it can be observed that in five of them the level is already in the Medium-High category. These are K. MELIDONIOY (7472), K. SISVN (7466), K. AGGELIANVN (7482), K. ALFAS (7525), and K. XOYMERIOY (7545). In all of them, although the hazard level is Low, the levels of exposure or vulnerability are High. Thus, while exposure is High and vulnerability is Medium-High in K. MELIDONIOY and K. SISVN, in the other three communities mentioned (K. AGGELIANVN, K. ALFAS and K. XOYMERIOY), exposure is Medium and vulnerability is High. K. MELIDONIOY and K. SISVN have the largest area of agricultural land by far and belong to municipalities with the largest population and employment rates. On the other hand, K. AGGELIANVN, K. ALFAS and K. XOYMERIOY show very high values of the HV index and some of the highest values of the ES index, which ultimately confirm this Higher vulnerability.

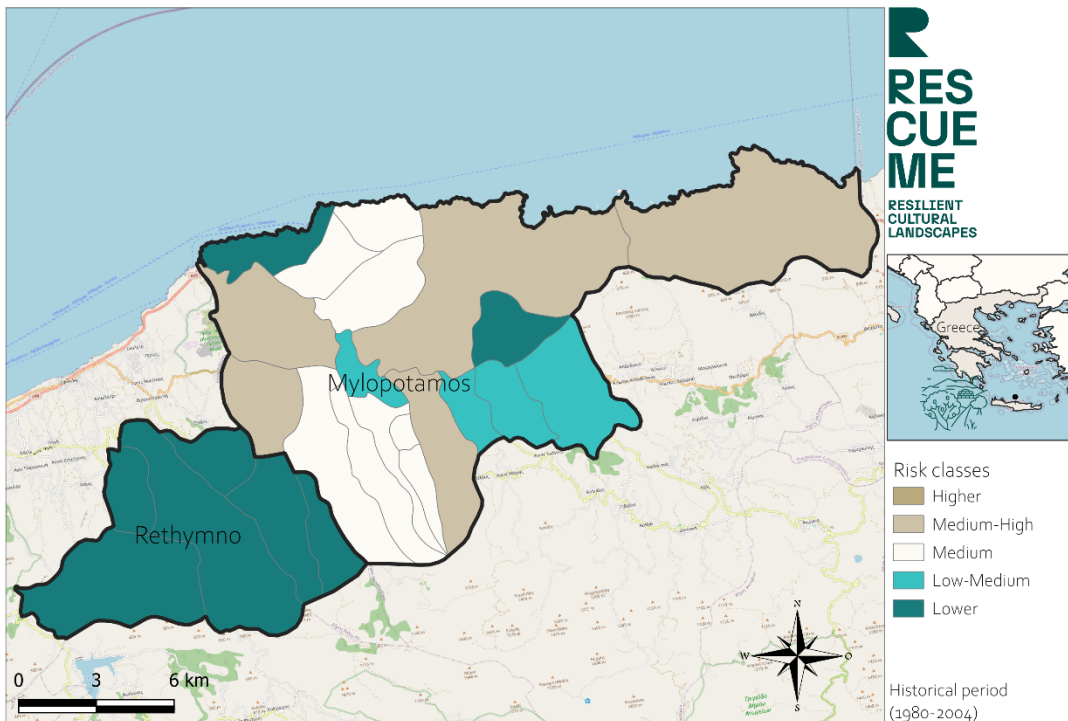


Figure 26. Impact of changes in precipitation on culture. Historical period (1980-2004).

## 5.2.5 RCP 4.5 (2075-2099)

The RCP 4.5 scenario for this period shows that the five communities that were at Medium-High risk in the reference period 1980-2004, i.e. K. MELIDONIOY (7472), K. SISVN (7466), K. AGGELIANVN (7482), K. ALFAS (7525) and K. XOYMERIOY (7545), now show a Higher risk level, attributed to the fact that the hazard increases from Low to Medium in all cases. XOYMERIOY (7545) now shows a Higher risk level, attributed to the hazard increasing from Low to Medium in all cases. In addition, other new communities are added to the Medium-High risk class, namely K. PASALITVN (7578), K. MARGARITVN (7538), K. KALANDARES (7559), K. ORUE (7549), K. AXLADE (7490), K. MELISSOYRGAKIOY (7597), K. MELISSOYRGAKIOY (7597) and K. ROYMELHS (7468). In all of these cases, while the hazard level is also Medium and exposure is Low-Medium or Medium, vulnerability reaches higher levels, i.e. Medium-High and High, again conditioned by very high values of the HV index, and medium and High values of the ES index.

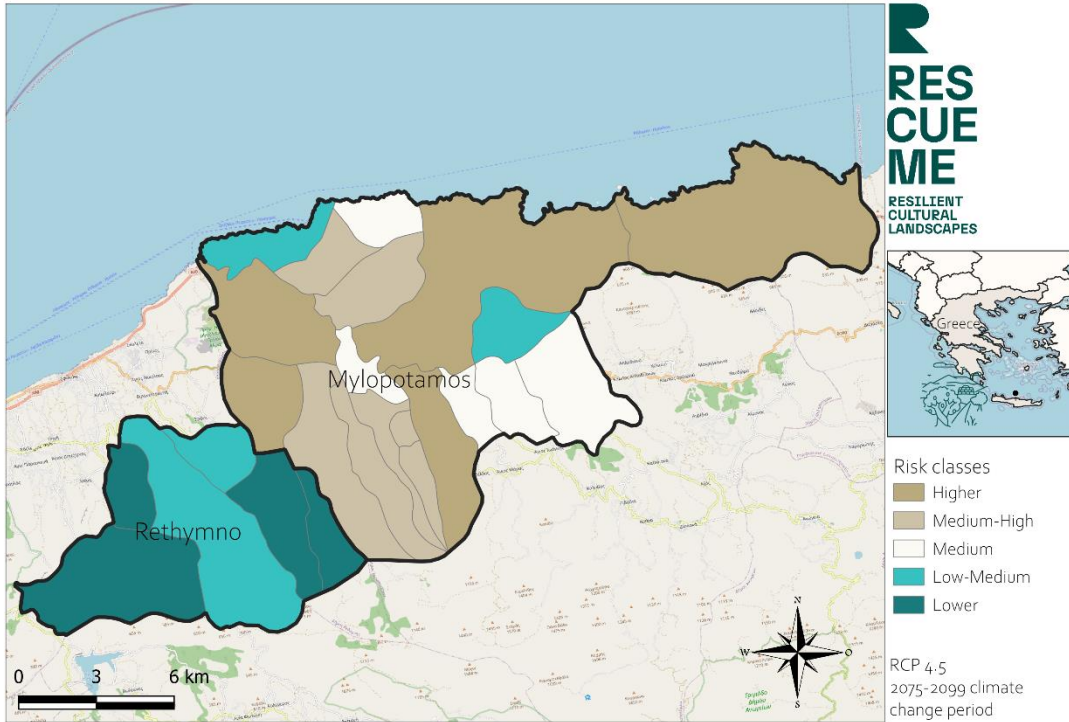


Figure 27. Impact of changes in precipitation on culture. RCP 4.5 (2075-2099).

## 5.2.6 RCP 8.5 (2075-2099)

Examining the data for the most unfavourable scenario in terms of potential Greenhouse Gas (GHG) emissions (RCP 8.5 scenario), all the communities that were categorised as being at Higher or Medium-High risk in the RCP 4.5 scenario now show a High risk level, with the exception of K. ROYMELHS. This is due to the increase in the only component that varies over the periods considered in the analysis. Specifically, the hazard level in all communities is Medium-High.

Two additional points to note are that three communities show Medium-High risk values: K. ROYMELHS, K. SKEPASTHS (7465) and K. PERAMATOS (7522). By contrast, in certain communities (K. AMNATOY, K. XARKIVN, K. ELEYUERNHS, K. SKOYLOYFIVN, K. KYRIANNAS and K. ARXAIA ELEYUERNA), the estimated hazard level is High, yet the resulting risk is Low-Medium or even Low due to Low-Medium levels of exposure and vulnerability.

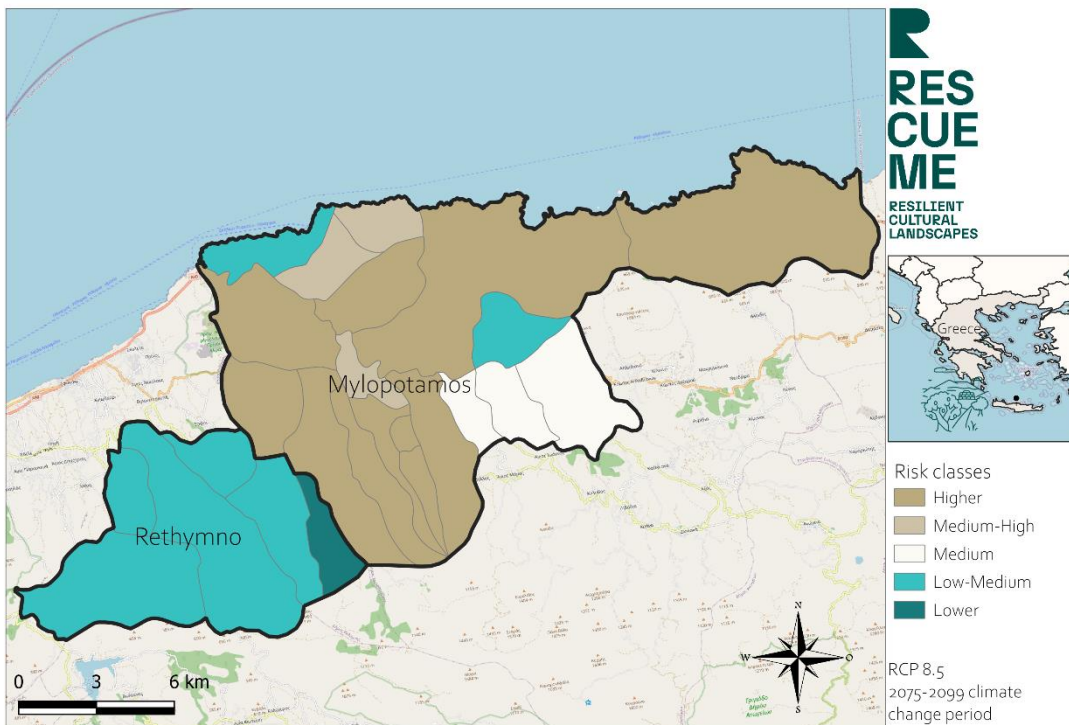


Figure 28. Impact of changes in precipitation on culture. RCP 8.5 (2075-2099)

## 5.3 Portovenere, Cinque Terre and the Islands

### Impacts of landslides on the terraced landscape

#### 5.3.1 Historical period (1981-2010)

The relative risk levels of the communities belonging to the Cinque Terre study area are in the Low to Medium range in most cases. Only in one of the regions, Pignone (11021) is Medium-High risk identified during this period. In this region, the value of risk is mainly attributed to Higher vulnerability values, while the exposure is Low and the hazard is low-Medium. This Medium-High vulnerability is primarily due to the fact that the HV index is the highest of all the regions, accounting for 40 % of the total vulnerability. Other indicators whose values also contribute a relevant load to this component are the categories of “pop\_change” and “elevation\_breakdow\_upland”.

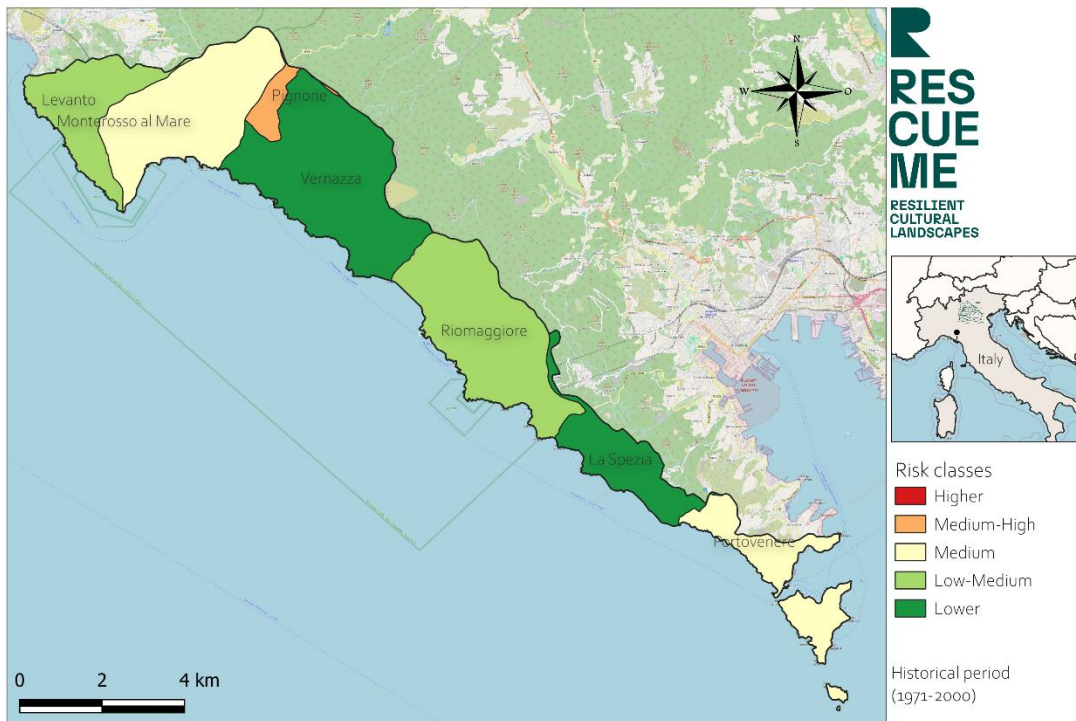


Figure 29. Impacts of landslides on the terraced landscape.

The situation is different in regions where the risk level is Medium, such as Monterosso al Mare (11019) and Portovenere (11022). While Portovenere is also considered more vulnerable, with a Low hazard and Medium exposure, in Monterosso al Mare it is the exposure, that contributes greatly to the increase in risk, with hazard and vulnerability remaining in the background with Low-Medium values.

In the case of Portovenere, the High vulnerability is largely due to the fact that the ES index is the highest of all the regions and has high values for the indicators “elevation\_breakdow\_low\_coast”, “elevation\_breakdow\_high\_coast” and “elevation\_breakdow\_inland”, although less important than that of the ES index. It should also be noted that, when considering all the time periods of the study, the index characterising the hazard is the lowest of all the regions.

The High exposure in Monterosso al Mare is especially explained by high values for the indicators “bed\_places” and “tourist\_acc\_stablis”.

On the other hand, the regions of Levanto (11017) and Riomaggiore (11024) present Low-Medium risk values, albeit with slightly different behaviour in their components. Thus, in Levanto they all have low-medium values. On the contrary, in Riomaggiore, the increase in the exposure value is compensated by a Low vulnerability and a Low-Medium hazard. Finally,

in Vernazza (11030) and La Spezia (11015) the risk levels are Low, with Low levels of hazard and vulnerability and Low-Medium to Medium levels of exposure.

### 5.3.2 RCP 4.5 scenario (2071-2100)

There are two regions where a potential increase in the risk values were identified: Pignone (11021) and Portovenere (11022) (Figure 30). Although vulnerability is High in both regions, the exposure components differ significantly. While in Pignone the hazard is High and the exposure is Low, in Portovenere both components have Medium values.

The region of Monterosso al Mare (11019) is the only one with a Medium-high risk. Here it is the case that, although vulnerability is Low-medium, hazard and exposure values are classified as High.

The level of risk in the regions of Levanto (11017) and Riomaggiore (11024) is Medium. In both cases the hazard is High. However, while exposure and vulnerability are Low-medium in Levanto, in Riomaggiore exposure is High and vulnerability Low.

Among the regions with Lower risk values, we find again Vernazza (11030) and La Spezia (11015), both with Low-medium risk. Vulnerability is Low, exposure is in the Medium range and hazard is in the Medium to Medium-high range.

In terms of hazard, there has been an increase in the values in all regions during this period, resulting in an increase in the assigned risk classes. Consequently, there are no regions with a Low risk, as was the case in the reference period.

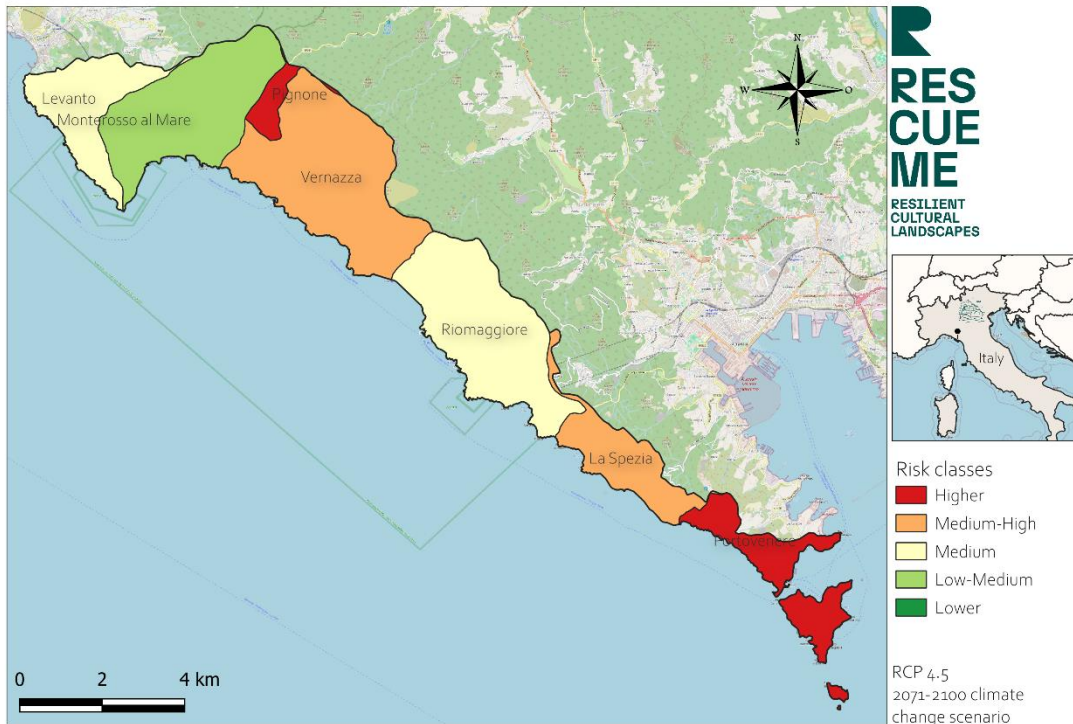


Figure 30. Impacts of landslides on the terraced landscape. RCP 4.5 (2071-2100).

### 5.3.3 RCP 8.5 scenario (2071-2100)

Although the highest risk levels are observed in this scenario for all regions, mainly because the highest hazard levels are observed for all climate scenarios, these changes are not significant enough to warrant a different risk classification for the regions than that already described for the RCP 4.5 scenario (2071 - 2100). Because of that reason, the RCP 8.5 maps and all the risk maps from scenario 4.5 for the period 2041–2070 up to this one can be found in Annex 2.

## 5.4 Defensive system of Zadar

As outlined in the hazard section, only some of the buildings are exposed to coastal flooding. Of the 13 buildings selected for the vulnerability analysis, only one is located within the exposed area. This building houses both the University Library and the Chapel of St. Demetrius.

It should be noted that this exposure only occurs in the long-term scenario projected to the end of the current century, when sea levels are expected to rise by 1.04 and 1.47.

Considering that exposure values for most of the analysed buildings (12 out of 13) are zero, there is no technical basis for conducting a conventional risk analysis in this context. For this reason, a comprehensive analysis of the intrinsic vulnerability of these architectural structures to the various effects of climate change was developed, which goes beyond mere exposure to the studied hazard.

The vulnerability assessment conducted reveals significant findings: nearly half of the evaluated heritage buildings (six out of 13) present vulnerability levels classified as medium or high (Figure 31). Three buildings stand out for their high vulnerability: the Ethnographic Department of the National Museum, St. Anastasia's Cathedral, and St. Donatus' Church. The Ethnographic Department of the National Museum presents the highest vulnerability index of the analysed set. This is primarily based on the exceptional valuation given by experts in two key dimensions which were deemed to be threatened by the hazard: its historical authenticity and its relevance as a tourist attraction and entertainment venue.

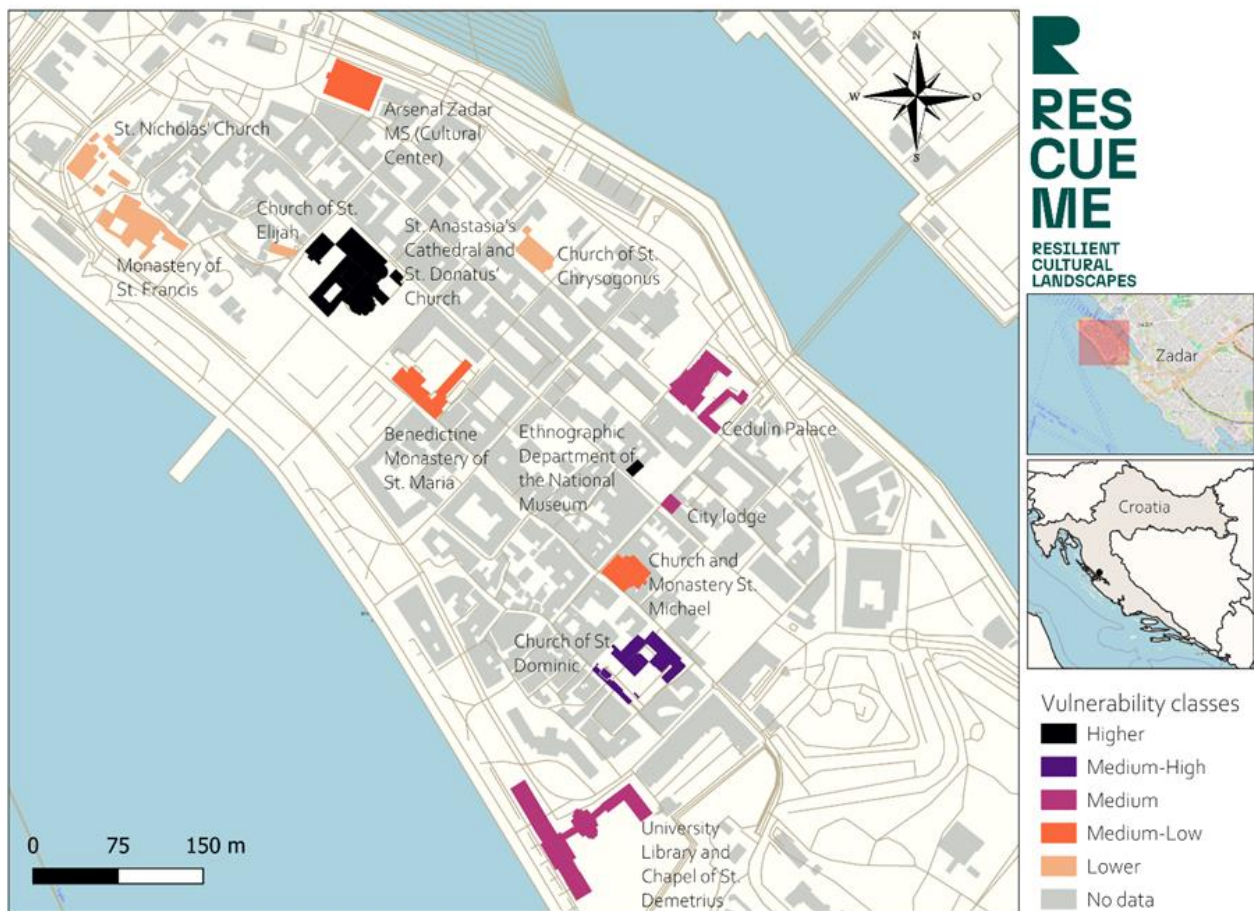


Figure 31. Climate change vulnerability. Source: UNIBO, using data collected through a survey conducted with R-Lab experts.

Regarding St. Anastasia's Cathedral and St. Donatus' Church, their High vulnerability derives mainly from three fundamental dimensions: the technical, workmanship, and traditional knowledge incorporated in their construction; their authenticity and historical importance; and their significant value as tourism and entertainment resources. Meanwhile, the Church of St. Dominic presents a vulnerability level categorised as medium-high. The aspects that significantly increase its vulnerability are primarily related to the technological, workmanship, and traditional knowledge incorporated in its structure and its considerable importance as a tourism and entertainment resource.

Three buildings present Medium vulnerability: the University Library, the Chapel of St. Demetrius, and Cedulin Palace. It is relevant to note that the University Library and the Chapel of St. Demetrius are precisely the only buildings that present direct exposure to climate hazards in the long-term scenario.

The remaining nine buildings present vulnerability levels classified as Medium-Low or Lower. In these cases, the various factors evaluated contribute predominantly to diminishing their vulnerability. This is primarily due to characteristics such as their lesser relevance in terms of historical authenticity, lower impact on tourism and educational character among others.

## 5.5 L'Horta de València

### Impact of torrential rainfall on the agricultural heritage system

#### 5.5.1 Historical period (1971-2000)

In the geographical area of L'Horta de Valencia, an increase in the spatial distribution of flood risk associated with torrential rainfall is observed towards the end of the century (see Figure 32, Figure 33 and Figure 34).

In the historical reference scenario, the spatial distribution of risk presents the following stratification: 18 municipalities (41.9%) are categorised as Low risk, 17 municipalities (39.5%) as Medium-Low risk, 2 municipalities (4.7%) as Medium risk, 6 municipalities (14%) as Medium-High risk, and there is a complete absence of municipalities classified as Higher risk.

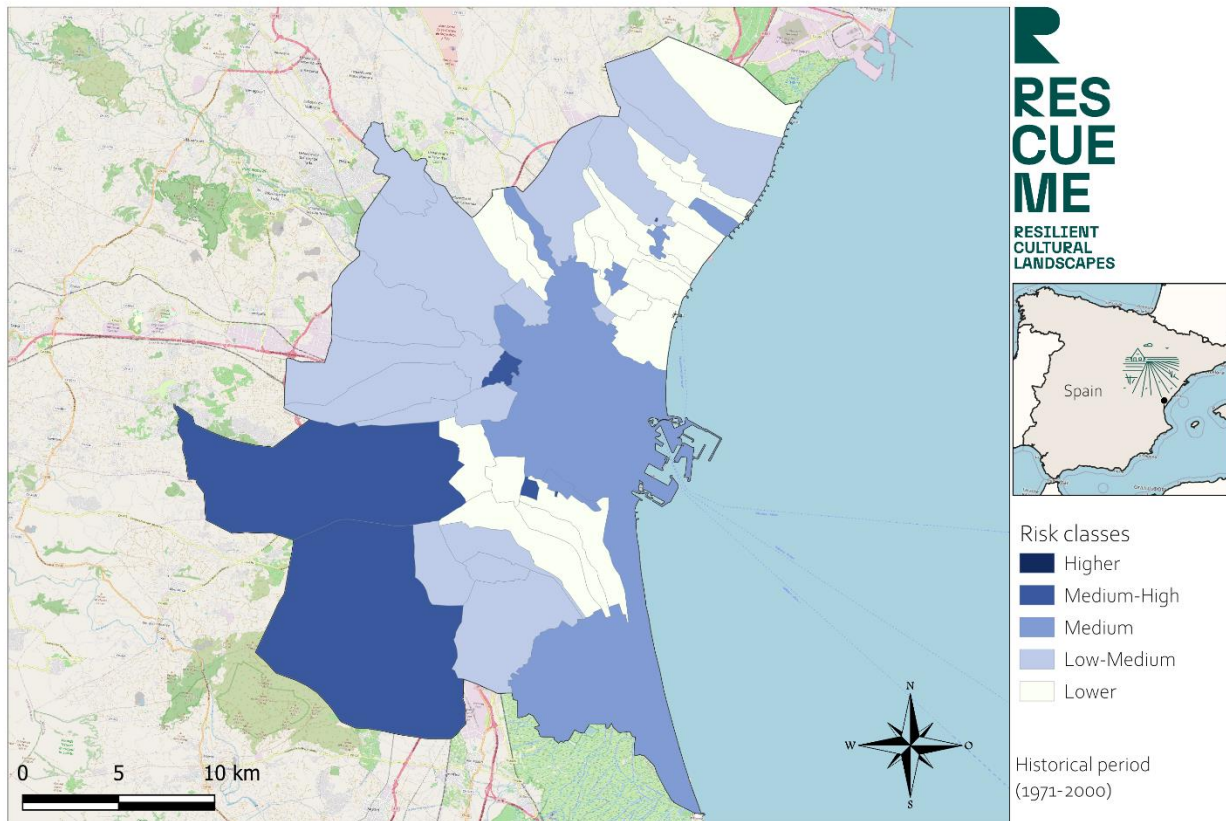


Figure 32. Impacts of torrential rainfall on the agricultural heritage system. Historical period (1971-2000).

The municipalities categorised as Medium-High risk (Benetússer, Mislata, Llocnou de la Corona, Picassent, Torrent, and Emperador) primarily attribute this classification to elevated vulnerability indices. Among these, only Picassent and Torrent exhibit High exposure values, while the remaining municipalities present Low-Medium and Lower exposure metrics.

Sedaví and Valencia are two particularly noteworthy municipalities, as both are classified as Medium risk—albeit for very different reasons. Valencia demonstrates the highest exposure coefficient in the study area, while Sedavi ranks among the lowest in this parameter. Conversely, the vulnerability pattern shows an inverse relationship: Sedavi vulnerability levels are High, whereas Valencia has one of the lowest vulnerability indices.

Exposure values are relatively homogeneous among municipalities classified in the lowest risk categories, with predominantly Lower values. Meanwhile, both hazard and vulnerability parameters are Lower or Low-Medium values across these jurisdictions.

## 5.5.2 RCP 4.5 (2071-2100)

Risk assessment values demonstrate significant alteration in the projections for the end of the century, showing a pronounced increase toward higher risk classifications (Figure 33). This temporal progression is evident in the substantial increase in municipalities categorised in elevated risk brackets. Specifically, 6 municipalities (14% of the regional total) are projected to reach High risk classification, 1 municipality (2.3%) is projected to reach a Medium-High risk category, and 16 municipalities (37.2%) are projected to reach a Medium-risk classification. The remaining 20 municipalities (46.5%) are classified to lie within the Lower risk spectrum (medium-low and low categories).

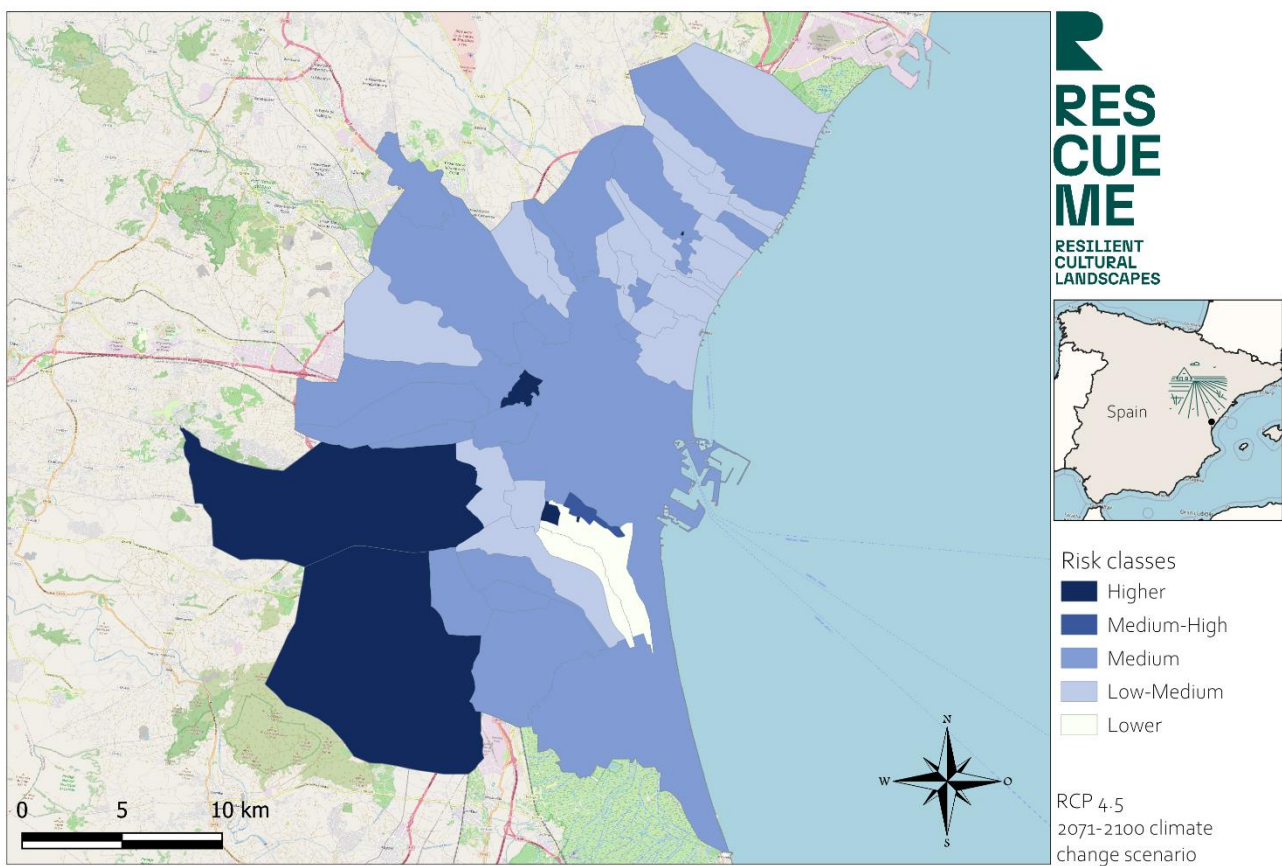


Figure 33. Impacts of torrential rainfall on the agricultural heritage system. RCP 4.5 (2071-2100).

In this scenario, the municipalities of Benetússer, Mislata, Llocnou de la Corona, Picassent, and Torrent exhibit High risk levels. This is primarily due to High values of both hazard and vulnerability. However, in some of these municipalities (Benetússer, Mislata, and Llocnou de la Corona), exposure values are Low or Medium-Low.

Sedaví shows a Medium-High level of risk, representing an increase compared to the previous scenario. This is also driven by High levels of hazard and vulnerability.

Overall, in all municipalities classified as Medium risk, a common pattern is observed: Low exposure, High or Medium-High hazard, and Medium or Low- Medium vulnerability. Given that vulnerability accounts for half of the weight in the risk calculation, even Higher hazard values are not sufficient to significantly raise the overall risk when vulnerability remains moderate or Low.

### 5.5.3 RCP 8.5 (2071-2100)

The RCP 8.5 scenario (high emissions) shows a slightly less severe risk redistribution: 5 municipalities (11.6%) present High risk, 2 municipalities (4.7%) Medium-High risk, 12 municipalities (27.9%) Medium risk, and the remaining 24 municipalities (55.8%) are classified in lower risk categories (Figure 34).

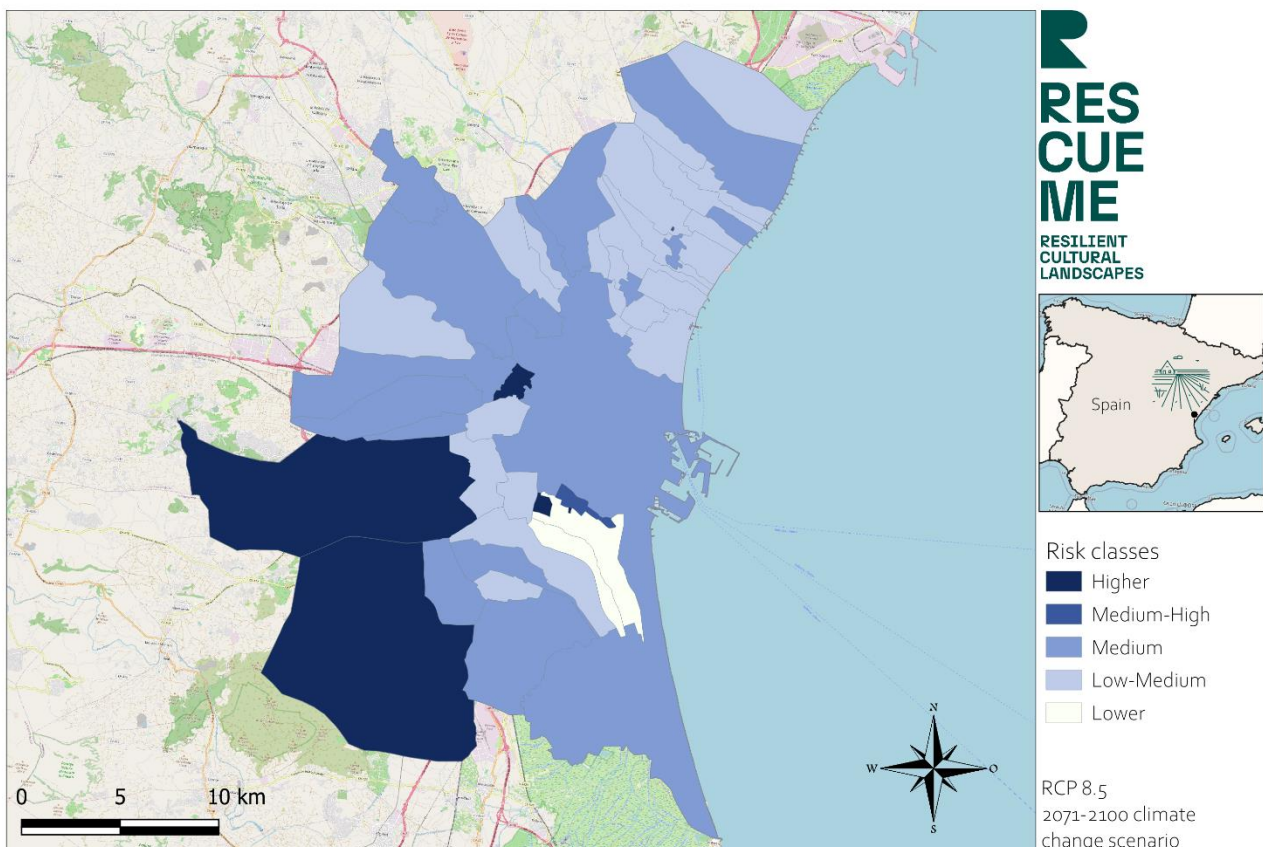


Figure 34. Impacts of torrential rainfall on the agricultural heritage system. RCP 8.5 (2071-2100).

Museros, Xirivella, and Beniparrell represent three significant cases of municipalities that exhibit an increase in their risk profile under the RCP 8.5 scenario compared to RCP 4.5, shifting from a Medium-Low to a Medium risk classification. In contrast, Tabernes Blanques displays a reverse trend, experiencing a reduction in its risk designation from Medium to

Medium-Low. For the remaining municipalities within the analysed area, risk values remain largely consistent with those estimated under the low-emissions scenario.

The prevailing risk pattern observed across all scenarios indicates that vulnerability is the predominant factor in determining overall risk. This conclusion is supported by the paradoxical observation that hazard intensity actually decreases under the high-emissions scenario (RCP 8.5) in comparison to the low-emissions scenario (RCP 4.5), with 12 municipalities classified as high hazard under RCP 4.5, versus only 6 under RCP 8.5. Despite this reduction in hazard, overall risk levels remain notably stable across scenarios, definitively confirming that vulnerability metrics exert the dominant influence on the integrated risk assessment outcomes.

## Impact of droughts on the agricultural heritage system

In the Valencia region, the impact of droughts on the agricultural heritage system is projected to intensify when comparing the historical reference scenario with future climate scenarios. In the historical scenario, the spatial distribution of risk shows that only five municipalities are classified as Medium-High risk, three as Medium, 29 as Medium-Low, and eight as Lower (Figure 35). By the end of the century, however, at least half of the municipalities are expected to experience risk levels of Medium or higher.

Unlike the previously analysed impact of torrential rainfall, a substantial divergence is observed between the two emissions scenarios in the case of drought-related risk. It is important to note that the data model used for both types of hazards applies the same weighting structure, with vulnerability accounting for 50% of the total risk score. This underlines that the projected increase in drought hazard – reflected in the significant reduction of wet days – is sufficient to drive the observed differences in risk levels between the RCP scenarios. A detailed breakdown of this analysis is presented in the following section.

### 5.5.4 Historical period (1971-2000)

In this scenario, drought risk is Medium or higher in only 8 out of 45 municipalities (approximately 20%). Of these 8, only 5 exhibit Medium-High risk, while the remaining 3 have Medium risk. The five municipalities with Medium-High risk are Benetusser, Mislata, Llocnou de la Corona, Torrent, and Emperador. As expected, these municipalities also present High vulnerability, given that the weighting of vulnerability accounts for half of the overall risk in this context.

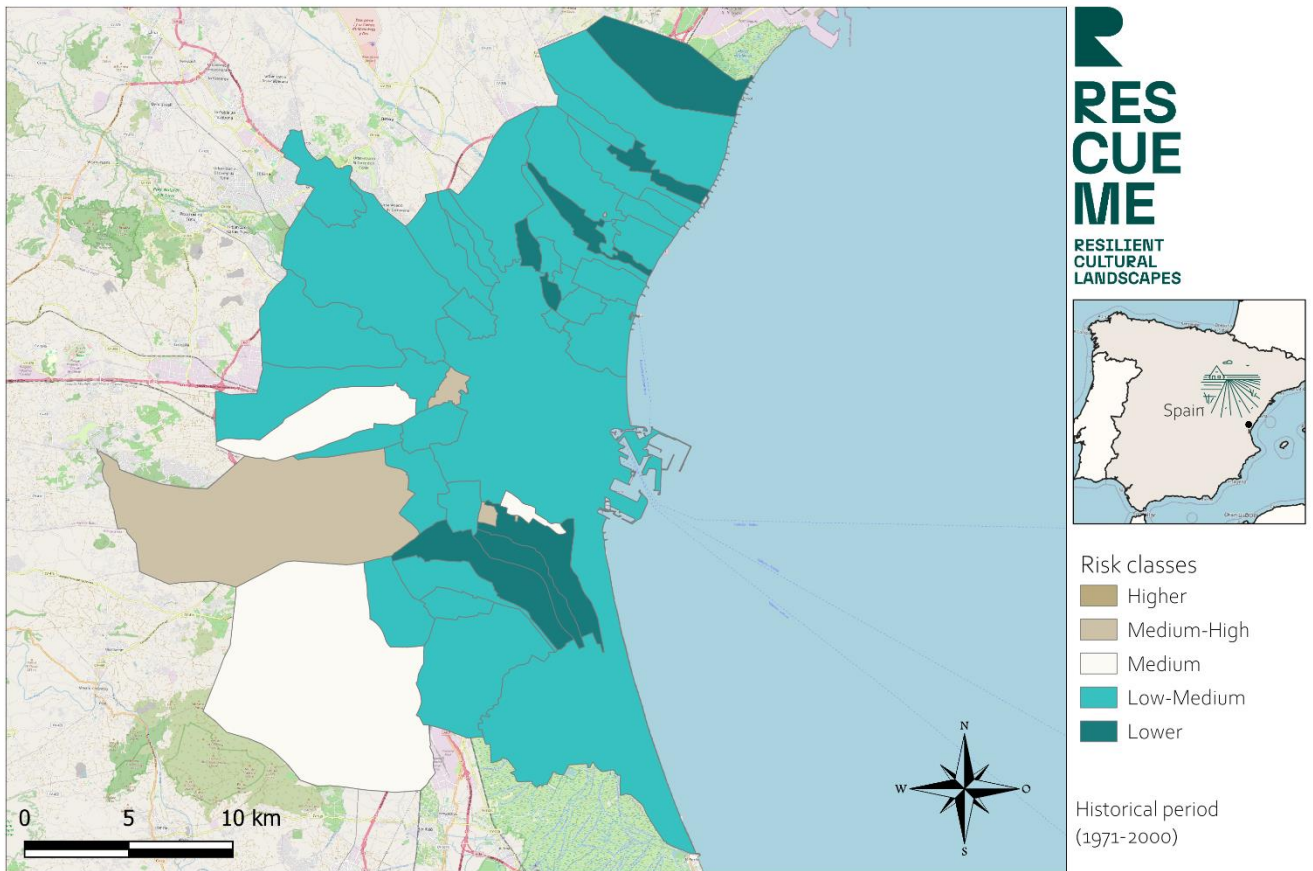


Figure 35. Impact of droughts on the agricultural heritage system. Historical period (1971-2000).

### 5.5.5 RCP 4.5 (2071-2100)

In the low-emission scenario for the end of the century, the situation changes considerably compared to the historical period. Seventeen municipalities exhibit Medium or higher risk, doubling the number compared to the historical scenario. Additionally, in this scenario, there are three municipalities with the highest risk level (Benetusser, Mislata, and Llocnou de la Corona). In contrast to that, the only three municipalities that remain at the lowest risk level are Massanassa, Alfafar, and Catarroja, although they still show Medium hazard values. In fact, hazard levels are Medium or Medium-High across the territory, except in eight municipalities. Exposure, meanwhile, has Low or Low-Medium values in 90% of the L’Horta de Valencia area.

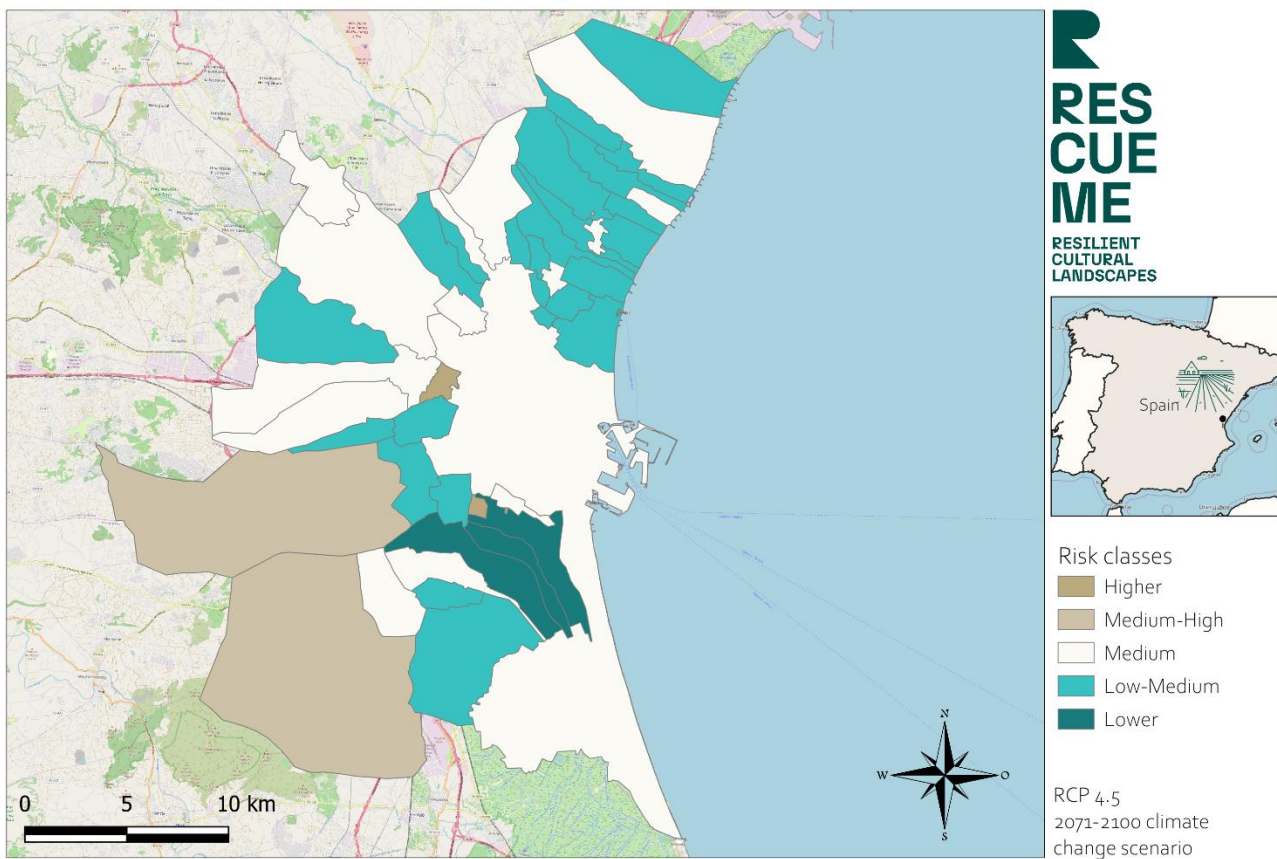


Figure 36. Impact of droughts on the agricultural heritage system. RCP 4.5 (2071-2100).

### 5.5.6 RCP 8.5 (2071-2100)

The high-emission scenario indicates greater water stress, which corresponds to an increased number of municipalities with high risk. In this case, ten municipalities exhibit Higher or Medium-High risk, while 23 have Medium risk. In other words, only twelve municipalities have Lower or Low-Medium risk, representing approximately 30% of the total area.

It is important to recall that vulnerability accounted for 50% of the weighting, while hazard only accounted for 20%. Therefore, it can be inferred that hazard values are Higher in this scenario to result in high-risk levels for so many municipalities. In fact, hazard values are High or Medium-High in all of them. With the exception of three municipalities, exposure levels are Low or Low-Medium.

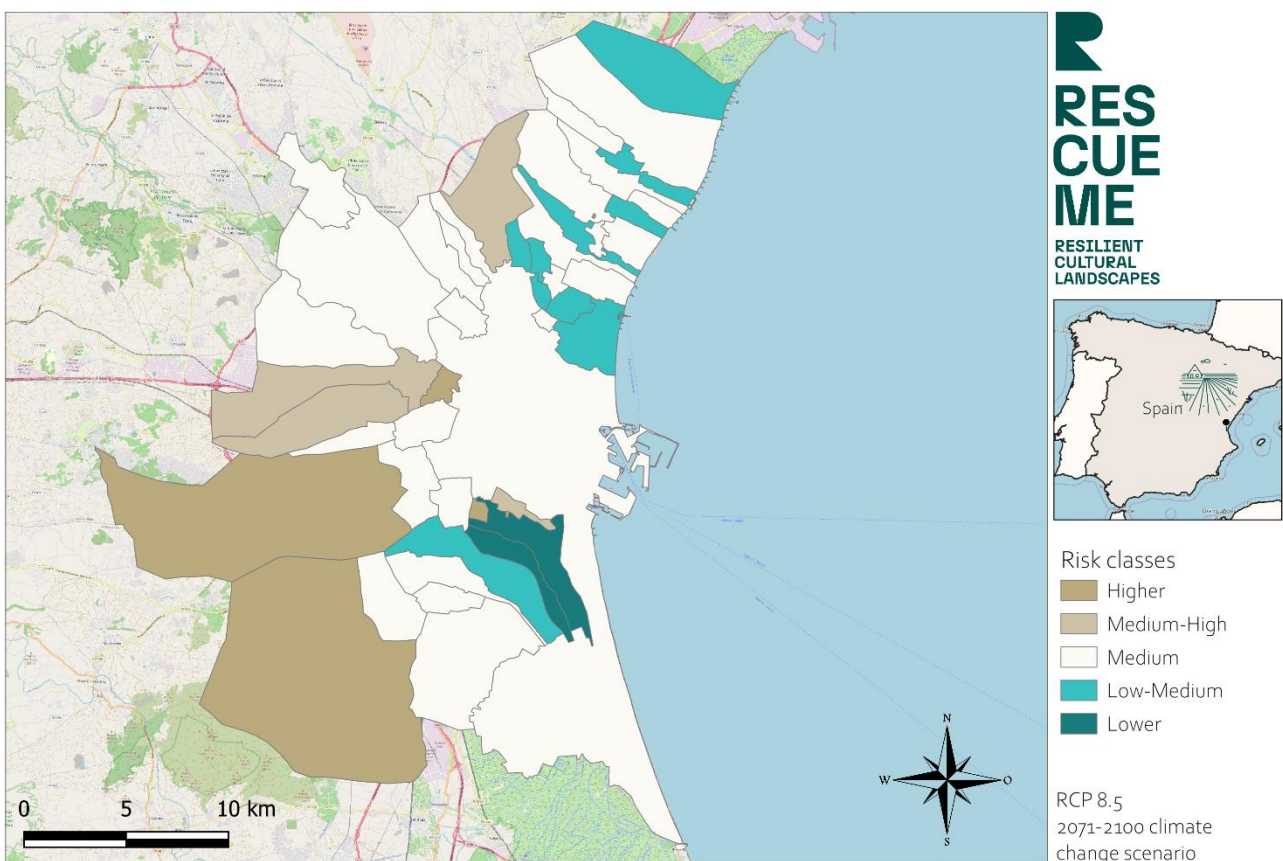


Figure 37. Impact of droughts on the agricultural heritage system. RCP 8.5 (2071-2100).

## 5.6 Comparing the local outcomes with the global outcomes

Analysing case studies from a local perspective makes it possible to focus the study on problems specifically identified by R-labs members. These problems, along with information provided by the R-Labs themselves, have already been identified in some cases through the risks analysed in the Atlas for all European coastal regions (NUTS3) (Klose et al., 2024). Many of the risks analysed at the local level are particularly relevant in the NUTS3 regions to which the case study areas belong. However, it should be noted that the results of the risk analyses are based on data models which, although relating to cultural heritage, differ in that they must consider the availability of data on a scale larger than Europe. Therefore, results obtained at the European level should not be compared with those of the case studies, even when the risk appears to be the same. Similarly, it is not advisable to compare results from one case study with those from another, as there are many reasons not to do so: local indicators may differ depending on data availability, periods and climate scenarios may not coincide, and the weights of indicators and risk components agreed by the R-Labs will not be identical. With this caveat in mind, the following presents the relationship identified between the two analyses, intended solely for exploratory purpose.

In Neuwerk (Hamburg, Germany), the study at NUTS3 level (Hamburg) of this coastal flood hazard confirmed that this is a hazard that will evolve negatively in all the scenarios. The data for the reference period (1981-2010) shows that the risk for this hazard could be classified as having a medium risk. However, projections for the period 2070–2100 under both RCP 4.5 and RCP 8.5 scenarios indicate a shift to a high-risk classification. Even under the more optimistic RCP 2.6 scenario, the risk class is expected to increase. Overall, the data reflects a consistent upward trend in flood risk, with a general increase of one risk level across future climate scenarios. At the local level, a hydrodynamic numerical modelling approach has been adopted to characterise and quantify the hazard posed by coastal flooding and storm surges under extreme conditions, specifically those corresponding to an RCP 8.5 scenario and horizon 2100. This assessment focuses on the island's buildings and agricultural lands. The risk analysis shows that in this case vulnerability is a more critical factor than the hazard itself. Parcels along the island's perimeter, associated with coastal infrastructure, exhibit moderate risk due to high vulnerability despite moderate hazard levels. Northern and southern parcels have higher risk due to high exposure and vulnerability, but most parcels on the island are characterized by low risk, primarily due to low exposure. Regions without significant population, tourism infrastructure, or agricultural activity have minimal risk compared to other parcels.

In the Psiloritis UNESCO Global Geopark, the shifting temperature and precipitation patterns have been analyzed and assessed locally. In the regional study (at the NUTS3 of Rethymno level), the risks were considered high in all the scenarios for heatwaves and very high for all the scenarios regarding the draught risk. In the local analysis, regarding the impact of changes on temperature on culture, during the historical period from 1980 to 2004, none of the 25 communities in the Psiloritis study area were classified as being at high risk. And only 5 communities were identified as having a medium-high risk level. The hazard level was low, but either exposure or vulnerability was elevated. Looking ahead to the RCP 4.5 scenario for the period 2075 to 2099, the same five communities previously at medium-high risk are projected to shift into the high-risk category. This change is primarily due to an increase in hazard levels from low to medium. Additionally, several new communities are expected to enter the medium-high risk category. In these areas, the hazard level is medium, exposure ranges from low-medium to medium, and vulnerability is medium-high to high. Again, high HV and ES index values are key contributors to their elevated risk. Under the more severe RCP 8.5 scenario for the same future period (2075–2099), nearly all communities that were previously at high or medium-high risk under RCP 4.5 are projected to face high risk. This is attributed to a further increase in hazard levels, which reach medium-high across these communities. Regarding the impact of changes in precipitation patterns on culture, during the historical period of 1980-2004, 5 communities already exhibited medium-high risk levels due to climate-related hazards, despite having low hazard levels. Their high exposure and vulnerability levels made them more susceptible. Climate scenarios predict increased risk levels for these 5 communities, with hazard levels expected to rise from low to medium. An additional 8 communities will also be at risk, with medium hazard levels and low-medium or medium exposure, but higher vulnerability levels. In the most extreme scenario, all 5 previously identified high-risk communities will face even greater hazards, with hazard levels increasing from medium to medium-high. In total, 14 communities will be at high or medium-high risk, with 3 more experiencing medium-high risk levels, and others being less affected due to reduced exposure and vulnerability.

As discussed in Section 4.4.1, shallow landslides triggered by rainfall are a major natural hazard in Cinque Terre and the surrounding Eastern Ligurian Riviera. Due to their frequency and potential for severe damage, they are considered the region's most critical geohazard. Regional-scale analysis, at La Spezia NUTS3 level, confirms that landslide risk, together with the pluvial floods risk, in this area is extremely high and is projected to remain so across all assessed climate scenarios. At local scale, we can see that during the historical period (1981–2010), landslide risk levels across the Cinque Terre study area were generally in the low to medium range. In most communities, the risk was moderate, with only one area showing a medium-high risk level. As we have seen in the other cases, this elevated risk was primarily due to high vulnerability, particularly influenced by demographic changes and topographic characteristics, while hazard and exposure remained relatively low. In other areas with medium risk, the contributing factors varied, some were driven by higher

vulnerability, while others were more affected by increased exposure, such as tourism-related infrastructure. Regions with low-medium or lower risk typically exhibited balanced or low values across all three components: hazard, vulnerability, and exposure. Under the RCP 4.5 climate scenario for the future period (2071–2100), risk levels increase across the entire region, with no areas remaining in the lower risk category. This shift is largely due to a general rise in hazard levels. In the RCP 8.5 scenario for the same future, the highest hazard levels are observed across all regions, making it the most severe scenario. However, the increase in hazard does not significantly alter the overall classification of risk levels compared to the RCP 4.5 scenario, resulting in no changes to the overall distribution of risk categories.

For Zadar R-Lab the identified hazards have been coastal flooding and storm. According to the regional assessment, at Zadarska županija NUTS3 level, the evolution of coastal flood risk over time indicates a clear upward trend. During the historical period (1981–2010), the risk class was categorized as medium. However, projections for the future under both RCP 4.5 and RCP 8.5 scenarios for the period 2070–2100 show an increase to a high-risk classification. For the local assessment, a detailed hazard modelling approach has been adopted and deployed, following the steps as given for the Neuwerk case. The analysis of coastal flood exposure in the study area reveals that only a small portion of buildings are at risk, with just one out of the 13 buildings selected for vulnerability assessment located within the projected flood zone. However, the vulnerability assessment yielded more significant insights: nearly half of the buildings analyzed exhibit medium to high vulnerability related to their cultural significance.

In the L'Horta de Valencia R-Lab, droughts and torrential rainfall are the most significant climate-related hazards, both driven by changes in precipitation patterns. In the analysis at the regional level, at Valencia/València NUTS3 level, risk from pluvial flooding has remained consistently high from the historical period (1981–2010) through all future climate scenarios (RCP 2.6, 4.5, and 8.5). Similarly, drought risk has been persistently very high, showing no change across scenarios, indicating a sustained vulnerability. In the study carried out at the local level, historical flood risk (1971–2000) was generally moderate, with no municipalities classified as high risk. Under RCP 4.5 scenario, six municipalities are projected to reach high risk, and under RCP 8.5, five municipalities fall into this category. Despite slightly lower hazard levels in RCP 8.5, overall risk remains stable due to the dominant influence of vulnerability again. For droughts, historical risk was medium or higher in only eight municipalities. By 2071–2100, under RCP 4.5, this number more than doubles, with three municipalities reaching the highest risk level. Under RCP 8.5, drought risk intensifies further, with ten municipalities at high or medium-high risk and only twelve remaining at low or very low risk. This increase is driven by higher hazard levels and persistent vulnerability, despite generally low exposure across the region.

It is essential to acknowledge, again, that the results presented in this report are not directly comparable across the case studies or with the European reference study due to the unique nature of each case and differences in methodology and parameters used. Each case study has its own specific characteristics and risk factors, making comparison challenging and rendering a common comparison framework infeasible. Therefore, each case study should be interpreted independently, considering the results in the context of its own specific conditions. While always bearing this in mind several conclusions can be drawn, based on a broad and general analysis rather than a detailed and exhaustive comparison:

- The importance of localized approaches in understanding and managing climate-related hazards should be highlighted. While regional (NUTS3-level) assessments provide a broad overview, local studies reveal more nuanced patterns shaped by specific exposure, vulnerability, and land-use characteristics. This localized perspective is essential for identifying context-specific vulnerabilities and designing targeted adaptation strategies.
- A consistent finding across all case studies (Neuwerk, Psiloritis, Cinque Terre, Zadar, and L'Horta de Valencia) and all analysis scales, is that vulnerability is the dominant perceived factor from the local stakeholders and therefore is influencing the overall risk. Even in areas where hazard levels are moderate or low, high vulnerability, often linked to cultural heritage, can significantly elevate risk levels. This underscores the need to prioritize vulnerability reduction in climate adaptation planning, particularly by adopting a cultural heritage-based approach when such planning is applied to cultural landscapes
- Risk trends observed at the regional level generally show an increase under future climate scenarios, particularly RCP 4.5 and RCP 8.5. Local analyses confirm these trends but often reveal lower or more varied risk levels, depending on the specific characteristics of each area. This variation reinforces the value of local assessments in complementing broader regional models.
- In Neuwerk and Zadar, detailed hydrodynamic modelling provided a more precise understanding of coastal flood risk. It identified specific zones of concern, such as coastal infrastructure and agricultural land, and reduced the perceived severity of risk at a regional scale. These insights would not have been apparent through regional-scale assessments alone, demonstrating the added value of localised hazard modelling.
- The inclusion of cultural heritage in risk assessments adds an additional, a necessary, layer of complexity. In Zadar, for example, although only one building is exposed to coastal flooding, nearly half of the assessed heritage buildings exhibit medium to high vulnerability due to their cultural significance. This highlights the importance of integrating qualitative cultural values into semiquantitative and quantitative risk frameworks to ensure that heritage assets are adequately protected in the face of climate change.

## 6 Conclusions

Effective climate change risk assessments must be based on robust, context-specific data aligned to the assessment's purpose and scale. Local-level assessments often require detailed datasets to support decision-making. These data cover climate scenarios, as well as information on the exposure and vulnerability of populations, infrastructure, natural environments, culture, and other assets. However, such assessments are often constrained by the limited availability of data, which rarely aligns with the initial theoretical model.

While detailed assessments offer more accuracy, they are complex and resource-intensive due to the comprehensive information required. Consequently, data constraints can pose significant barriers and must be addressed at the very beginning of the assessment process. This is particularly true when accessing data that may conflict with data protection regulations, especially when the level of detail is high. However, access to precompiled administrative data through statistical portals can ease this challenge, particularly in regions where municipalities serve as the basic territorial units. Establishing the boundaries of a risk assessment involves defining its core elements: setting the guiding principles, selecting appropriate methodologies, and outlining the scope, objectives, timeframe, climate scenarios, and geographic boundaries. The primary goal is to identify key climate risks by analysing hazards, vulnerabilities, and exposures across different sectors and communities. This analysis must strike a balance between data availability, the resources needed to obtain additional data, and the prioritisation of critical assessment components.

RescueME encompasses a diverse range of R-Labs that differ in terms of the types of climate risks and landscape features they cover, as well as geographic scale and data maturity. When designing each assessment, it is essential to identify which landscape characteristics have different values and could significantly affect vulnerability across spatial units.

For example, the island of Neuwerk presents a small-scale case where territorial units correspond to cadastral lots. Although hazard and exposure values can be modelled, assessing vulnerability requires identifying essential elements that vary meaningfully across units. Early discussions centred on the island's inhabited and build-up areas, however, since the number of buildings is limited, they are spatially concentrated and share similar constructive characteristics, collecting data through in-situ surveys was considered too resource-intensive for the limited analytical benefit they would provide. Instead, the focus shifted to factors that differ across units and contribute more directly to landscape vulnerability, but still related to properties, agricultural holdings, and tourism facilities.

In the case of Neuwerk, the main results indicate that by the year 2100, under a sea-level rise scenario of 1 meter, storms will pose a medium risk to the peripheral areas of the island.

In the island's interior, high risk is projected for specific parcels – particularly those hosting residential areas and tourist facilities – while most of the island will remain within the low-risk category. For both the baseline scenario and the 2050 projection, storm-related hazard was not significant in any parcel, and therefore, no exposure of grazing areas or tourism assets was identified. It is important to note that the hazard assessment may be subject to limitations, given the complexity and number of variables involved in storm modelling for an island such as Neuwerk.

L'Horta de València covers a much broader area – 45 municipalities – where more data are typically available, as the unit of analysis matches with statistical units. This enables a data-rich, indicator-based analysis that includes cultural practices and agricultural traditions. Here, specific indicators for the R-Lab were identified and selected to reflect the heritage value of the region's historical irrigation systems.

In L'Horta de Valencia, the impact of torrential rainfall on the agricultural heritage system is projected to rise over the course of the century, with a significant number of municipalities expected to experience high or medium-high risk levels compared to the historical scenario. However, it is important to note that the hazard projections do not differ substantially under the high-emissions scenario. As a result, overall risk levels remain similar under both RCP 4.5 and RCP 8.5. In fact, in some municipalities, the projected risk under RCP 8.5 is slightly lower than under RCP 4.5.

Regarding the impact of droughts on the agricultural heritage system, the spatial distribution of high-risk values changes significantly over time. In the historical scenario, most municipalities exhibit low or very low risk levels. However, by the end of the century, under both RCP 4.5 and RCP 8.5, this distribution shifts markedly, with most municipalities transitioning to medium, medium-high, or high-risk categories. Although RCP 8.5 yields slightly higher risk values than RCP 4.5, the difference between the two scenarios is not substantial in terms of overall spatial risk patterns.

The Portovenere, Cinque Terre and the Islands case followed a similar approach at the municipal level, although with fewer analysis units, compared to L'Horta de Valencia. While several indicators were available, stakeholders emphasised the need to identify areas undergoing land abandonment – critical information that was not readily accessible. Given its importance, targeted efforts were made to derive this data to ensure a comprehensive understanding of vulnerability.

In this R-Lab, the impacts of landslides on the terraced landscape increase substantially from the historical scenario to the projected future scenarios. While most municipalities exhibit medium-low or low risk levels in the historical baseline, under future conditions, more than 70 % of the territory is classified as having medium or medium-high risk. Although

the hazard component shows a slight increase over the course of the century, this change is not significant enough to alter the overall risk classification. As a result, risk levels remain stable between future scenarios despite minor variations in hazard intensity.

In Zadar, the focus was on the historic peninsula, but data availability was limited to the municipal level and could not be disaggregated to suit the finer scale required. Assigning the same values to all units would have added little analytical value. Therefore, the building level was selected as the unit of analysis, requiring significant effort to collect data and construct a new GIS database from scratch. This low-data scenario provided a starting point for an evolving information system, with a dedicated survey conducted to assess vulnerabilities in the absence of sufficient quantitative data.

The results show that approximately half of the buildings analysed exhibit medium to higher levels of vulnerability. Among them, only the University Library and the Chapel of St. Demetrius are currently exposed to the identified hazard. It should be noted that the hazard modelling may contain certain inaccuracies. Therefore, a more detailed and in-depth analysis is recommended to enhance its accuracy and reliability.

Finally, the Psiloritis Geopark in Crete, although most data were available at the municipal level, the limited number of areas involved justified using a sub-municipal scale (communities) for the assessment. Some relevant indicators, including those related to agricultural exposure and ecosystem services, were available and supported a more granular analysis.

The results for the Psiloritis Geopark indicate that risk levels, related to temperature changes, will increase substantially under the projected scenarios. While all communities currently fall within the low to medium risk categories in the historical baseline, they are expected to shift toward medium to high risk levels in future scenarios. Although hazard levels increase across the entire territory, the centre and the northeastern sector (Municipality of Mylopotamos) is projected to experience more pronounced changes. As a result, communities in this area are expected to face higher risk compared to those within the Municipality of Rethymno.

A similar pattern is observed in the impact associated with changes in precipitation patterns. While none of the 25 communities exhibited the highest level of risk under the historical scenario, in the high-emissions scenario most communities within the Municipality of Mylopotamos show the highest risk levels. This increase is primarily attributed to a more pronounced decrease in the hazard component in Mylopotamos compared to other areas.

In conclusion, it is useful to compare the weights assigned to the different risk components across the various R-Labs, as these weights fundamentally shape the risk results summarized above.

Vulnerability consistently received the highest weight across all case studies – except in Zadar, where this methodological step was omitted due to the absence of hazard, exposure, and therefore risk. In the remaining cases, vulnerability was assigned a minimum weight of 40 %, reaching up to 50 % in some instances. This highlights the significant influence of the intrinsic characteristics of each analysis unit on the final risk values.

The hazard component, by contrast, was uniformly assigned a lower weight across all case study areas, typically ranging between 20 % and 30 %, reflecting a consensus among experts on its comparatively lesser influence in the overall risk calculation.

Exposure was the most variable component in terms of expert weighting, with assigned values ranging from 20 % to 40 %. This variation suggests that the perceived importance of exposure is more context-dependent, likely influenced by the specific socio-spatial dynamics and data availability in each study area.

## 7 References

- AEMET. (n.d.). Valencia Aeropuerto: Valencia Aeropuerto - Absolute extreme values - Selector - State Meteorological Agency - AEMET - Spanish Government. Agencia Estatal de Meteorología (AEMET). Retrieved 22 September 2024, from [https://www.aemet.es/en/serviciosclimaticos/datosclimatologicos/efemerides\\_extremos](https://www.aemet.es/en/serviciosclimaticos/datosclimatologicos/efemerides_extremos)
- Azzopardi, E., Kenter, J. O., Young, J., Leakey, C., O'Connor, S., Martino, S., Flannery, W., Sousa, L. P., Mylona, D., Frangoudes, K., Béguier, I., Pafi, M., da Silva, A. R., Ainscough, J., Koutrakis, M., da Silva, M. F., & Pita, C. (2023). What are heritage values? Integrating natural and cultural heritage into environmental valuation. *People and Nature*, 5(2), 368–383. <https://doi.org/10.1002/pan3.10386>
- BOE-A-2023-4378. Law 6/2022, of 5 December 2022, on Climate Change and Ecological Transition of the Valencian Community. <https://www.boe.es/eli/es-vc/l/2022/12/05/6>
- Bogaard, T., Geco, R., (2018). Invited perspectives: Hydrological perspectives on precipitation intensity-duration thresholds for landslide initiation: proposing hydro-meteorological thresholds, *NHESS*, 18, 31–39, 2018, <https://doi.org/10.5194/nhess-18-31-2018>
- Bollmeyer, C., Keller, J. D., Ohlwein, C., Wahl, S., Crewell, S., Friederichs, P., ... & Steinke, S. (2015). Towards a high-resolution regional re-analysis for the European CORDEX domain. *Quarterly Journal of the Royal Meteorological Society*, 141, 1–15. <https://doi.org/10.1002/qj.2486>
- Brunetti, M., Melillo, M., Gariano, S.-L., Guzzetti, F., Bartolini, D., Brutti, F., ... & Peruccacci, S. (2024). e-ITALICA (enhanced ITALian rainfall-induced Landslides CAtalogue) [Data set]. Zenodo. <https://doi.org/10.5281/zenodo.14204473>
- Conforti, M., Rago, V., Muto, F., & Versace, P. (2016). GIS-based statistical analysis for assessing shallow-landslide susceptibility along the highway in Calabria (Southern Italy). *Rendiconti Online della Società Geologica Italiana*, 39, 155–158. <https://doi.org/10.3301/ROL.2015.184>
- Croatian Hydrometeorological Office (Državni hidrometeorološki zavod). (2025). Retrieved February 2025, from <https://hidro.dhz.hr/>
- Di Napoli, M.; Di Martire, D.; Bausilio, G.; Calcaterra, D.; Confuorto, P.; Firpo, M.; Pepe, G.; Cevasco, A. Rainfall-Induced Shallow Landslide Detachment, Transit and Runout Susceptibility Mapping by Integrating Machine Learning Techniques and GIS-Based Approaches. *Water* 2021, 13, 488. <https://doi.org/10.3390/w13040488>

Di Napoli, M., Di Martire, D., Bausilio, G., Calcaterra, D., Confuorto, P., Firpo, M., ... & Cevasco, A. (2021). Rainfall-induced shallow landslide detachment, transit and runoff susceptibility mapping by integrating machine learning techniques and GIS-based approaches. *Water*, 13(4), 488. <https://doi.org/10.3390/w13040488>

ESPON (2022). ESPON-CLIMATE Update 2022. Updating and Integrating CLIMATE Datasets and Maps. Final Report. (D. Navarro, J. Lizundia-Loiola, J. Paz, B. Abajo-Alda, C. Cantergiani, G. García, & E. Feliu, Eds.). ESPON EGTC. <https://www.espon.eu/projects/espon-2020/monitoring-and-tools/climate-data-and-maps-update>

EurOtop Manual. (2018). Retrieved May 2025, from <https://www.overtopping-manual.com/eurotop/downloads/>

European Environmental Agency. (2016). European Digital Elevation Model (EU-DEM). <https://sdi.eea.europa.eu/catalogue/srv/api/records/d08852bc-7b5f-4835-a776-08362e2fbf4b>

Faggian, P., Trevisiol, A. (2024) Climate extreme scenarios affecting the Italian energy system with a multi-hazard approach. *Bull. of Atmos. Sci. & Technol.* 5, 4 (2024). <https://doi.org/10.1007/s42865-024-00067-w>

Flanders Marine Institute (VLIZ), & Intergovernmental Oceanographic Commission (IOC). (2025). Sea level station monitoring facility. <http://www.ioc-sealevelmonitoring.org>

Freie und Hansestadt Hamburg, Landesbetrieb Geoinformation und Vermessung (LGV). (2022). Digitales Höhenmodell Hamburg DGM 1. <https://suche.transparenz.hamburg.de/?q=dgm>

Fröhle, P., & Manojlovic, N. (2022). Project TideelbeKlima. <https://www.tuhh.de/wb/forschung/aktuelle-projekte/tideelbeklima>

Gandini, A., Egusquiza, A. (2023). RescueME Deliverable D1.1: Actionable resilient historic landscape framework.

GEBCO Compilation Group. (2019). GEBCO 2019 Grid. <https://doi.org/10.5285/836f016a-33be-6ddc-e053-6c86abc0788e>

Greco, S., Ishizaka, A., Tasiou, M. *et al.* On the Methodological Framework of Composite Indices: A Review of the Issues of Weighting, Aggregation, and Robustness. *Soc Indic Res* 141, 61–94 (2019). <https://doi.org/10.1007/s11205-017-1832-9>

Greek Water Authority. (2025). Retrieved April 2025, from <https://www.apdkritis.gov.gr/el>

Hamel, P., Bosch, M., Tardieu, L., Lemonsu, A., de Munck, C., Nootenboom, C., Viguí, V., Lonsdorf, E., Douglass, J. A., & Sharp, R. P. (2024). Calibrating and validating the Integrated Valuation of Ecosystem Services and Tradeoffs (InVEST) urban cooling model: Case studies in France and the United States. *Geoscientific Model Development*, 17(12), 4755–4771. <https://doi.org/10.5194/gmd-17-4755-2024>

Hong, Y., & Adler, R. F. (2008). Estimation of global SCS curve numbers using satellite remote sensing and geospatial data. *International Journal of Remote Sensing*, 29(2), 471–477. <https://doi.org/10.1080/01431160701264292>

Hu, Y., Wang, C., & Li, J. (2023). Assessment of Heat Mitigation Services Provided by Blue and Green Spaces: An Application of the InVEST Urban Cooling Model with Scenario Analysis in Wuhan, China. *Land*, 12(5), Article 5. <https://doi.org/10.3390/land12050963>

IFFI. (2025). Italian Landslide Inventory. <https://www.progettoiffi.isprambiente.it/>

IPCC. «Annex VII Glossary». En *Climate Change 2021: The Physical Science Basis. Contribution of Working Group I to the Sixth Assessment Report of the Intergovernmental Panel on Climate Change*, 2215-56. Cambridge, United Kingdom and New York, NY, USA: Cambridge University Press, 2021. [https://www.ipcc.ch/report/ar6/wg1/downloads/report/IPCC\\_AR6\\_WGI\\_AnnexVII.pdf](https://www.ipcc.ch/report/ar6/wg1/downloads/report/IPCC_AR6_WGI_AnnexVII.pdf).

ITALICA. (2025). Retrieved May 2025, from <https://zenodo.org/records/8009366>

Kabir, R., Akter, M., Karim, D. S., Haque, A., Rahman, M., & Sakib, M. (2019). Development of a Matrix Based Statistical Framework to Compute Weight for Composite Hazards, Vulnerability and Risk Assessments. *Climate*, 7(4), Article 4. <https://doi.org/10.3390/cli7040056>

Kappes, M. S., Papathoma-Köhle, M., & Keiler, M. (2012). Assessing physical vulnerability for multi-hazards using an indicator-based methodology. *Applied Geography*, 32(2), 577–590. <https://doi.org/10.1016/j.apgeog.2011.07.002>

Klose A., Abajo-Alda B., Lopez de Aguilera A., Gandini A., Egusquiza A., Usobiaga E., Benedito M., Zubiaga M., Simon A., Santangelo A., Salpina D., Manojlovic N., Durrant L. (2024). RescueME Deliverable D1.2: Atlas of European coastal heritage landscape typologies and climate change impacts

Kolokotsa, D., Psomas, A., & Karapidakis, E. (2009). Urban heat island in southern Europe: The case study of Hania, Crete. *Solar Energy*, 83(10), 1871–1883. <https://doi.org/10.1016/j.solener.2009.06.018>

Kuhn, M., Wickham, H., & Hvitfeldt, E. (2025). recipes: Preprocessing and feature engineering steps for modeling (Version 1.3.0) [R package].  
<https://github.com/tidymodels/recipes>

Lombardini, G., & Scorza, F. (2016). Resilience and Smartness of Coastal Regions. A Tool for Spatial Evaluation. In O. Gervasi, B. Murgante, S. Misra, A. M. A. C. Rocha, C. M. Torre, D. Taniar, B. O. Apduhan, E. Stankova, & S. Wang (Eds.), *Computational Science and Its Applications—ICCSA 2016* (pp. 530–541). Springer International Publishing.  
[https://doi.org/10.1007/978-3-319-42111-7\\_42](https://doi.org/10.1007/978-3-319-42111-7_42)

Lonsdorf, E. V., Nootenboom, C., Janke, B., & Horgan, B. P. (2021). Assessing urban ecosystem services provided by green infrastructure: Golf courses in the Minneapolis-St. Paul metro area. *Landscape and Urban Planning*, 208, 104022.  
<https://doi.org/10.1016/j.landurbplan.2020.104022>

Ludwig, W., Dumont, E., Meybeck, M., & Heussner, S. (2009). River discharges of water and nutrients to the Mediterranean and Black Sea: Major drivers for ecosystem changes during past and future decades? *Progress in Oceanography*, 80, 199–217. <https://doi.org/10.1016/j.pocean.2009.02.001>

Marino, D., Palmieri, M., Marucci, A., Soraci, M., Barone, A., & Pili, S. (2023). Linking Flood Risk Mitigation and Food Security: An Analysis of Land-Use Change in the Metropolitan Area of Rome. *Land*, 12(2), Article 2. <https://doi.org/10.3390/land12020366>

MeteoBlue. (2025). Retrieved April 2025, from [https://www.meteoblue.com/de/wetter/historyclimate/climatemodelled/kreta\\_griechenland\\_258763](https://www.meteoblue.com/de/wetter/historyclimate/climatemodelled/kreta_griechenland_258763)

MeteoItalia. (2025). Retrieved May 2025, from <https://www.agenziaitaliameteo.it/en/climatology/climate-projections/italy-weather-scenarios/>

Millennium Ecosystem Assessment. (2005). *Ecosystems and human well-being: Synthesis*. Island Press.

Ministry for the Ecological Transition and the Demographic Challenge (MITECO). (2025). *AdapteCCa Platform*. <http://adaptecca.es/en/what-adaptecca>

NASA Sea Level Change Team. (n.d.). IPCC AR6 Sea Level Projection Tool. NASA. <https://sealevel.nasa.gov/ipcc-ar6-sea-level-projection-tool>

National Oceanography Centre. (2025). *Permanent Service for Mean Sea Level*. [https://psmsl.org/about\\_us/](https://psmsl.org/about_us/)

Natural Capital Project. (2023). InVEST (Version 3.14.2) [Computer software]. Stanford University, University of Minnesota, Chinese Academy of Sciences, The Nature Conservancy, World Wildlife Fund, Stockholm Resilience Centre and the Royal Swedish Academy of Sciences. <https://naturalcapitalproject.stanford.edu/software/invest>

Navarro, D., Cantergiani, C., Abajo-Alda, B., Gomez de Salazar, I., & Feliu, E. (2023). Territorial vulnerability to natural hazards in Europe: A composite indicator analysis and relation to economic impacts. *Natural Hazards*. <https://doi.org/10.1007/s11069-023-06165-w>

OECD, European Union, & EC-JRC. (2008). Handbook on constructing composite indicators: Methodology and user guide. OECD Publishing. <https://doi.org/10.1787/9789264043466-en>

Ogden, F. L., Crouch, T. D., Stallard, R. F., & Hall, J. S. (2013). Effect of land cover and use on dry season river runoff, runoff efficiency, and peak storm runoff in the seasonal tropics of Central Panama. *Water Resources Research*, 49(12), 8443–8462. <https://doi.org/10.1002/2013WR013956>

Osman, S. M., Khalil, D. A. H., & Ibrahim, N. M. (2022). The aesthetic values of the (Tally) heritage craft and its role in enriching small projects. *International Design Journal*, 12(1), 165–178. <https://doi.org/10.21608/idj.2022.210328>

Papathoma-Köhle, M., Cristofari, G., Wenk, M., & Fuchs, S. (2019). The importance of indicator weights for vulnerability indices and implications for decision making in disaster management. *International Journal of Disaster Risk Reduction*, 36, 101103. <https://doi.org/10.1016/j.ijdr.2019.101103>

Pedregosa, F., Varoquaux, G., Gramfort, A., Michel, V., Thirion, B., Grisel, O., Blondel, M., Prettenhofer, P., Weiss, R., Dubourg, V., Vanderplas, J., Passos, A., Cournapeau, D., Brucher, M., Perrot, M., & Duchesnay, É. (2011). Scikit-learn: Machine learning in Python. *Journal of Machine Learning Research*, 12, 2825–2830. <https://scikit-learn.org/stable/modules/preprocessing.html>

Peng, Y., Welden, N., & Renaud, F. G. (2024). Incorporating ecosystem services into comparative vulnerability and risk assessments in the Pearl River and Yangtze River Deltas, China. *Ocean & Coastal Management*, 249, 106980. <https://doi.org/10.1016/j.ocecoaman.2023.106980>

Peña-Alonso, C., Hernández-Calvento, L., Pérez-Chacón, E., & Ariza-Solé, E. (2017). The relationship between heritage, recreational quality and geomorphological vulnerability in the coastal zone: A case study of beach systems in the Canary Islands. *Ecological Indicators*, 82, 420–432. <https://doi.org/10.1016/j.ecolind.2017.07.014>

Petrou, A. M., John. (n.d.). Meteo.gr. meteo.gr - Προγνώσεις καιρού για όλη την Ελλάδα.  
Retrieved 12 May 2025, from <http://www.meteo.gr/>

Phelan, P. E., Kaloush, K., Miner, M., Golden, J., Phelan, B., Iii, H. S., & Taylor, R. A. (2015). Urban Heat Island: Mechanisms, Implications, and Possible Remedies. *Annual Review of Environment and Resources*, 40(Volume 40, 2015), 285–307.  
<https://doi.org/10.1146/annurev-environ-102014-021155>

Politi, N., Vlachogiannis, D., Sfetsos, A. et al. (2023) High resolution projections for extreme temperatures and precipitation over Greece. *Clim Dyn* 61, 633–667 (2023).  
<https://doi.org/10.1007/s00382-022-06590-w>

Poulos. (2020). The Mediterranean and Black Sea Marine System: An overview of its physico-geographic and oceanographic characteristics.

Puertos del Estado. (2025). *Portus*. <https://portus.puertos.es/#/?locale=en>

Ravankhah, M., Schmidt, M., & Will, T. (2021). An indicator-based risk assessment framework for World Heritage sites in seismic zones: The case of “Bam and its Cultural Landscape” in Iran. *International Journal of Disaster Risk Reduction*, 63, 102405.  
<https://doi.org/10.1016/j.ijdr.2021.102405>

Rocatti, A., Pailaga., G, Luino, F., Faccini, F., Turconi, L. (2021): GIS-Based Landslide Susceptibility Mapping for Land Use Planning and Risk Assessment, *Land* 2021, 10(2), 162;  
<https://doi.org/10.3390/land10020162>

Roccati, Anna; Paliaga, Guido; Luino, Fabio; Faccini, Francesco; Turconi, Laura. *Atmosphere*; Basel Bd. 11, Aug. 12, (2020). Rainfall Threshold for Shallow Landslides Initiation and Analysis of Long-Term Rainfall Trends in a Mediterranean Area 1367.  
DOI:10.3390/atmos11121367

Ross, C. W., Prihodko, L., Anchang, J., Kumar, S., Ji, W., & Hanan, N. P. (2018). Global Hydrologic Soil Groups (HYSGs250m) for Curve Number-Based Runoff Modeling [Dataset]. ORNL DAAC. <https://doi.org/10.3334/ORNLDAAC/1566>

Tapia, C., Abajo-Alda, B., Feliu, E., Mendizabal, M., Martínez-Sáenz, J. A., Fernández, G., Laburu, T., & Lejarazu, A. (2017). Profiling urban vulnerabilities to climate change: An indicator-based vulnerability assessment for European cities. *Ecological Indicators*, 78, 142-155. <https://doi.org/10.1016/j.ecolind.2017.02.040>

Tekken, V., Spangenberg, J. H., Burkhard, B., Escalada, M., Stoll-Kleemann, S., Truong, D. T., & Settele, J. (2017). “Things are different now”: Farmer perceptions of cultural ecosystem

services of traditional rice landscapes in Vietnam and the Philippines. *Ecosystem Services*, 25, 153–166. <https://doi.org/10.1016/j.ecoser.2017.04.010>

Torres-Carrión, P. V., González-González, C. S., Aciar, S., & Rodríguez-Morales, S. (2018). Methodology for systematic literature review applied to engineering and education. In *2018 IEEE Global Engineering Education Conference (EDUCON)* (pp. 1364–1373). <https://doi.org/10.1109/EDUCON.2018.8363388>

USGS. (2025). *Basemaps*. <http://www.usgs.gov/>

Wischott, V., Ugalde, I., Pirazán-Palomar L., Angelone S., Milde, K., Lückerath D., Klose A. (2024). RescueME Deliverable D4.3: Local resilience baseline and local impact chains for R-Labscapes

Wischott, V., Ugalde, I., Pirazán-Palomar L., Angelone S., Milde, K., Lückerath D., Klose A. (2024). RescueME Deliverable D4.3: Local resilience baseline and local impact chains for R-Labscapes

Zanaga, D., Van De Kerchove, R., Daems, D., De Keersmaecker, W., Brockmann, C., Kirches, G., Wevers, J., Cartus, O., Santoro, M., Fritz, S., Lesiv, M., Herold, M., Tsendbazar, N.-E., Xu, P., Ramoino, F., & Arino, O. (2022). ESA WorldCover 10 m 2021 v200 [Dataset]. Zenodo. <https://doi.org/10.5281/zenodo.7254221>

Zardo, L., Geneletti, D., Pérez-Soba, M., & Van Eupen, M. (2017). Estimating the cooling capacity of green infrastructures to support urban planning. *Ecosystem Services*, 26, 225–235. <https://doi.org/10.1016/j.ecoser.2017.06.016>

Zomer, R. J., Xu, J., & Trabucco, A. (2022). Version 3 of the Global Aridity Index and Potential Evapotranspiration Database. *Scientific Data*, 9(1), 409. <https://doi.org/10.1038/s41597-022-01493-1>

# 8 Appendices

## Annex 1. R-Labs Data models

Table A- List of data used in the island of Neuwerk in Hamburg

Risk component	Vulnerability dimension	HV/ES	Name of indicator	Unit
Hazard	-	-	Wave run up under different SLR scenarios	[m]
Exposure	-	-	Population	Number
			Bed places	Number
			Number of agricultural holdings	Number
			Owned houses with summer use only	Number
			Number of properties	Number
Vulnerability	Adaptive capacity	Heritage values	Number of cultural facilities open to the public and aiming at promoting arts and culture per population	Number/ha
	Adaptive capacity	Heritage values	Area with outdoor recreation potential	Percentage
	Adaptive capacity	Heritage values	Cultural vibrancy - number of cultural sites exposed to coastal floods	Number/ha
	Adaptive capacity	Ecosystem services	Share of agricultural land	Percentage
	Adaptive capacity	Ecosystem services	Share of forest land	Percentage
	Adaptive capacity	Ecosystem services	Share of natural land + water	Percentage
	Adaptive capacity	-	Households with access to the internet at home	Percentage

Risk component	Vulnerability dimension	HV/ES	Name of indicator	Unit
	Adaptive capacity	-	Emergency operators	Percentage

**Table B- List of data used in Psiloritis Geopark**

Risk component	Vulnerability dimension	HV/ES	Name of indicator	Unit
Hazard	-	-	Maximum temperature (based on the monthly values taken from the observation stations*)	[°C]
			Mean annual precipitation	[mm]
Exposure	-	-	Population number	Number
			Employed persons	Number
			Agricultural area	[m <sup>2</sup> ]
Vulnerability	Adaptive capacity	Heritage values	Protected areas under national laws	Percentage
			Number of sites accessible by people with disabilities	Number/km <sup>2</sup>
			Annual number of festivals or cultural events connected to traditions/culinary practices/local products	Number/1,000 inhabitants
			Number of local associations connected to traditions/culinary practices/local products	Number/1,000 inhabitants
			Number of shops, restaurants and tourism facilities selling local products (0 Km)	Number/1,000 inhabitants
			Attendance and participation in cultural activities and events	Number/1,000 inhabitants
			Cultural vibrancy - number of cultural sites	Number/km <sup>2</sup>

Risk component	Vulnerability dimension	HV/ES	Name of indicator	Unit
		Ecosystem services	Runoff retention/cooling capacity*	Dimensionless
	Sensitivity	-	Proportion of population aged 65 years and more	Percentage
	Adaptive capacity	-	Share of tenant agricultural area	Percentage
	Adaptive capacity	-	Share of farmers with full or basic agricultural training	Percentage

\*Runoff retention is used for the changing precipitation patterns hazard, while cooling capacity for rising temperatures.

Table C- List of data used in Porto Venere, Cinque Terre and the islands

Risk component	Vulnerability dimension	HV/ES	Name of indicator	Unit	
Hazard	-	-	Landslide trigger index	Dimensionless	
Exposure	-	-	Population number	Number	
			Bed places	Number	
			Number of Agricultural holdings	Number	
			Number of educational facilities	Number	
			Tourist accommodation establishments	Number	
Vulnerability	Adaptive capacity	Heritage values	Share of Natura2000 area	Percentage	
			Surface cultivated with vineyards	Percentage	
			Surface cultivated with olive trees	Percentage	
			Share of protected areas surface	Percentage	
			Protected natural and agricultural areas with international designation exposed to landslides	Percentage	
			Percentage of terraced vineyards on the total land used for viticulture	Percentage	
	Sensitivity		Percentage of abandonment of terraces on the total terraced area	Percentage	
	Adaptive capacity		Ecosystem services	Share of forest land	Percentage
				Share of agricultural area	Percentage
	Sensitivity		Degree of urbanisation - Share of urban areas	Percentage	

Risk component	Vulnerability dimension	HV/ES	Name of indicator	Unit
	Sensitivity	-	Population density	persons/ km <sup>2</sup>
			Unemployment rate	% of Working Age Population (15 and older)
			Arrivals at tourist accommodation establishments per population	number/1,000 inhabitants
			Share of region with high or very high landslide susceptibility	Percentage
			Share of elevation breakdown - low coast	Percentage
			Share of elevation breakdown - high coast	Percentage
			Share of elevation breakdown - inland	Percentage
			Share of elevation breakdown - upland	Percentage
			Share of elevation breakdown - mountains	Percentage
	Adaptive capacity	-	Population change	Number/ 1,000 inhabitants

Table D- List of data used for the defensive system of Zadar

Risk component	HV/ES	Name of indicator	Unit
Hazard	-	Wave run up under different SLR scenarios	[m]
Exposure	-	Number of buildings exposed	Number
Vulnerability	Heritage value	HV index	Dimensionless

Table E- List of data used for the L'Horta de Valencia risk assessment

Risk component	Vulnerability dimension	HV/ES	Name of indicator	Unit
Hazard	-	-	95th percentile of daily rainfall	[mm/d]
			Number of days with rainfall less than 1 mm	[-]
			Accumulated rainfall in 24 h	[mm/a]
Exposure	-	-	Population number	Number
			Number of Agricultural holdings	Number
			Agricultural area	m <sup>2</sup>
Vulnerability	Adaptive capacity	Heritage value	Share of Natura 2000 area	% of area
			Share of protected areas surface	% of area
			Incentives for the maintenance of traditional agricultural activities	€/farmer/year
			Number of PDO/PGI agriculture firms	Number/km <sup>2</sup>
			Area with outdoor recreation potential	% of area
			Protected areas under national laws	% of area
			Diversity of landscape	Number
			Traditional channels of irrigation	m/km <sup>2</sup>
			Area used for traditional cultivations	% of area

Risk component	Vulnerability dimension	HV/ES	Name of indicator	Unit
			Number of architectural and infrastructural elements representing the traditional way of living and cultivating	Number/km <sup>2</sup>
	Adaptive capacity	Ecosystem services	Average hydric resources for crops	m <sup>3</sup> /ha/year
			Organic farming activities	% of area
			Share of arable land	% of area
			Permanent cultivations surface	% of area
			Ramsar site wetland area	% of area
			Runoff Retention (calculated with InVEST)	m <sup>3</sup> /25m <sup>2</sup>
	Sensitivity		Unemployment rate	% of Working Age Population (15 and older)
	Adaptive capacity		Availability of action plans or adaptation strategies at municipal level	0=has neither nor, 1=has one of them, 2=has both
	Adaptive capacity		Share of holdings with a full-time manager	Percentage
	Adaptive capacity		Social Security affiliation in Agriculture	Percentage
	Adaptive capacity		Public land tenure	Percentage

Risk component	Vulnerability dimension	HV/ES	Name of indicator	Unit
	Adaptive capacity		Share of female farm managers	Percentage
	Adaptive capacity		Farm manager with agricultural studies	Percentage
	Adaptive capacity		Municipal budget	Euro/inhabitant/year
	Adaptive capacity		Number of Bio agriculture firms	Percentage
	Adaptive capacity		Share of young farmers (25 to 34 years)	Percentage
	Adaptive capacity		Number of water management bodies/structures	Percentage
	Sensitivity		Mid agriculture value	€/ha
	Adaptive capacity		Share of farmers with full or basic agricultural training	Percentage

## Annex 2. Risk maps

These maps include the mid-century time frame scenarios. It is worth noting that in some cases (Psiloritis Geopark, in the map showing the impact of changes in temperature patterns, and Portovenere, Cinque Terre and the Islands), these maps are identical. That is, although the risk does change, it is not significant enough to shift to a different category, so the cartography appears the same across the different scenarios.

### PSILORITIS GEOPARK

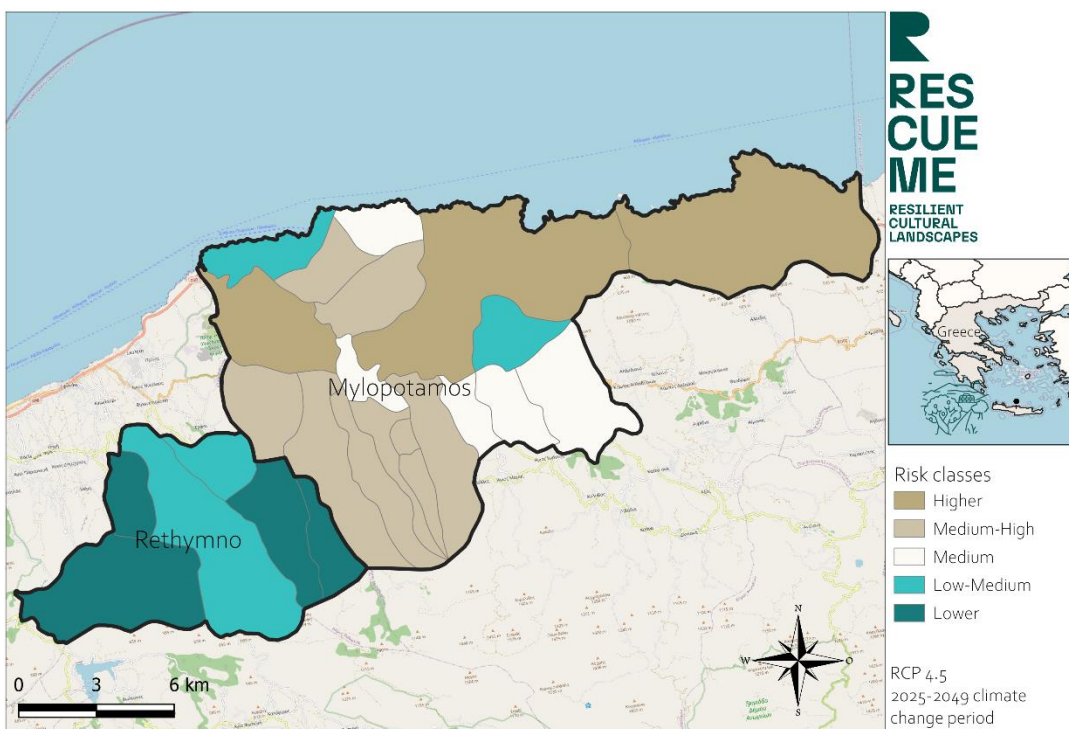


Figure 38. Impact of changes in precipitation patterns on culture. RCP 4.5 (2025-2049)

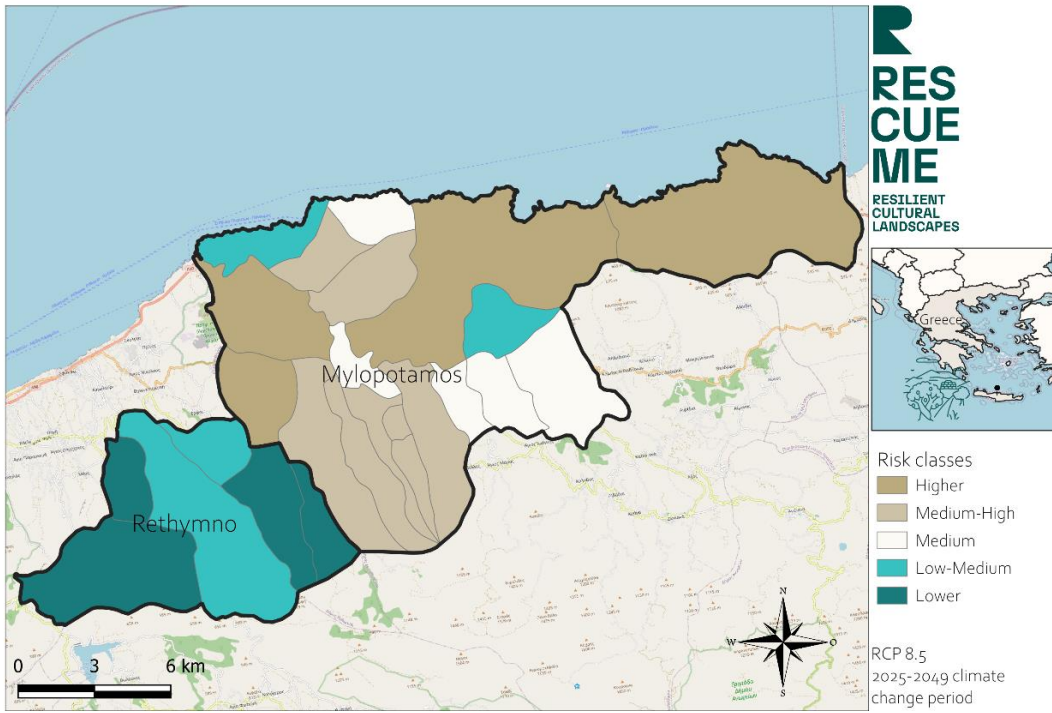


Figure 39. Impact of changes in precipitation patterns on culture. RCP 8.5 (2025-2049)

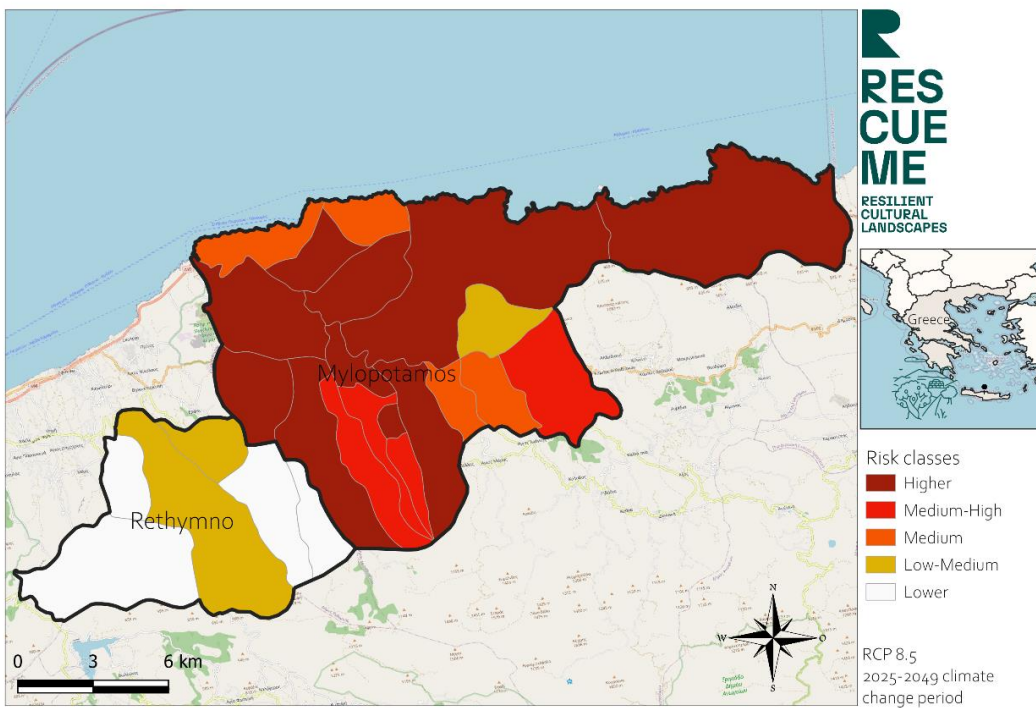


Figure 40. Impact of changes in temperature on culture. RCP 8.5 (2025-2049)

## L'HORTA DE VALENCIA

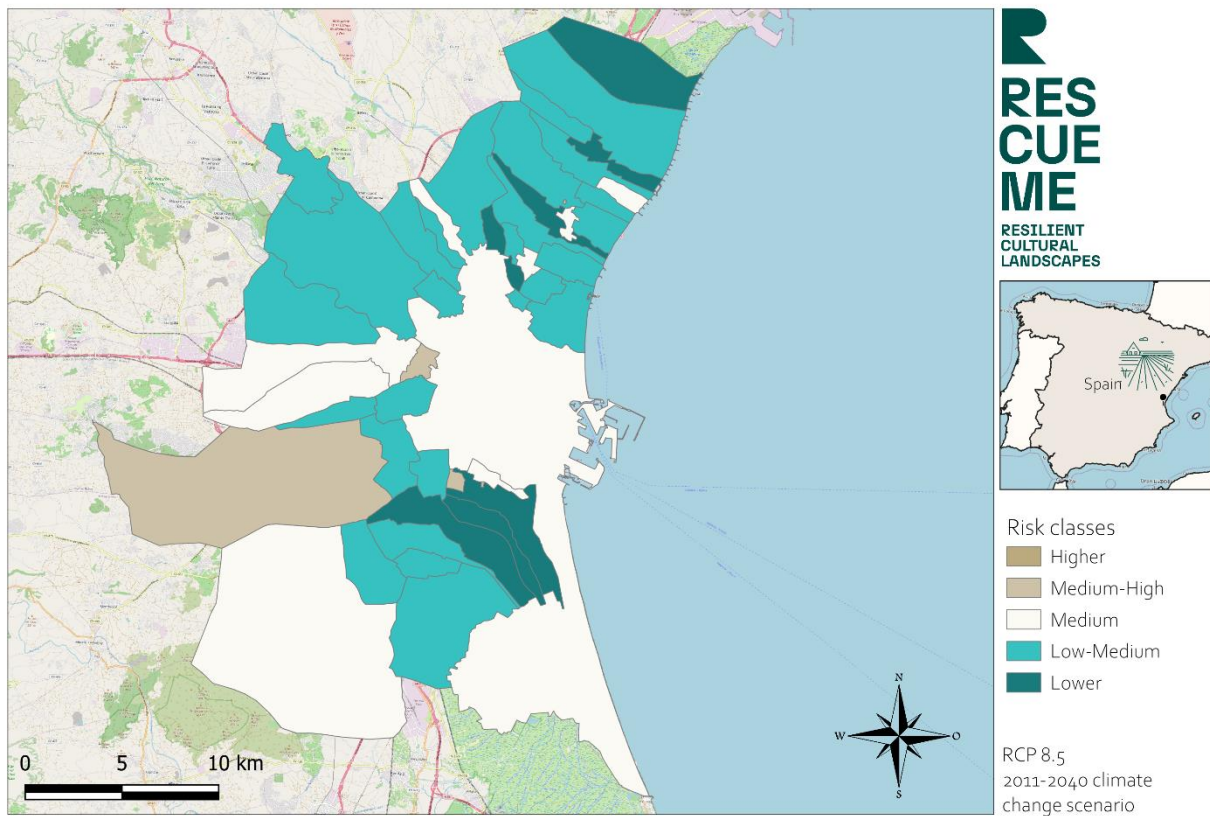


Figure 41. Impact of droughts on the agricultural heritage system. RCP 8.5 (2011-2040)

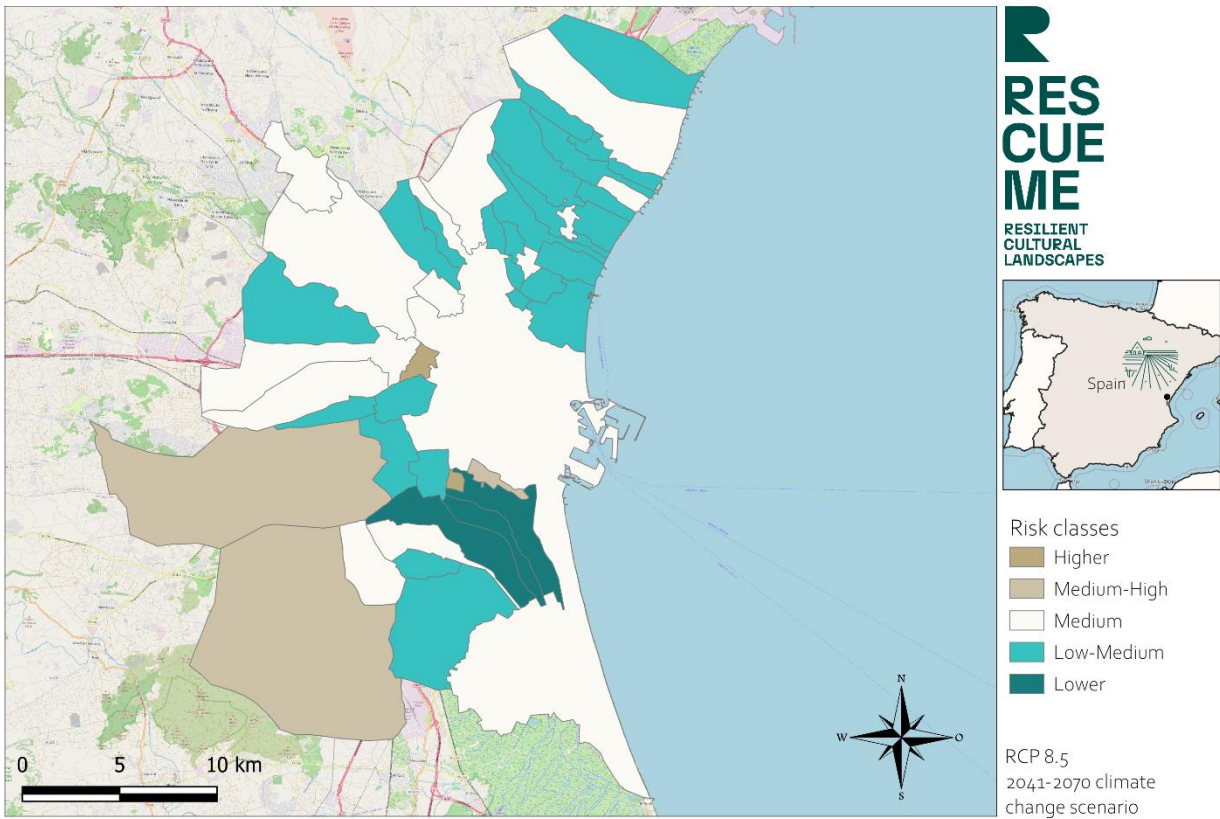


Figure 42. Impact of droughts on the agricultural heritage system. RCP 8.5 (2041-2070)

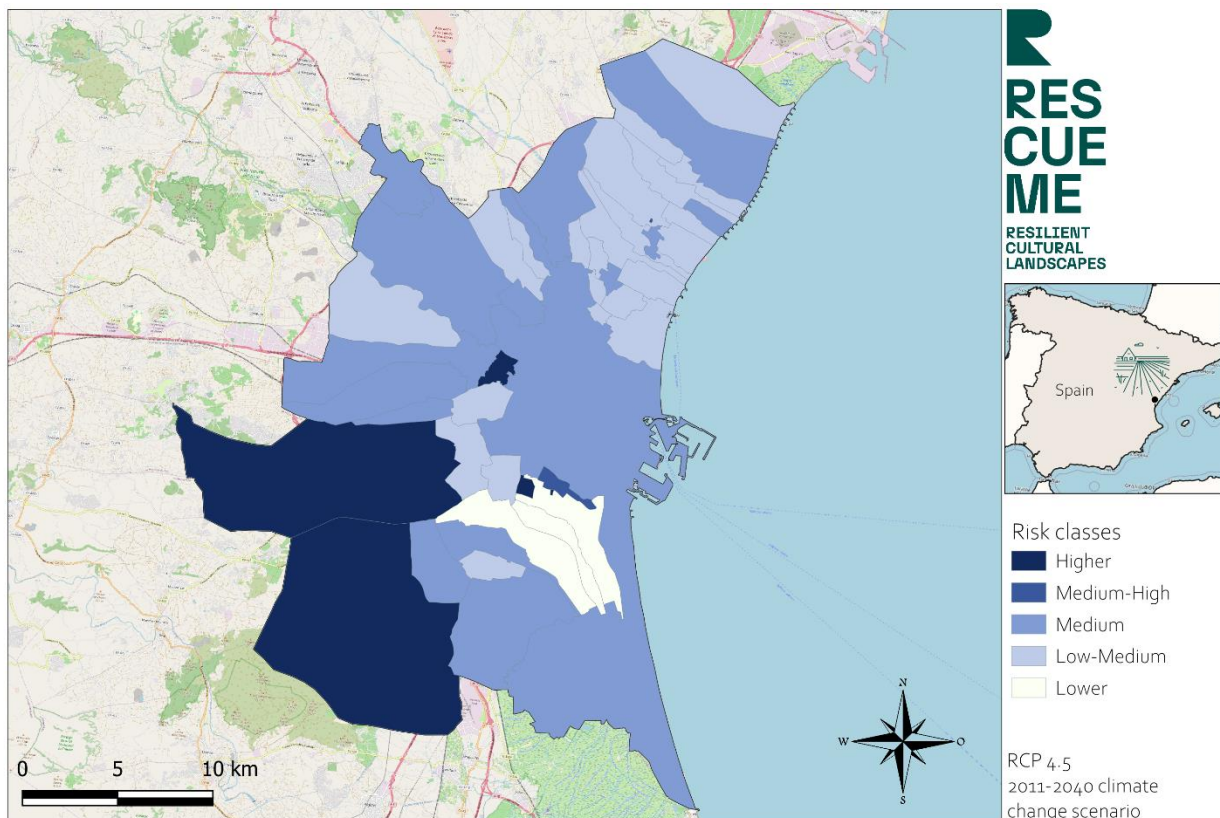


Figure 43. Impacts of torrential rainfall on the agricultural heritage system. RCP 4.5 (2011-2040)

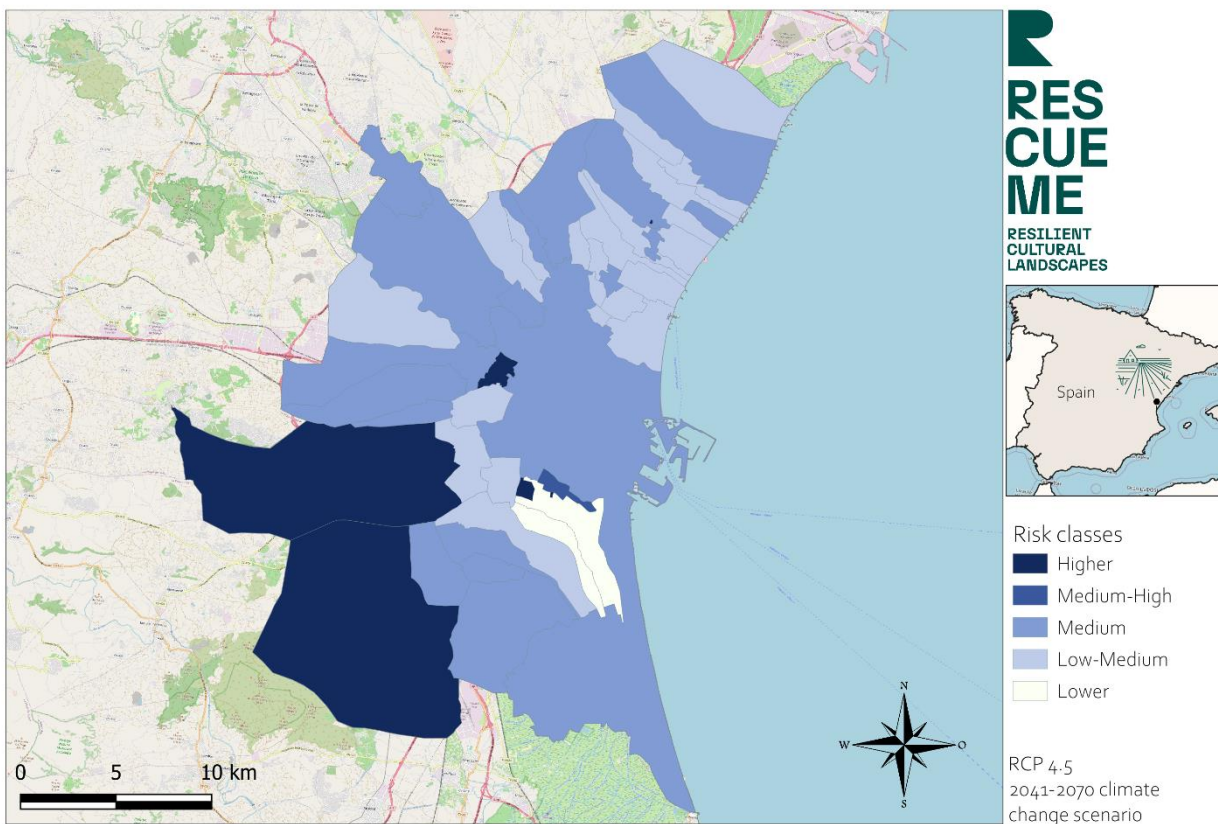


Figure 44. Impacts of torrential rainfall on the agricultural heritage system. RCP 4.5 (2041-2070)

## PORTOVENERE, CINQUE TERRE AND THE ISLANDS

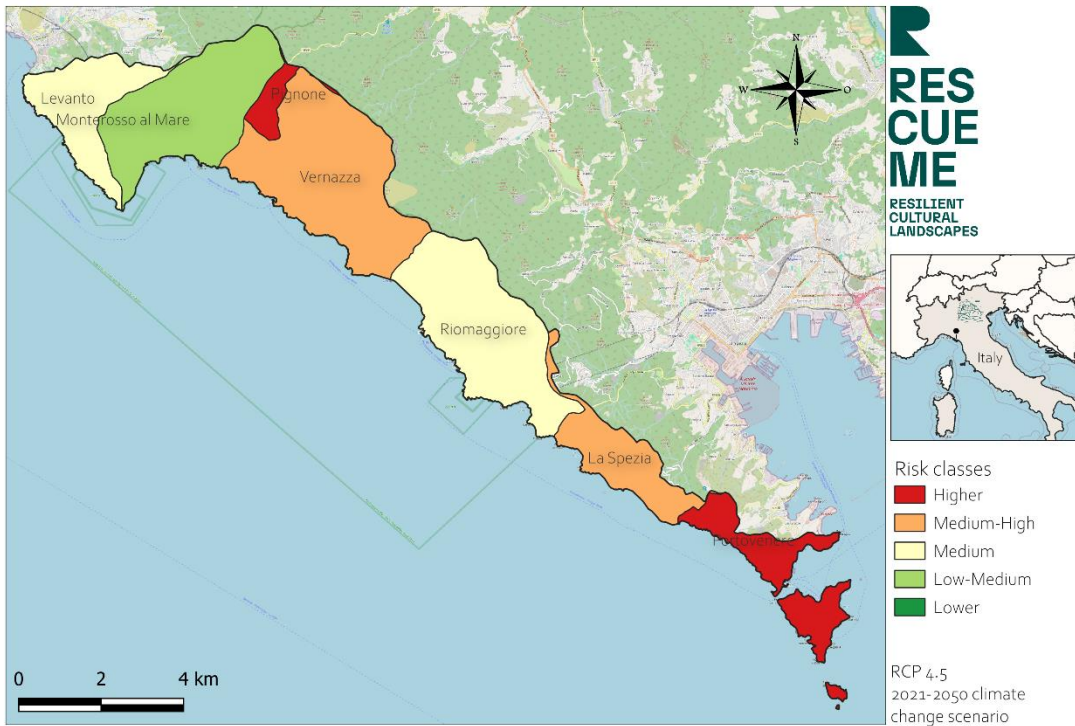


Figure 45. Impacts of landslides on the terraced landscape. RCP4.5 (2021-2050)

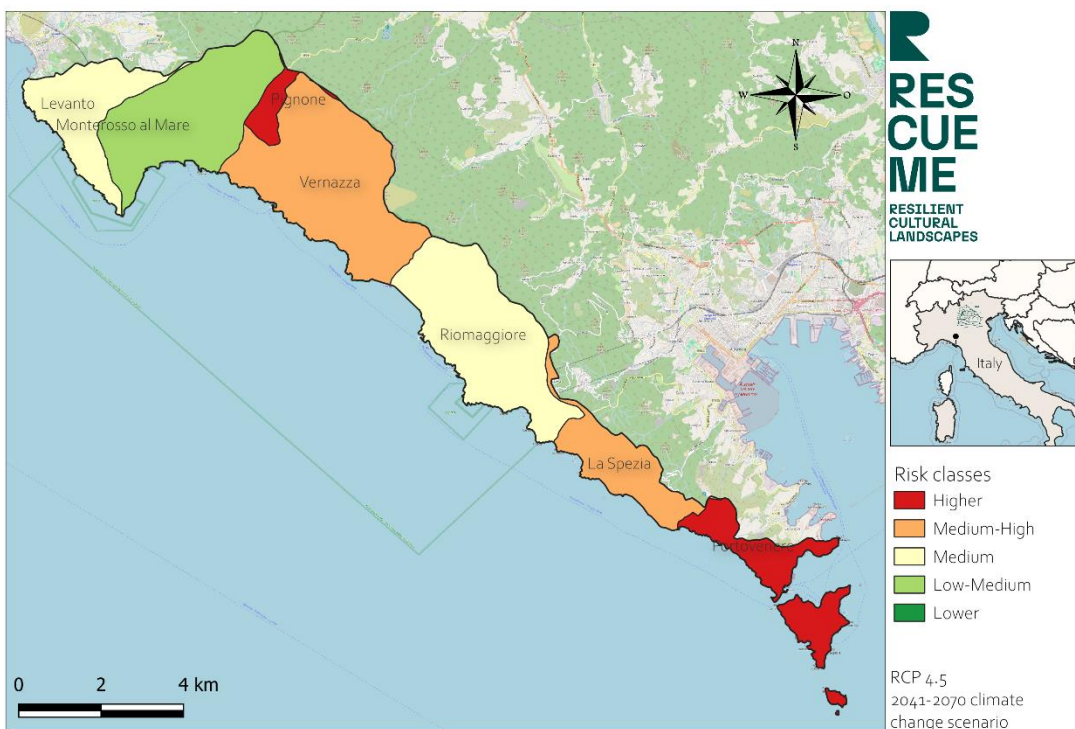


Figure 46. Impacts of landslides on the terraced landscape. RCP4.5 (2041-2070)

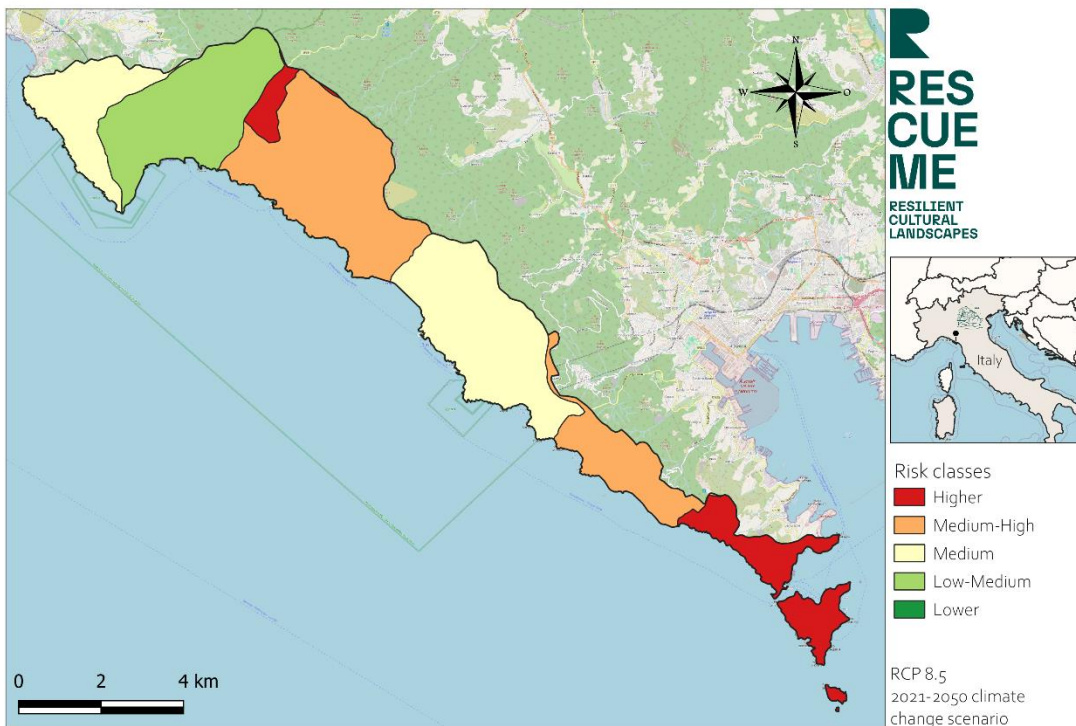


Figure 47. Impacts of landslides on the terraced landscape. RCP8.5 (2021-2050)

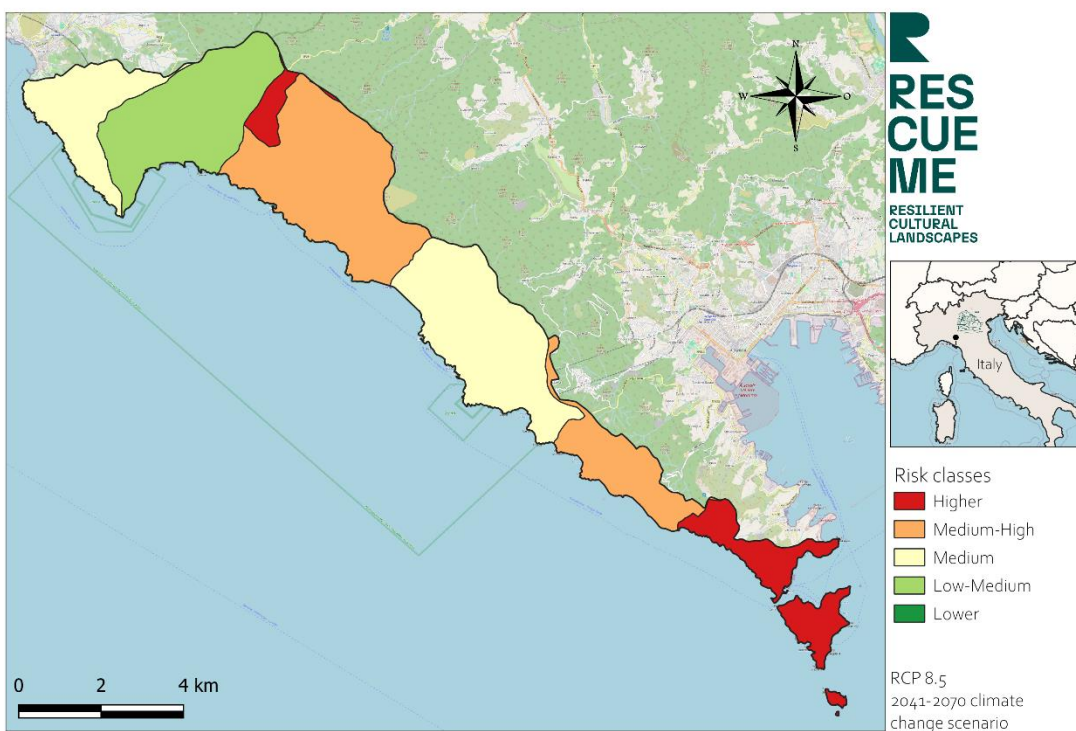


Figure 48. Impacts of landslides on the terraced landscape. RCP8.5 (2041-2070)

# Partners

**tecnal:a**

MEMBER OF BASQUE RESEARCH  
& TECHNOLOGY ALLIANCE



ALMA MATER STUDIORUM  
UNIVERSITÀ DI BOLOGNA  
DIPARTIMENTO DI ARCHITETTURA



CONEXIONES  
**improbables**



**LAS NAVES**



# Contact us

[www.resilientculturallandscapes.eu](http://www.resilientculturallandscapes.eu)

**AITZIBER EGUSQUIZA ORTEGA**  
PROJECT COORDINATOR  
[aitziber.egusquiza@tecnalia.com](mailto:aitziber.egusquiza@tecnalia.com)

**ALESSANDRA GANDINI**  
WP LEAD  
[alessandra.gandini@tecnalia.com](mailto:alessandra.gandini@tecnalia.com)

**MARIA AYELEN CALVET**  
TASK LEAD  
[maria.ayelen@tecnalia.com](mailto:maria.ayelen@tecnalia.com)

**KATHERINE PEINHARDT**  
COMMUNICATIONS LEAD  
[Katherine.peinhardt@iclei.org](mailto:Katherine.peinhardt@iclei.org)

Follow us

LinkedIn: [www.linkedin.com/company/rescuemeeu/](http://www.linkedin.com/company/rescuemeeu/)

Twitter: [twitter.com/RescueME\\_EU](https://twitter.com/RescueME_EU)



Funded by  
the European Union

Funded by the European Union. Views and opinions expressed are however those of the author(s) only and do not necessarily reflect those of the European Union or Research Executive Agency (REA). Neither the European Union nor the granting authority can be held responsible for them.